CALIFORNIA
ENERGY COMMISSION

Energy Research and Development Division

FINAL PROJECT REPORT

Natural Gas Dedicated Exhaust Gas Recirculation Engine for Improved On-Highway Efficiency

Gavin Newsom, Governor
July 2020 | CEC-500-2020-044

PREPARED BY:

Primary Authors:
Thomas E. Briggs, Jr.
Michael C. Kocsis
Scott A. Sjovall

Southwest Research Institute
6220 Culebra Road
San Antonio, TX 78238
210-522-3751
https://www.swri.org

Contract Number: PIR-16-025

PREPARED FOR:
California Energy Commission

Peter Chen
Project Manager

Jonah Steinbuck, Ph.D.
Office Manager
ENERGY GENERATION RESEARCH OFFICE

Laurie ten Hope
Deputy Director
ENERGY RESEARCH AND DEVELOPMENT DIVISION

Drew Bohan
Executive Director

ACKNOWLEDGEMENTS

The work described in this report was conducted by Southwest Research Institute under contract with and funding by the California Energy Commission. In addition to the California Energy Commission, the authors would like to thank Southern California Gas Company, Woodward, Inc., Garrett – Advancing Motion, Oak Ridge National Laboratory and KS Kolbenschmidt US, Inc. for providing technical and hardware support.

PREFACE

The California Energy Commission's (CEC) Energy Research and Development Division manages the Natural Gas Research and Development Program, which supports energy-related research, development, and demonstration not adequately provided by competitive and regulated markets. These natural gas research investments spur innovation in energy efficiency, renewable energy and advanced clean generation, energy-related environmental protection, energy transmission and distribution and transportation.

The Energy Research and Development Division conducts this public interest natural gas-related energy research by partnering with research, development, and demonstration entities, including individuals, businesses, utilities and public and private research institutions. This program promotes greater natural gas reliability, lower costs and increases safety for Californians and is focused in these areas:

- Buildings End-Use Energy Efficiency.
- Industrial, Agriculture and Water Efficiency
- Renewable Energy and Advanced Generation
- Natural Gas Infrastructure Safety and Integrity.
- Energy-Related Environmental Research
- Natural Gas-Related Transportation.

Natural Gas Dedicated Exhaust Gas Recirculation Engine for Improved On-Highway Efficiency is the final report for the Research and Development of a Natural Gas D-EGR Engine for Improved On-Highway Efficiency project (Contract Number PIR-16-025) conducted by Southwest Research Institute. The information from this project contributes to the Energy Research and Development Division's Natural Gas Research and Development Program.

For more information about the Energy Research and Development Division, please visit the CEC's research website (www.energy.ca.gov/research/) or contact the CEC at 916-327-1551.

ABSTRACT

A Cummins Westport ISX12 G heavy-duty natural gas engine was modified to use dedicated exhaust gas recirculation (Dedicated EGR®), an innovative configuration where specific cylinders directly feed their exhaust to the intake of the engine. This configuration enables higher levels of EGR dilution with reduced pumping work when compared to traditional high-pressure EGR systems typically seen on heavy-duty engines. This system was used in combination with an advanced continuous discharge ignition system, a variable geometry turbocharger, and a low-squish, high compression ratio piston. The combined hardware modifications enabled a 12 percent improvement in engine fuel economy while maintaining oxides of nitrogen (NO_X) emissions at levels 90 percent below the current 2010 heavy-duty NO_X standard. Heavy-duty natural gas vehicles using high efficiency Dedicated EGR engines can displace diesel vehicles and help California meet its greenhouse gas emission reduction goals, while simultaneously addressing air quality improvement needs of regions such as the South Coast Air Basin.

Keywords: natural gas, heavy-duty engine, ISX12 G, Dedicated EGR, D-EGR, advanced ignition, variable nozzle turbine, VNT turbocharger

Please use the following citation for this report:

Kocsis, Michael, Thomas Briggs and Scott Sjovall. 2020. *Natural Gas Dedicated Exhaust Gas Recirculation Engine for Improved On-Highway Efficiency.* California Energy Commission. Publication Number: CEC-500-2020-044.

TABLE OF CONTENTS

LIST OF FIGURES

Page

LIST OF TABLES

EXECUTIVE SUMMARY

Introduction

Meeting California's aggressive goals for greenhouse gas emission reduction requires reduced carbon dioxide (CO_2) emissions from the transportation sector. Criteria pollutants such as oxides of nitrogen (NO_X), a precursor to smog, must be simultaneously reduced to address the air quality needs of regions such as the South Coast Air Basin. Regulations are already in place to address these needs for light-duty transportation by deploying a combination of advanced conventional vehicle technologies and electric vehicles. However, the heavy-duty vehicle market is more challenging because of their reliance on diesel engines for their durability and utility. Switching to natural gas engines is a potential alternative for many heavy-duty vehicle applications. Previous work funded by the California Air Resources Board (CARB) has demonstrated a cost-effective technology pathway to update these engines to meet stringent NO_X emission reductions required for air quality improvement. However, this pathway compromised the efficiency of the engine to meet the NO_X targets.

The relatively small market for heavy-duty natural gas engines has limited the commercial investment to develop advanced combustion approaches, which could improve efficiency while maintaining the emissions reductions already achieved. Until a larger market base is available, it is unlikely the industry can justify the cost of such development without support from government entities. This has led to financial support from the California Energy Commission to help accelerate the development of more efficient natural gas engines that can replace diesel engines in the California on-highway heavy-duty truck market.

Project Purpose

To improve natural gas engine efficiency, this project developed an improved combustion system for natural gas engines based on previous developments at Southwest Research Institute® on light-duty gasoline engines. Past demonstrations have shown the combustion system's ability to provide 10 percent or greater improvement in gasoline engine efficiency. Southwest Research Institute anticipated the system would offer similar benefits to natural gas engines when combined with suitable technologies (such as advanced ignition systems, improved combustion chamber design, advanced turbocharger systems, and high compression ratio piston design) because of the similarities between gasoline and natural gas combustion engines. As the key characteristics of the engine that enabled tailpipe emissions consistent with future CARB regulations remained unchanged, implementing this system can improve efficiency while simultaneously meeting the desired low NO_X emission targets.

Replacing diesel engines with low NO_X emission natural gas engines can improve air quality, with important benefits particularly for areas of poor ambient air quality such as the South Coast Air Basin. Successful deployment would also expand the market for natural gas use in California's transportation sector, which can reduce CO_2 emissions by displacing petroleum fuels. Natural gas engines can also use renewable natural gas, a low carbon transportation fuel captured from waste sources such as wastewater treatment plants and dairies, for additional reductions in lifecycle CO_2 emissions.

The results of this project will be transferred to engine manufacturers who could then adapt the technology to a production scale. These engines would then be available for installation in trucks sold in the California market, realizing the desired NO_X and CO_2 emission reduction benefits.

Project Approach

The research team was comprised of experts at Southwest Research Institute, a multidisciplinary laboratory with a 70-year history of research and development for the automotive industry. Through previous work, Southwest Research Institute has developed advanced ignition and combustion systems, which were directly applicable to the technical scope of this project. The team at Southwest Research Institute was supported by Woodward Inc., a company that develops advanced ignition systems for natural gas engines as well as advanced engine control solutions. The team also included Garrett Advancing Motion, a company that develops turbochargers for light-duty and heavy-duty engines and supplied the high efficiency turbocharger hardware that enabled the engine to achieve the project's efficiency target.

Southwest Research Institute modified a production model of the Cummins Westport ISX12 G, a common heavy-duty natural gas engine for the on-highway truck market, to use an innovative combustion approach known as dedicated exhaust gas recirculation (Dedicated EGR®). Dedicated exhaust gas recirculation is a combustion system where one or more cylinders of an engine are dedicated to producing exhaust gas that is directed back to the engine intake. The current state of the art heavy-duty engines use cooled exhaust gas recirculation in a high-pressure (before turbine) configuration. The turbine is sized to provide the restriction necessary to drive exhaust gas recirculation. To balance the exhaust gas recirculation rate and engine breathing performance, the exhaust gas recirculation rate is typically limited to approximately 20 percent. The dedicated exhaust gas recirculation routing approach allows the engine to exceed this limit by mixing approximately 33 percent of the engine's exhaust gases with fresh air from the intake.

The high percentage of exhaust gas dilution allowed by Dedicated EGR® reduces knock tendencies by lowering combustion chamber temperatures. Mitigating engine knock enables Southwest Research Institute to increase the compression ratio of the pistons, which yields higher efficiency. After modifying the base ISX12 G engine to a high compression ratio dedicated exhaust gas recirculation engine with a high efficiency turbocharger, the team tested the modified engine's ability to meet the base power requirements while yielding higher fuel efficiency.

Careful development decisions and tuning identified the optimum combination of ignition system, piston design, and dedicated cylinder equivalence ratio to enable the engine to properly run with the dedicated exhaust gas recirculation system. The base engine's flat cylinder head design prevented the engine from utilizing the full potential of the dedicated exhaust gas recirculation system. Ideally, the engine would use a pent-roof combustion chamber, which is better suited for stable spark-ignited combustion at high dilution levels. Non-technical barriers were primarily related to coordination of the supply of hardware from Woodward and Garrett, as prototype parts were difficult to schedule for production. Southwest Research Institute held regular conferences with Woodward and Garrett to ensure supply of hardware in time to address key program milestones.

Technology costs for the final configuration of the modified engine are expected to be similar to current engine technology. The advanced ignition system will add minor costs, as it has higher voltage and energy requirements than conventional systems. The remaining hardware used in the program is essentially equivalent to current engine technology, so no significant cost increases would be expected for most of the engine systems.

The researchers formed a technical advisory committee to monitor technical progress and offer opportunities for independent input to the program team. Advisory committee members included experts from Garrett Advancing Motion, Oak Ridge National Laboratory, Southern California Gas Company, and Woodward Inc. The advisory committee was instrumental in planning for the ignition system studies by discussing test plans and reviewing test results to further refine the test plan. Additionally, the committee provided valuable support in steering the data analysis to convey impact of the efficiency improvements on the market.

Project Results

Southwest Research Institute modified a Cummins Westport ISX12 G engine to achieve improved efficiency while maintaining ultra-low NO_X emission levels. The engine met the project objectives by:

- Demonstrating an average 12.3 to 13.5 percent improvement in engine fuel economy using the combined hardware modifications.
- Demonstrating the potential for achieving an ultra-low NOX emission level of 0.02 grams per brake horsepower hour (g/bhp-hr), a 90 percent reduction relative to the United States Environmental Protection Agency’s current 2010 heavy-duty NOX standard.
- Evaluating and ranking advanced ignition systems for best performance under high exhaust gas recirculation rates.
- Designing and selecting improved engine components using simulations as well as physical hardware testing. The optimal configuration consisted of the following components: Dedicated exhaust gas recirculation arrangement with two cylinders dedicated to producing the exhaust gas recirculation, a variable geometry turbocharger, a continuous discharge ignition system, and custom piston designs.

To further improve the engine efficiency, Southwest Research Institute recommends the following development activities:

- Improve exhaust gas recirculation tolerance and reduce heat transfer losses through the development of a pent-roof combustion chamber, which is more suitable for stable spark-ignited combustion at high dilution levels.
- Improve exhaust gas recirculation tolerance through the further development of pre-chamber ignition systems.

Technology/Knowledge Transfer/Market Adoption

Southwest Research Institute advanced the technology readiness level of dedicated exhaust gas recirculation for heavy-duty natural gas engines from TRL 5 to TRL 7, but it requires additional development before commercial adoption. Southwest Research Institute is making the knowledge gained from this project available to the public and promoting the technical and economic benefits of this project through a number of technology transfer activities, which will help advance this research to the market:

- Conference Presentations: Southwest Research Institute regularly attends and presents at conferences, technology forums and industry events. Southwest Research Institute plans to include the details of the engine efficiency improvement with ultra-low NO_X potential technology at these events.
- Consortium presentations: Southwest Research Institute provided updates to the High Efficiency Dilute Gasoline Engine® consortium members throughout the project at regularly scheduled technical advisory committee meetings. As of October 2019, the members of the consortium consist of original equipment manufacturers and suppliers from across the globe.
  - Original equipment manufacturers: Cummins, Fiat Chrysler Automotive, Ford, GAC Group, General Motors, Honda, Hyundai Motor Group, Isuzu, Kia Motors, Nissan, PSA Peugeot Citroen, Renault, Toyota, Volkswagen.
  - Suppliers: BorgWarner, Convergent Science, Garrett Advancing Motion, Hanon Systems, IHI Turbochargers, Lubrizol, Sejong Industrial, Woodward.
- Technical papers: Southwest Research Institute regularly publishes technical papers to convey detailed results to the industry. These papers focused on individual technical challenges, observations, and provide a summary of the development process and project results.
- Original equipment manufacturer/supplier visits: Southwest Research Institute regularly visits Original equipment manufacturers and suppliers to discuss current challenges and future opportunities for their product line. These visits often include presentations on publicly funded projects, such as this project.

The results of this project presented in the final report and disseminated through technology transfer activities could be used in the following ways:

- Government emissions regulators will be able to use the results to confirm that natural gas engines are capable of delivering a low CO_2 solution with "near-zero" NO_X potential. This provides valuable insight into the potential of future technology in order to make informed decisions on the content and timing of future emissions regulations.
- Southwest Research Institute is engaged with many of the major vehicle original equipment manufacturer and engine manufacturers in the on-road heavy-duty vehicle market. These entities, if not already aware of dedicated exhaust gas recirculation, will be informed of the potential benefits of using the technology along with challenges to implementation. This may alter research and development plans to include similar technologies to those demonstrated in this project.

Benefits to California

Natural gas-fueled heavy-duty vehicles offer significant environmental advantages to California ratepayers relative to conventional diesel-fueled vehicles. Natural gas engines produce very low particulate emissions, and their gaseous emissions can be effectively controlled by passive aftertreatment to achieve NO_X emission levels 90 percent below the current regulation. The higher exhaust temperatures of natural gas engines also enable the aftertreatment to remain effective even under extended low- and no-load conditions, as is frequently experienced for bus operation and other urban traffic conditions. These lower emissions can improve ambient air quality and reduce the negative health effects associated with transportation emissions.

Natural gas engines power transit buses, refuse hauling trucks, local and short-haul freight trucks, and other applications that directly touch California ratepayers through their provided services as well as through their environmental impacts. Depending on the application, natural gas engines typically have 10 to 20 percent lower efficiency compared to a diesel engine, which reduces the incremental greenhouse gas benefit of using natural gas. The greater than 10 percent efficiency improvement demonstrated by this project represents a significant step toward achieving parity with diesel engines. An engine with the optimal dedicated exhaust gas recirculation configuration developed in this project can reduce greenhouse gases by 16 to 20 percent compared to a diesel engine.

There are nearly 19,000 medium- and heavy-duty vehicles operating in California. The additional cost savings achieved from eliminating the efficiency deficit of natural gas vehicles may provide incentives for more fleets to adopt natural gas vehicles. Transitioning an additional 10,000 heavy-duty vehicles from diesel to using natural gas engines with the optimal dedicated exhaust gas recirculation configuration developed in this project could reduce statewide NO_x emissions by 13,741 tons/year and CO_2 emissions by 594,920 tons/year.

A second benefit of the 10 percent efficiency improvement is the reduction in total operating cost for fleets that convert to natural gas vehicles. A major barrier to broader adoption of natural gas vehicles lies in the incremental cost of the natural gas engine. With little competition in the market, natural gas engines are often sold at a premium to an equivalent diesel engine plus the added cost of the complex fuel storage system, which can cost as much as the engine itself. For example, a fleet owner may purchase a natural gas vehicle at an incremental cost of $37,500 over an equivalent diesel vehicle. The fuel efficiency improvement from using the dedicated exhaust gas recirculation configuration combined with the lower cost of compressed natural gas compared to diesel can save the fleet to save $39,000 over two years. This allows the fleet to recover the higher upfront cost of natural gas vehicles in two years and makes natural gas vehicles a more economically competitive alternative to diesel vehicles.

CHAPTER 1: Introduction

Background

There is strong interest in California to displace on-highway diesel engines with natural gas engines and other alternatives. The switch in fuel type offers a number of benefits to the environment and to California citizens. Natural gas engines are cleaner and rely on a much simpler technical path to treating the harmful emissions from the combustion process than diesel engines. This improves air quality and reduces health problems associated with transportation. Natural gas also offers greenhouse gas benefits relative to diesel fuel. The production and distribution of natural gas can offer reduced greenhouse gas (GHG) emissions relative to the production and distribution of diesel fuel. There is also a reduction in the CO_2 emissions from burning an equivalent mass of natural gas when compared to diesel fuel.

Despite the benefits of natural gas as a diesel fuel alternative, there are technical and economic challenges which prevent wide adoption in the marketplace. These challenges are linked and primarily centered on the reduced efficiency of a natural gas engine when compared to a diesel engine of equivalent utility (power and torque production). Current state-of-the-art natural gas engines are stoichiometric spark-ignited engines that experience efficiency losses associated with pumping work and the lower compression ratio required by the combustion system to prevent damaging engine knock. Even with the relatively high equivalent octane number of compressed natural gas (CNG), natural gas engines have a propensity to knock related to the slow burn rate of the fuel. A diesel engine can run lean, which allows a significant reduction in the air pumping losses. Diesel engines also do not suffer from knock, so the compression ratio can be higher.

A 12-15 liter displacement diesel engine used for heavy-duty truck applications will generally be 44-46 percent efficient at converting fuel to useful work. An equivalently sized natural gas engine using current technology will be 36-38 percent efficient. The benefits of natural gas described above cannot offset this large reduction in efficiency, leading to higher fuel consumption costs for fleet operators.

Southwest Research Institute® (SwRI®) has been developing high efficiency combustion systems for spark ignited engines for many years, and one technology which has shown great promise for gasoline engines is Dedicated EGR® (D-EGR®). D-EGR is a combustion system where one or more cylinders of an engine are dedicated to the production of exhaust gas that is directed back to the engine intake. Through past work, SwRI has shown that a gasoline-fueled passenger car engine can achieve 10 percent higher fuel economy by using the D-EGR combustion system [1]. SwRI has also worked to extend this system to natural gas engines, which can respond less favorably to EGR because of the different chemistry of natural gas combustion [2].

SwRI has also demonstrated the potential for natural gas engines to easily meet future emissions standards as proposed by the California Air Resources Board (CARB), with up to a 90 percent reduction in NO_X emissions possible relative to the current regulations [3]. This significant reduction in NO_X emissions would have a direct impact on the smog and ground level ozone problems that remain in some regions of California. Unfortunately, achieving these reduced NO_X emissions led to an increase in fuel consumption for the engine under development. The engine required higher fuel consumption during cold starts to rapidly bring the three-way catalyst to a functional operating temperature which resulted in a ~1 percent CO_2 penalty on the Heavy-Duty FTP cycle.

Dedicated Exhaust Gas Recirculation Technology

SwRI has developed high efficiency, dilute gasoline engine technology to the point where it is ready to be commercialized on all SI engines. The technology involves using higher than typical levels of cooled EGR to improve the efficiency and reduce the engine-out emissions from SI engines. When combined with stoichiometric operation and a TWC, the end result is diesel-like efficiency with ultra-low tailpipe emissions. The key enabling technologies, developed by SwRI over the last seven years, include a robust ignition system and a modified combustion chamber, both of which serve to promote high EGR tolerance. Cooled EGR has been shown to be more effective than air dilution (lean burn) at suppressing knock, reducing exhaust temperatures, lowering engine-out NOx emissions, and improving engine efficiency in CNG applications over non-dilute engines. SwRI's technology has been shown to improve the EGR tolerance in spark ignition engines, which significantly increases the benefits that can be realized by the use of cooled EGR. The presence of a TWC and stoichiometric exhaust has been shown in previous applications to result in near-zero emissions of NO_X, CO, HC and PM in pre-mixed engines. This technology is a cost-effective solution for reducing NO_x and CO_2 in vehicles using stoichiometric spark-ignited engines.

D-EGR® is an extension of cooled EGR technology. SwRI initially conceptualized D-EGR in 2007 as a solution to the combustion deterioration associated with high levels of EGR dilution and to simplify EGR controls for gasoline engines. The concept was to route the exhaust from one or more cylinders of a multi-cylinder engine directly back to the intake to create the entirety of the EGR for the engine. This effectively decouples the exhaust of the EGR generating cylinders, henceforth known as "dedicated cylinder(s)", from the aftertreatment system thereby allowing the air-fuel ratio of the dedicated cylinders to be optimized for best overall engine performance. A schematic of D-EGR being used on a four-cylinder engine is shown in Figure 1. This arrangement results in a nominal 25 percent EGR rate. In a six-cylinder application, as would be typical of a heavy-duty natural gas engine, the configuration can be varied to select either 17 percent or 33 percent EGR if one or two cylinders are used to produce EGR. A diagram of the D-EGR concept as applied to a 6-cylinder engine is shown in Figure 2.

Figure 1: D-EGR Schematic of a 4-Cylinder Application

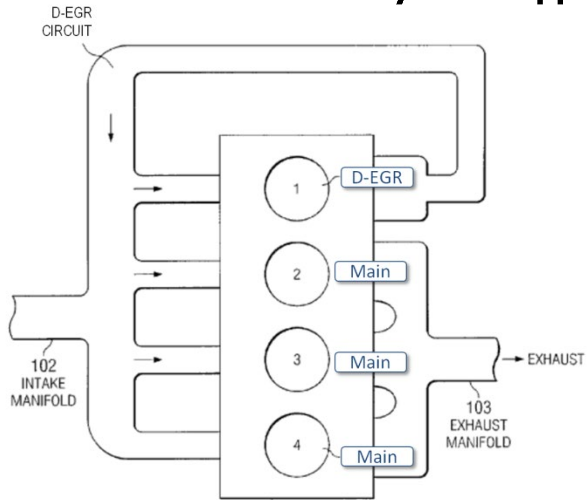

Source: Southwest Research Institute

Figure 2: D-EGR Schematic of a 6-Cylinder Application

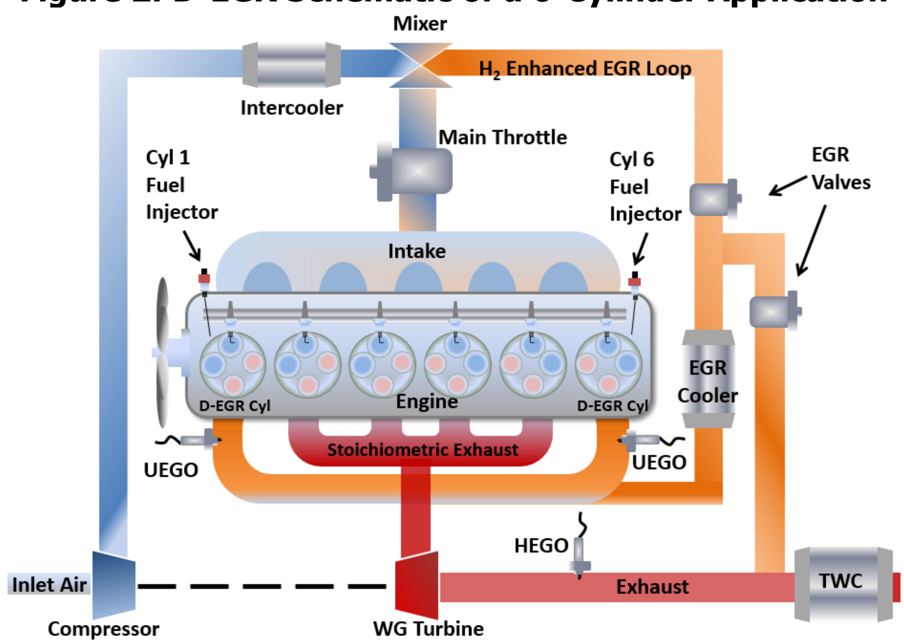

Source: Southwest Research Institute

Reforming a fuel such as gasoline or natural gas into syngas (products of partial oxidation that include carbon monoxide (CO) and hydrogen (H_2)) has been shown to offer many advantages for dilute, high efficiency engines. The biggest advantages from adding syngas to the combustion mixture are improved knock resistance, improved EGR tolerance, lower necessary ignition energy, faster combustion rates, and improved flame quench distance. CO is a very high octane fuel; the antiknock index (AKI) is approximately 108 compared to gasoline which has an AKI of 87 to 93. H_2 also has improved knocking resistance because of its high research octane number (RON); however, the main benefit is the its fast burn rate which helps overcome the reduction in flame speed from dilute combustion. The faster burn rate also allows more EGR to be used, which further suppresses knock. The downside to conventional methods of reforming fuel into syngas (external to the engine) is that ~23 percent of the heating value of the fuel is lost in the process through a combination of heat generation (partial oxidation is an exothermic reaction) and increasing entropy (increase in the number of moles due to breaking chemical bonds). Syngas will make the engine more efficient, but the loss in heating value from the fuel offsets much of the benefit from external reforming.

The D-EGR concept is unique in that the engine acts as the reformer. A D-EGR system enables using combustion temperature and pressure to reform fuel by running fuel rich, but without the conventional chemical energy loss associated with rich cylinder operation and thermal losses from external reforming. Specifically, rich combustion in the dedicated cylinder creates the syngas. The difference is that the energy released during combustion is extracted via expansion in the cylinder rather than being rejected to the environment. Therefore, the D-EGR concept realizes all of the efficiency benefits of syngas while reducing the effect of the heating value loss. The result is an engine that can tolerate high rates of EGR and achieve high thermal efficiency.

Previous D-EGR research has primarily focused on four-cylinder gasoline engines, but natural gas engines can also take advantage of the D-EGR concept. There are some differences between using gasoline or natural gas as a fuel. With gasoline as the fuel, the presence of reformate effectively increases the octane of the in-cylinder fuel because the reformate has a higher AKI rating that typical pump grade gasoline. The knock resistance of gaseous fuels is determined through the Methane Number (MN), which is a similar concept to the octane number of a liquid fuel. Pure methane has a MN of 100 by definition whereas hydrogen has a MN of 0. This implies that the presence of H_2 within the reformate may cause the engine to become knock limited with enrichment of the dedicated cylinders. However, it was unknown at the start of the project whether the increased burn rates from H_2 would offset the reduced MN.

Natural gas has a higher octane/methane rating than gasoline, but knock is still a concern with high brake mean effective pressure (BMEP) natural gas engines, in particular with heavy-duty engines where the engines operate at higher loads over both certification cycles and in the field. External cooled EGR (not a D-EGR configuration) can effectively mitigate knock to allow the engine to run at or near maximum brake torque (MBT) ignition timing at all speed and loads.

As external cooled EGR is currently used in modern heavy-duty natural gas engines, the efficiency gains from adding additional EGR is expected to be marginal. Increasing EGR beyond what is needed for knock mitigation can actually lower efficiency, unless compression ratio is increased, combustion speed is improved, or other combustion losses such as heat transfer and combustion inefficiency are addressed. Natural gas burns slower than gasoline, and when the mixture is diluted (such as with EGR), the burn rates can become even slower. Slow burn rates reduce engine efficiency due to added heat losses, increased engine instability, and increased potential for knock. A faster burn rate provided by the hydrogen from the dedicated cylinder(s) can potentially improve efficiency at higher EGR rates. The hydrogen increases combustion speeds, which is more of a problem for natural gas engines than for gasoline engines.

In addition to the combustion advantages, D-EGR offers a potential breathing efficiency advantage. Significant past work has sought to improve the pumping mean effective pressure (PMEP), or the network gain/loss observed during the exhaust and intake strokes, for turbocharged heavy-duty engines. For an efficiently turbocharged engine, it is very possible to achieve positive work out of the pumping loop, or positive PMEP. This is enabled by a turbocharging setup that achieves positive “delta P” or an intake manifold pressure higher than the exhaust manifold pressure. With the advent of higher pressure EGR (HP-EGR), this approach has not been available due to the need to have negative delta P to drive the EGR flow. With D-EGR, it again becomes possible to have a positive delta P on the non-dedicated cylinders and minimal negative delta P on the dedicated cylinders therefore greatly improving engine-average PMEP relative to a HP-EGR approach. As shown in Figure 3, initial quantification of this effect shows a potential 60 kPa advantage which should equate to a roughly 3 percent improvement in fuel efficiency of the engine from the PMEP advantage. SwRI has observed the pumping work reduction during some of its D-EGR investigations; however, it is uncertain if this benefit applies to all engines when D-EGR is applied.

Figure 3: Pumping Work Reduction via Reduced Engine Average Delta Pressure Across Cylinder Head With D-EGR

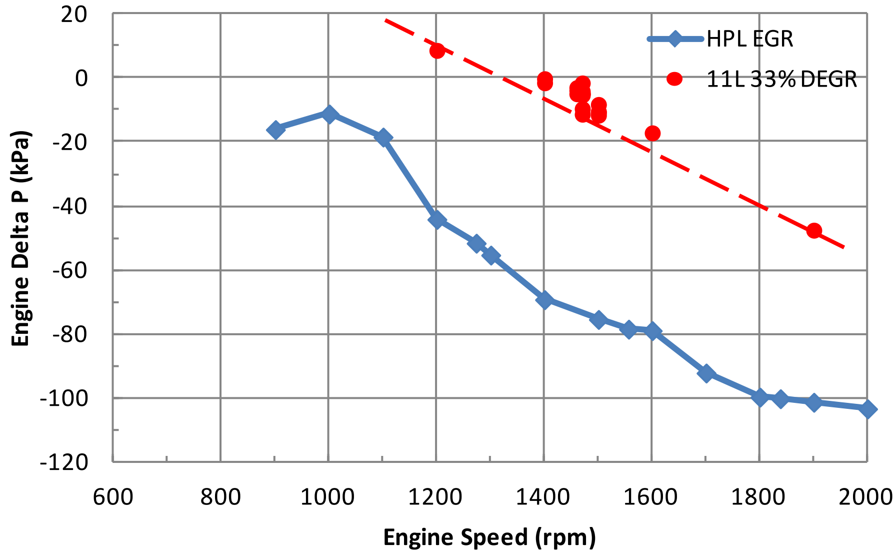

Source: Southwest Research Institute

California Air Resources Board Project Overview

SwRI has previously demonstrated 0.02 g/bhp-hr NOX on the Cummins Westport ISX12 G engine in a project sponsored by the California Air Resources Board, Agreement Number 13-312. The project investigated ultra-low NO_X technologies for both natural gas and diesel engines. The development of the CNG engine platform to meet ultra-low NOx levels was generally more straightforward than the diesel platform. Although a considerable amount of development effort was still required, the fact that the engine was a stoichiometric spark ignition (SI) unit allowed the use of the more mature three-way catalyst (TWC) technology that is capable of very high NO_X reduction, as long as the engine's air-fuel ratio (AFR) can be appropriately controlled.

The primary development efforts on the CNG engine involved:

- Selection of a TWC system from the options provided by the Manufacturers of Emission Controls Association (MECA)
- Implementation of advanced AFR controls in the ISX12 G engine
- Calibration of the AFR controls to achieve maximum performance
- Development of a cold-start warm-up strategy to get the TWC system to light off temperature as quickly as possible

An advanced third-party system produced by E-Controls was installed on the engine. This system used a model-based control approach and employed proprietary injection and mixing hardware. The ISX12 G engine employed a high-pressure loop EGR system, which allowed for control of engine-out NO_X levels. It was essential to ensure very good mixing between air-fuel- and EGR, and this was done via the proprietary mixing hardware that was part of the EControls system. The final catalyst system chosen was a combination of a close-coupled three-way catalyst (ccTWC) and a conventional under-floor TWC (ufTWC), which is similar to configurations used on Tier 2 gasoline light-duty passenger vehicles. Accepted aging methods were used to evaluate the final aftertreatment system over a full useful life.

Table 1 and Table 2 summarize the final tailpipe test results on the CNG Low NO_X demonstration engine using the final aged parts. The results are shown in comparison to results for the Baseline engine before modifications. In general, the results show roughly an order of magnitude reduction in tailpipe NO_X emissions for the Low NO_X engine, as compared to the Baseline. For all regulatory test cycles, tailpipe NO_X emissions were below the 0.02 g/bhp-hr target. In addition, the Low NO_X engine generally showed significantly lower NH_3 and methane emissions, as compared to the Baseline engine. This was generally the result of improved air-fuel ratio control with the Low NO_X engine.

Table 1: CNG Engine NO_X Emissions Comparison
Low NO_X Engine Versus Baseline, g/bhp-hr

Engine	FTP			RMC-SET	WHTC		
	Cold	Hot	Composite		Cold	Hot	Composite
Baseline	0.247	0.093	0.115	0.012	0.310	0.308	0.308
Low NO_X Engine	0.065	0.001	0.010	0.001	0.043	0.006	0.011
% Reduction	74%	99%	91%	92%	86%	98%	96%

Source: Southwest Research Institute, CARB Final Report: Agreement Number 13-312

Table 2: CNG Engine Comparison of Other Emissions
Low NO_X Engine Versus Baseline

Engine	Pollutant	FTP	RMC-SET	WHTC
Baseline	CH_4, g/bhp-hr	0.96	1.20	1.54
	NH_3, avg ppm	76	162	100
	CO_2, g/bhp-hr	542	454	510
Low NO_X Engine	CH_4, g/bhp-hr	0.15	0.93	0.10
	NH_3, avg ppm	52	37	44
	CO_2, g/bhp-hr	547	445	513
% Change from Baseline	CH_4	-84%	-23%	-94%
	NH_3	-32%	-77%	-56%
	CO_2	0.9%	-2.0%	0.6%

Source: Southwest Research Institute, CARB Final Report: Agreement Number 13-312

The CO_2 emissions impact of varied by cycle, but in general there was an increase of about 1 percent on duty cycles which featured a cold-start, due to the impact of the rapid cold-start warm-up strategy. However, this was generally offset by lower methane emissions in terms of overall GHG impact. It should be noted that NH_3 did exceed the program target of 10 ppm cycle average. However, this was due to a shortcoming of the air/fuel ratio (AFR) controller, which did not include an oxygen storage model for the catalysts at the time of development. However, such controls technology is in production on Tier 2 gasoline engines and could be added to a heavy-duty CNG engine given sufficient development time and resources. The resulting improved AFR control would likely result in lower NH_3 emissions.

High Efficiency, Low NO_x Engine Concept

The work presented in this report, as funded by the California Energy Commission, was designed to combine two successful technologies that were separately demonstrated in the past by SwRI. The emissions reduction performance of the CARB demonstration project would be coupled with the efficiency improvement potential of the D-EGR combustion system to develop a more competitive pathway to low achieving low NO_x emissions.

The engine chosen for this project was the Cummins Westport ISX12 G; a 12 L stoichiometric natural gas engine that is available for commercial sale in the California market. This engine is frequently used in heavy-duty truck applications and meets the 2010 heavy-duty NO_X standards as well as the United States Environmental Protection Agency's (USEPA) Phase 1 GHG standards. This was also the engine used in the CARB-funded work to demonstrate lower NO_X emissions. In 2018, Cummins Westport released an updated version of this engine, marketed as the ISX12N, certified to the California Air Resources Board and USEPA's Optional Low NO_X emissions standard of 0.02 g/bhp-hr.

In this project, the Cummins Westport ISX12 G was modified to use the D-EGR configuration. Combustion system development was then performed to increase the compression ratio of the combustion system in order to take advantage of the higher EGR rates. Advanced ignition and turbocharger systems were also identified and integrated into the engine to maximize the air pumping efficiency and the combustion efficiency of the engine.

Project Objectives

The goal of this project was to obtain a 10 percent improvement in fuel consumption over the stock Cummins Westport ISX12 G while demonstrating 0.02 g/bhp-hr NO_X emissions potential. These goals were achieved through the following objectives:

- Extend dilution limit using advanced ignition systems.
- Extend dilution limit and reduce heat transfer losses through combustion system development.
- Increase compression ratio as much as possible.
- Reduce pumping work through optimization of turbocharger hardware and EGR delivery method.

This report details the technical accomplishments of the project, the final demonstration results, and the potential benefits to California ratepayers if these technologies can be successfully commercialized and made available to California's bus and truck operators.

CHAPTER 2: Project Approach

Project Plan

At the start of the project, SwRI® developed a detailed project plan to improve the overall engine efficiency using a systems engineering approach. A conceptual view of the project plan is shown in Figure 4. The project plan focused on improving the engine efficiency and demonstrate low NO_X potential using methodologies developed by SwRI in a previous project for CARB that demonstrated 0.02 g/bhp-hr NO_X on the Cummins Westport ISX12 G.

Figure 4: Conceptual Project Plan

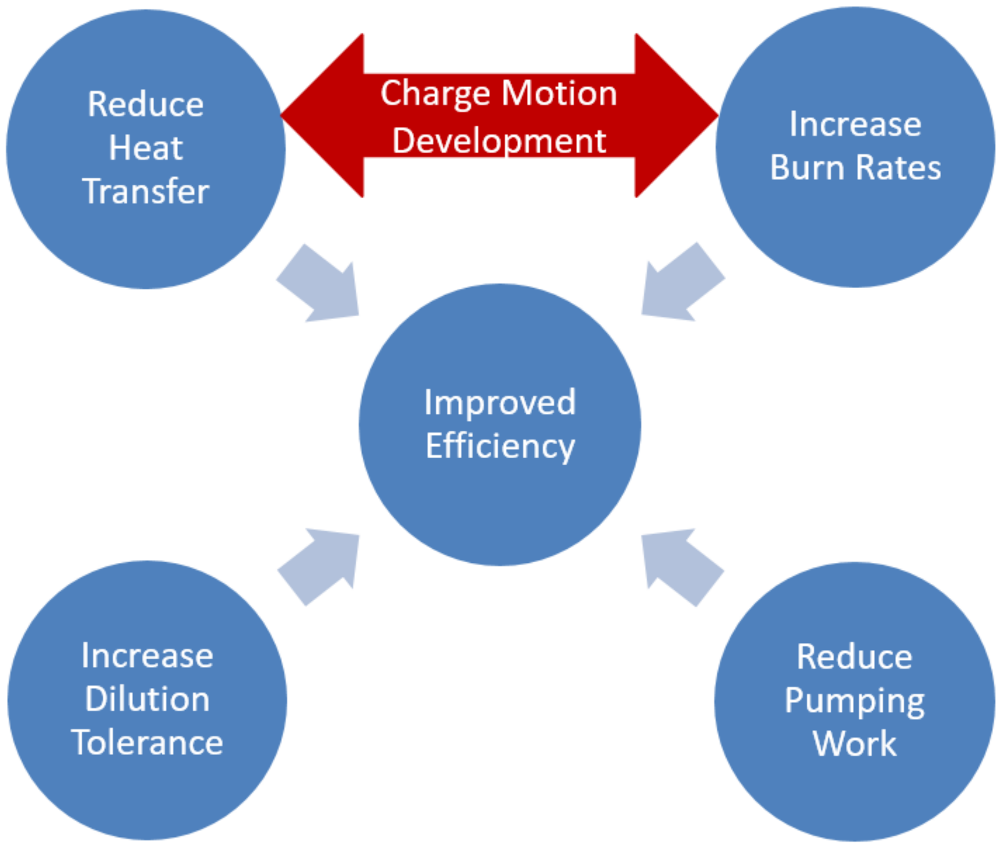

Source: Southwest Research Institute

Engine Testing

The test engine was installed into a development test cell and was be instrumented with cylinder pressure sensors for combustion analysis, Micro Motion fuel flow meter, Horiba emissions bench and other instrumentation necessary to monitor engine operation. A stock engine control unit was used to acquire the baseline engine data. An open development engine control unit (ECU), provided by Woodward Inc., was used to explore the dilution tolerance and rich limit of the engine. A development ECU was necessary during this phase as it allowed for various parameters to be easily modified while the engine is running. A development ECU also provided the flexibility needed to operate prototype ignition systems. A set of three-way catalysts with the same configuration as the CARB Low NO_X project was installed during all engine operation, unless there was potential to damage the catalyst during development. The CARB project utilized a 9 L close-coupled catalyst installed approximately 0.5 meters from the turbine outlet and a 20 L underfloor catalyst installed approximately 2 meters from the turbine outlet.

The engine performance was compared over the ramped mode cycle supplemental emissions test (RMC SET) points as well as peak torque and peak power. For compression ratio selection, peak torque usually determines the maximum compression ratio allowable as that is the most knock prone condition. Therefore, the early development process focused on maximizing the dilution tolerance at peak torque using the different ignition system options. It was important however, to understand the balance between the performance at peak torque, peak power and part load conditions. Should the turbocharger be sized to optimize peak torque performance only, which usually means a small turbine housing, peak power may become the knock limited condition because of the high back pressure trapping hot residuals in the combustion chamber.

Engine hardware was modified based upon the results from the air handling and combustion system development tasks. Combined with the best ignition system, the remaining engine testing focused on optimizing the calibration for best fuel economy and lowest tailpipe out emissions. To verify the engine’s potential to achieve a 0.02 g/bhp-hr NO_X emission level, SwRI had to develop a custom cold-start cycle because the changes to the engine hardware prevented the development ECU from controlling the engine on a transient test cycle. This data was compared to the CARB Low NO_X project results.

Air Handling System Development

Baseline engine data was used to construct a validated GT-Power model. The model was modified using inputs from further engine testing and computational fluid dynamics (CFD) modeling to represent the expected final hardware solution. The model utilized a proprietary knock sub-model in order to determine the maximum compression ratio that can be used without the engine knocking at full load. Working with Garrett, advanced pre-production boosting solutions were investigated to size a new turbocharger with the goal of meeting the baseline torque curve with reduced pumping work.

Combustion System Development

SwRI modeled the combustion system using a combination of reactive and non-reactive flow simulations using advanced CFD software packages combined with proprietary reaction mechanisms and ignition models developed in the High Efficiency Dilute Gasoline Engine (HEDGE®) Consortium. During the engine baseline task, data was acquired that served to develop the baseline flow model. Modifications to the piston were made with the goal of designing a combustion system that improved dilution tolerance and maintained burn rates with a reduced squish area ratio, thereby reducing heat transfer losses.

Base Engine

The base engine selected for this project was the Cummins Westport ISX12 G. The specifications of the engine are shown in Table 3. In 2018, Cummins Westport released an updated version of this engine, marketed as the ISX12N, certified to the California Air Resources Board and USEPA Optional Low NOx emissions standard of 0.02 g/bhp-hr.

Table 3: Cummins Westport ISX12 G Engine Specifications

Parameter	Units	Value
Displacement (L)	L	11.9
Bore x Stroke (mm)	mm	130 x 150
Rated Power	kW	293
Rated Speed	rpm	1699
Peak Torque	Nm	2098
Peak Torque Speed	rpm	1200
Fuel System	-	Compressed Natural Gas
Turbocharger	-	Fixed Geometry
EGR System	-	Cooled, high pressure
Emission Certification	-	US 2010 (0.2 g/bhp-hr NOx)
Application	-	Regional-haul, truck/tractor, vocational, and refuse

Source: Southwest Research Institute

To obtain the 10 percent fuel economy improvement, the following brake thermal efficiency targets were initially set as shown in Table 4.

Table 4: Baseline Efficiency and Improved Efficiency Targets

Engine Test Condition	Engine Speed (rpm)	Torque (N-m)	BSFC* (g/kW-hr)	BTE Baseline (%)	BTE Target (%)
A100	1272	2012	178	36.6	40.3
A75	1272	1509	177	36.8	40.5
A50	1272	1005	185	35.4	38.9
A25	1272	503	222	29.4	32.3
B100	1555	1791	180	36.3	39.9
B75	1554	1345	180	36.3	39.9
B50	1554	897	193	33.9	37.3
B25	1554	452	234	27.9	30.7
C100	1836	1494	186	35.0	38.5
C75	1836	1124	190	34.4	37.8
C50	1836	752	207	31.5	34.7
C25	1836	372	265	24.7	27.2
Peak Torque	1200	2098	200	37.6	40.7
Peak Power	1699	1648	203	35.4	39.3
Idle	700	65	605	12.0	13.2

***Using 49.6 MJ/kg LHV fuel.**

Source: Southwest Research Institute

These targets were based upon a 10 percent improvement for every modal point to provide an indication of overall improvement during the development process. The final efficiency improvement is determined by a weighted average using the steady state weighting factors for the Heavy-Duty Supplemental Emissions Test. Several components of the engine were assessed for their contributions to the improvements in engine efficiency to achieve these targets. The major components that were investigated include:

- Ignition systems
- Combustion chamber configurations
- Compression ratio of the engine
- Optimization of the turbocharger hardware
- EGR delivery method

Overview of Research and Development Tasks

Combustion System Evaluation

The baseline engine performance was measured using the stock engine controller and calibration. The EGR rate was varied to understand the limitations of the base engine at elevated dilution levels. The fuel used for baseline engine operation consisted of approximately 96.9 percent methane (CH_4) and 2.7 percent ethane (C_2H_6) (balanced with trace gasses) with a lower heating value of 49.63 MJ/kg.

Figure 5 shows the baseline engine's BTE, including extra test points.

Figure 5: ISX12 G Baseline BTE

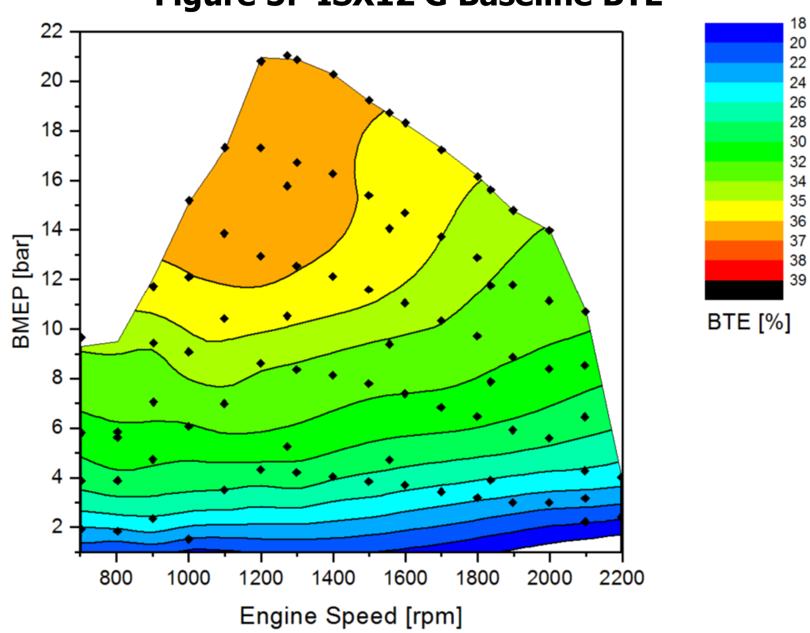

Source: Southwest Research Institute

The peak efficiency occurs at peak torque due to the compression ratio being selected to maintain combustion phasing near MBT timing as shown in Figure 6. A slight combustion phasing retard from MBT (~7 degrees) is observed at peak torque. The losses associated with this combustion phasing retard are likely offset by the ability to utilize a slightly higher compression ratio (CR) than if MBT timing was required.

Figure 6: ISX12 G Baseline Combustion Phasing (CA50)

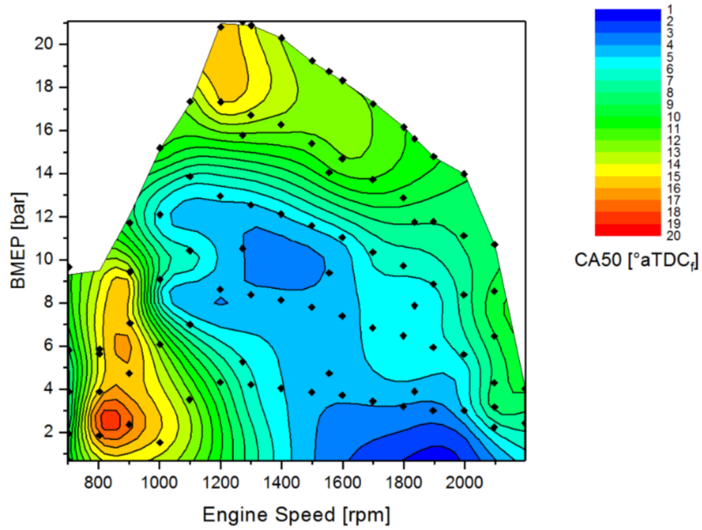

Source: Southwest Research Institute

The baseline engine calibration utilizes 15-20 percent high pressure EGR (HP-EGR) for emissions control and efficiency purposes (Figure 7). With HP-EGR, the turbine is undersized to provide the driving force to flow EGR. This can lead to high pre-turbine pressure, as shown in Figure 8, and therefore high pumping work as the pre-turbine pressure is always higher than the intake manifold pressure.

Figure 7: ISX12-G Baseline EGR Rate

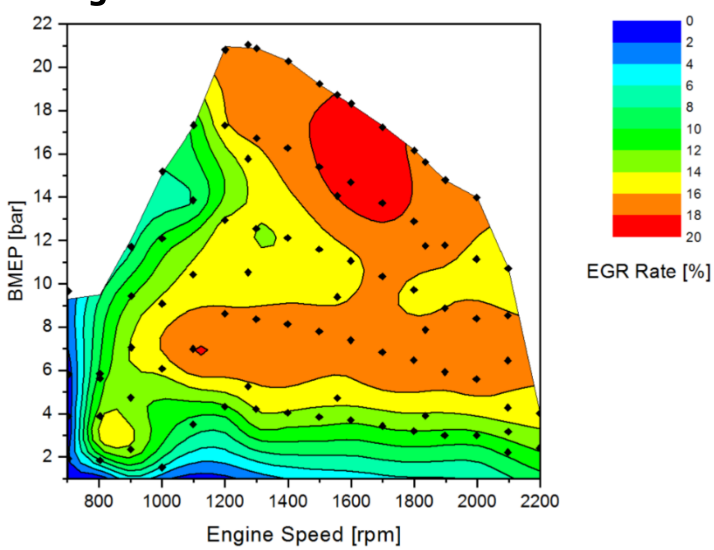

Source: Southwest Research Institute

Figure 8: ISX12-G Baseline Pre-Turbine Pressure

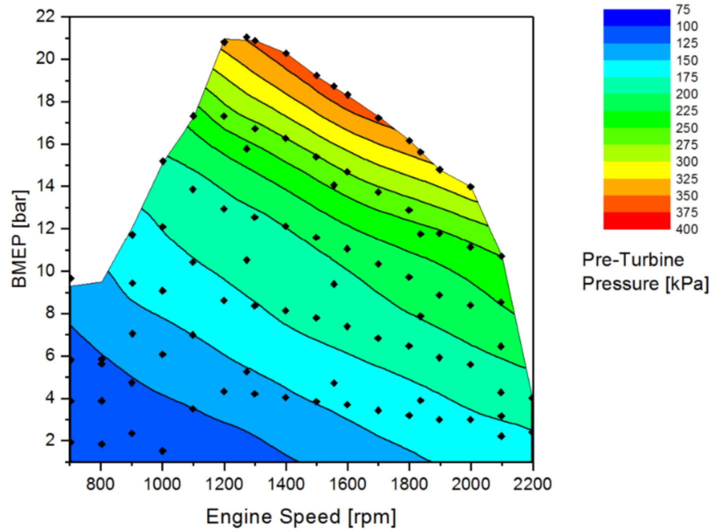

Source: Southwest Research Institute

To determine the engine's dilution tolerance, the HPEGR valve was opened to increase EGR rate from 0 percent to the maximum possible at the speed and load condition. The maximum EGR rate was determined by either the physical flow limit or when the engine reached a combustion stability limit. The combustion stability limit was defined as the coefficient of variation of the gross indicated mean effective pressure (CoV gIMEP) greater than 5 percent. Ignition timing was set individually for each cylinder. Data was collected at varying EGR rates until the combustion stability limit was reached.

Along the torque curve, pre-turbine pressures are high and the system achieves a maximum EGR rate typically around 16-18 percent. At this EGR rate, the engine is normally not at the combustion stability limit. The EGR rate can be increased by throttling the intake to reduce manifold pressure, which increases the pressure differential. However, this also reduces the load the engine is able to achieve as air flow is reduced. The team decided that once maximum EGR flow was reached, fuel enrichment would be increased across all cylinders until the stability limit is reached. This would give some insight as to what level of enrichment the dedicated cylinders could potentially achieve.

Table 5 shows the dilution tolerance results. The B and C speeds reached the combustion stability limit with EGR dilution alone and did not require fuel enrichment. The average maximum EGR rate across the eight points was 19 percent. The EGR dilution tolerance results for the A speed points show that the combustion stability limit was not reached with EGR dilution alone and required fuel enrichment. The average maximum EGR rate across the four points was 19 percent.

Table 5: Maximum Dilution Level for Modal Points

Modal Point	Maximum EGR [percent]	Equivalence Ratio [-]	Modal Point	Maximum EGR [percent]	Equivalence Ratio [-]	Modal Point	Maximum EGR [percent]	Equivalence Ratio [-]
A100	14	1.11	B100	16	1.02	C100	17	1.02
A75	22	1.10	B75	19	1.02	C75	18	1.00
A50	18	1.19	B50	21	1.00	C50	19	1.00
A25	23	1.04	B25	21	1.00	C25	19	1.00

Source: Southwest Research Institute

Boosting System Development

The conversion to the D-EGR configuration significantly impacted the selection of the turbocharger utilized to achieve the desired torque curve. The increased EGR rate pushes the compressor into a higher pressure ratio operating region which can cause compressor surge. As the dedicated cylinders effectively act as an EGR pump, sizing the turbine for EGR flow rate is no longer a consideration. This allows for more optimal turbine matching for efficiency improvements. However, the D-EGR configuration reduces the energy to the turbine, which needs to provide additional energy to operate the compressor at a higher pressure ratio. Further details of the mechanical conversion to D-EGR are provided in Appendix A. To select a turbocharger that can achieve the desired torque curve and reduce pumping work, the team created a one-dimensional engine simulation using GT-Power. The GT-Power model was calibrated to baseline engine data, including knock prediction, and was then modified to D-EGR configuration.

Due to the long lead time associated with procuring a prototype turbocharger, the initial airflow requirements were predicted using the GT-Power model before the model could be calibrated to engine data in D-EGR configuration. Additionally, the stock turbocharger maps were replaced with simple compressor and turbine models. The assumed compressor and turbine efficiencies were determined based upon SwRI's and Garrett's experience with next generation turbocharging hardware. Combustion was assumed to be at MBT phasing and a constant duration consistent with advanced ignition systems. The compression ratio was increased to 12.5:1 and the MBT phasing assumption was later validated once the calibrated knock model was available. The model was run targeting the stock torque curve and the results were provided to Garrett for initial map selection.

Garrett used the provided airflow data to screen available turbine and compressor maps that can be assembled into a new unit. The team did not expect an off-the-shelf unit to achieve the target performance requirements because the turbine is missing two cylinders worth of flow in D-EGR configuration. Two solutions were identified that had the potential to achieve the desired torque with both requiring prototype wheels to be manufactured. Garrett provided the map data to input into GT-Power to select the primary unit choice. Figure 9 show the maps for the GT3571V unit, which uses a variable geometry turbine (VNT) mechanism to control the power produced by the turbine. Figure 10 shows the GT3067 unit, which uses a traditional wastegate mechanism.

Figure 9: VNT Turbocharger (GT3571V) Turbine and Compressor Map

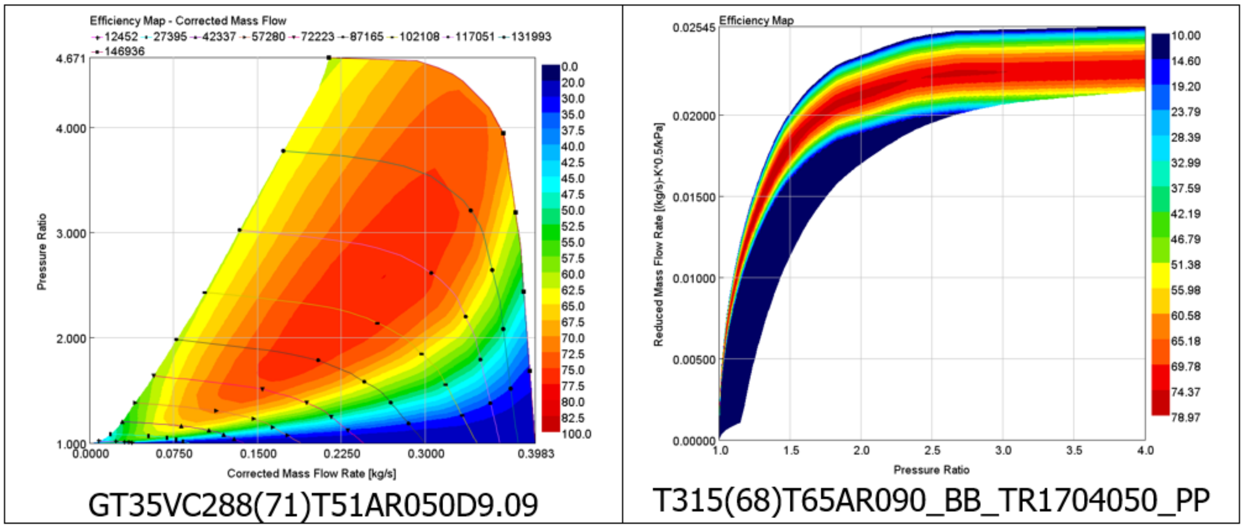

Source: Southwest Research Institute

Figure 10: Wastegate Turbocharger (GT3067) Turbine and Compressor Map

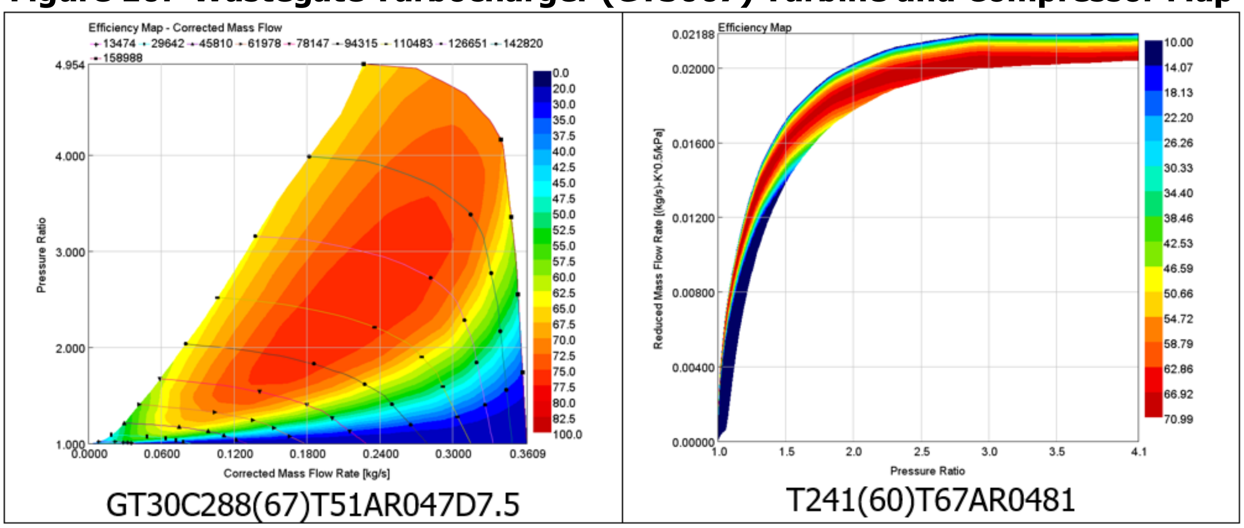

Source: Southwest Research Institute

The map data was input into GT-Power to replace the simple turbine and compressor models. Figure 11 shows the predicted performance of the two turbochargers along the torque curve. The VNT turbocharger achieved the desired torque at all the engine speeds whereas the wastegate turbocharger could only achieve the desired load at speeds above 1200 rpm. The VNT had some operational margin with the VNT mechanism at lower engine speeds while the wastegate was fully closed below the peak torque speed. The simulations also predicted lower fuel consumption, primarily through lower pumping work, with the VNT turbocharger. As the VNT turbocharger has wider operational margin and lower fuel consumption, the team selected the VNT turbocharger as the primary turbocharger for physical engine testing. Further details of the one-dimensional modeling and turbocharger selection are provided in Appendix B.

Figure 11: Predicted Torque Curve Performance with VNT and Wastegate Turbocharger

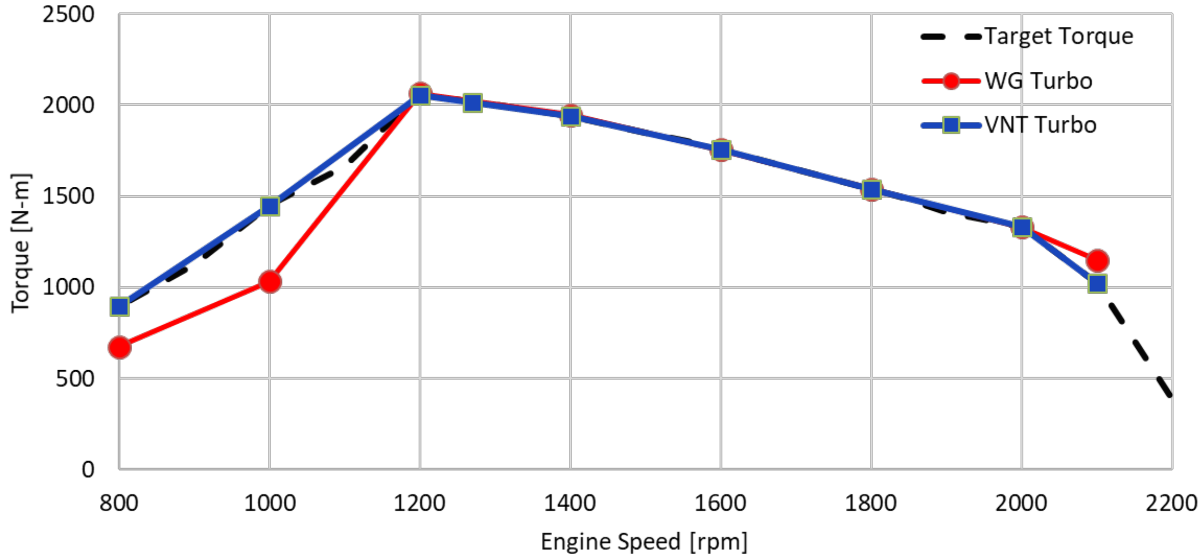

Source: Southwest Research Institute

Piston Development

A 3D computational fluid dynamics tool was used to develop the increased compression ratio piston design. The stock piston had a re-entrant bowl design with a high squish area ratio of 0.8. This piston design is carried over from the base diesel engine and offers significant areas for optimization with a dedicated piston design for natural gas combustion. The following section summarizes the development process, details are provided in Appendix C. The evolution of the piston design is shown in Figure 12.

Figure 12: Piston Design Modifications

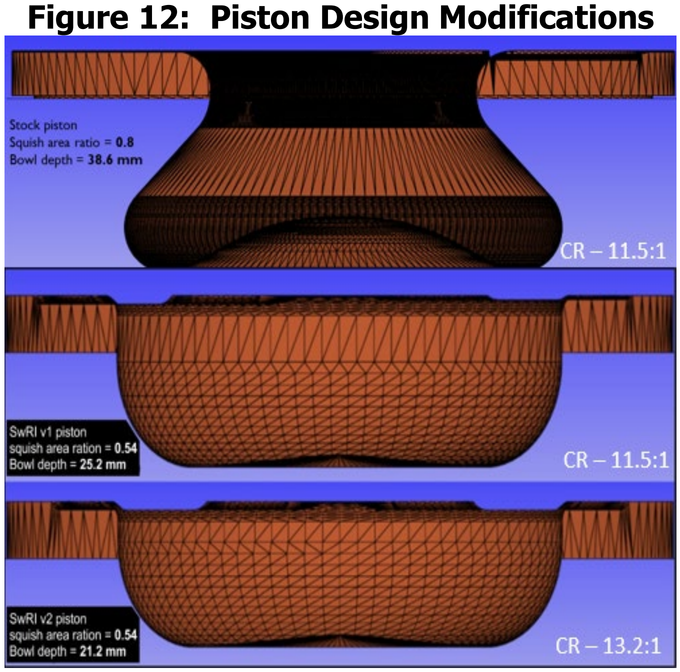

Source: Southwest Research Institute

The first iteration (SwRI v1) was a more open bowl piston design. The squish area ratio was decreased from 0.8 to 0.54 while maintaining the same clearance from the top of the piston to the head. To maintain the stock compression ratio, the bowl depth was reduced by 13.4 mm. The stock engine had fast burn rates due to the high level of squish. A decrease in burn rates, especially during the early flame kernel formation period, may negatively impact EGR tolerance. The results in Figure 13 show that the burn rates were maintained with the reduced squish piston design.

Figure 13: Apparent Heat Release Rate Comparison for SwRI v1

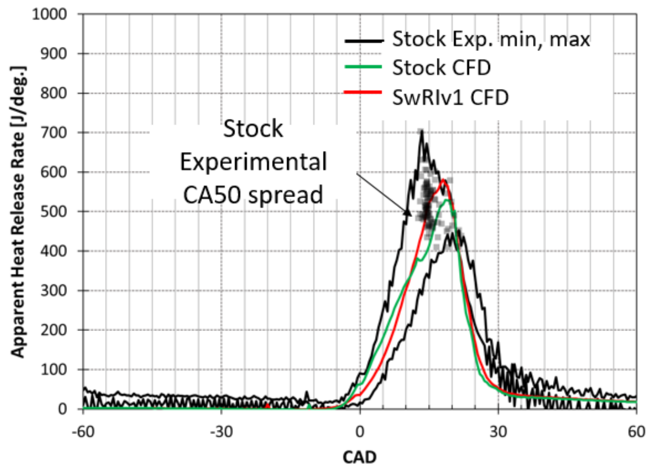

Source: Southwest Research Institute

Results from the GT study suggested that 12.5:1 was an achievable compression ratio when using the baseline combustion phasing. Considering that the baseline calibration was near MBT phasing at peak torque, further drive cycle efficiency improvements could be achieved by increasing compression ratio beyond 12.5:1 and allowing for some spark retard at peak torque. The increase in compression ratio was achieved by reducing the bowl depth to 21.2 mm while maintain the SwRI v1 squish area ratio of 0.54. The removal of the valve pockets necessary for engine braking resulted in a final compression ratio of 13.2:1 (SwRI v2 design). An analysis of the CFD results was performed to ensure that the compression ratio was achievable before the pistons were machined (shown in Figure 14). Engine testing confirmed that 13.2:1 was not too high as the combustion phasing at high loads was near MBT, Figure 15.

Figure 14: Machined SwRI v2 Piston

Source: Southwest Research Institute

Figure 15: Combustion Phasing for Optimum Configuration at High Loads – Engine Test Results

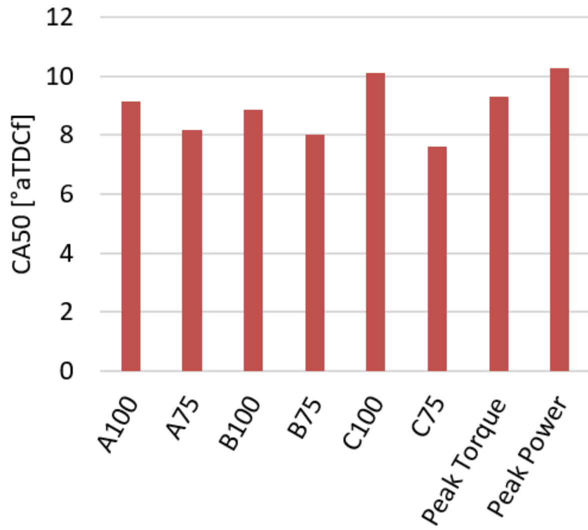

Source: Southwest Research Institute

Ignition System Evaluations

A key enabler of the targeted efficiency improvement was higher levels of EGR resulting from the D-EGR configuration. Operating a natural gas engine with high levels of dilution is especially challenging owing to the inherently slow laminar burning velocity of natural gas, which is further slowed with the addition of dilution. This leads to combustion stability challenges at high EGR dilution levels. A robust ignition system is required to operate the engine with stable combustion at high EGR rates. SwRI evaluated three advanced ignition systems and ranked for their potential to effectively operate at high EGR rates. The three ignition systems were SwRI's Dual Coil Offset (DCO) ignition system (a continuous discharge design) and two pre-chamber designs provided by Woodward (pre-chamber spark plug and Advanced Fast Ignitor with larger pre-chamber volume). Appendix D provides more details on the ignition system evaluation.

With the DCO system and stock pistons, the dilution tolerance was extended, and the engine could run at the full D-EGR rate and achieve between 5 and 40 percent dedicated cylinder enrichment. However, the SwRI v2 pistons had reduced EGR tolerance compared to the stock pistons and required bleeding off EGR at the B and C speeds, though the overall EGR rate was increased over the baseline with the DCO system. The EGR dilution tolerance for both pre-chamber designs showed marginal improvement over the baseline. The Advanced Fast Ignitors showed diesel-like stability with CoV gIMEP of ~0.6 percent and marked improvement in combustion duration over the baseline at the same EGR level. This led to similar brake thermal efficiency as the DCO system with a lower EGR rate, as shown in Figure 16. However, both pre-chamber systems experienced similar issues: pre-ignition, narrow ignition timing authority for stable combustion, low EGR tolerance, and misfires at EGR rates below the 33 percent EGR target. Neither pre-chamber system successfully operated at full load conditions as the EGR tolerance was not high enough to mitigate the pre-ignition. Even though the Advanced Fast Ignitors showed high efficiency potential, further refinement of the design to the specific combustion chamber is required to fully realize the potential. Therefore, the DCO ignition system with stock J-gap plugs was chosen as the optimal ignition system.

Figure 16: Best BTE points for DCO and Advanced Fast Ignitor

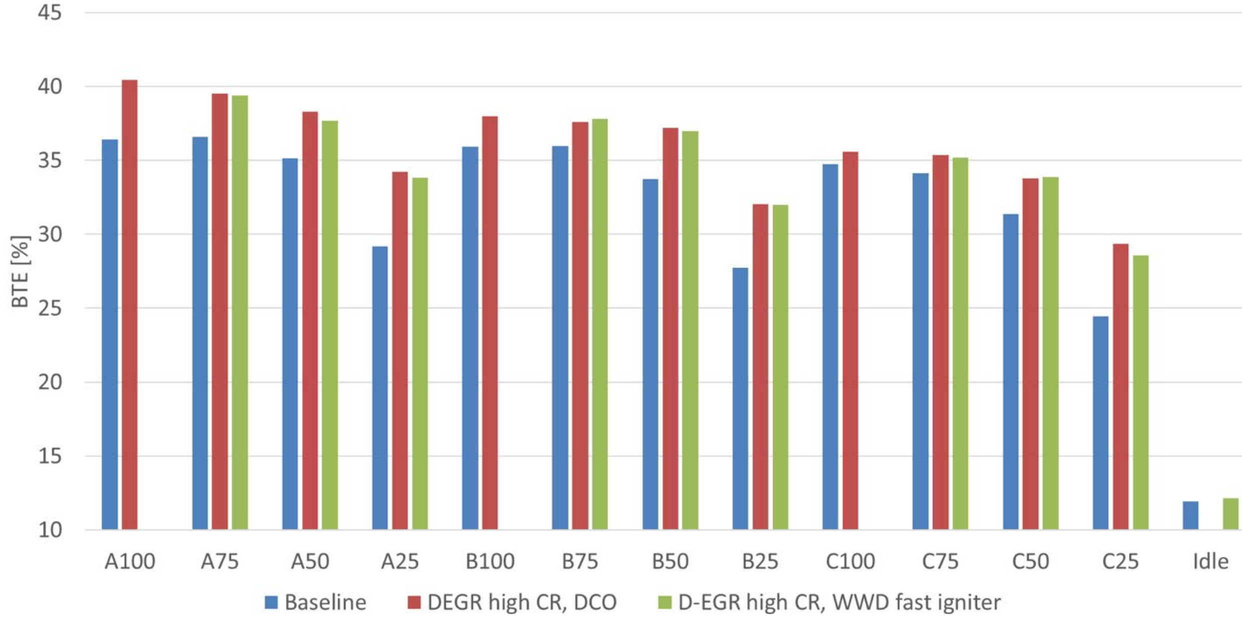

Source: Southwest Research Institute

CHAPTER 3:
Project Results

Optimal Engine Configuration

Table 6 summarizes the final optimum engine configuration that resulted from this study. The EGR delivery method was changed to a D-EGR configuration where two of the six cylinders were used for EGR production, as shown Figure 17. This arrangement allowed for higher EGR delivery than the baseline HP-EGR configuration due to the EGR generating cylinders acting as EGR pumps. A bypass was installed to reduce the EGR rate when necessary to maintain stable combustion. A high-energy Dual Coil Offset (DCO®) ignition system was utilized to extend the EGR tolerance of the engine. Increasing external EGR aided with knock mitigation allowing the compression ratio to be increased to 13.2:1. The stock pistons were replaced with a shallow-bowl and low squish area design to reduce heat transfer losses. A prototype variable geometry turbine (VNT) turbocharger was provided by Garrett to achieve the baseline toque curve while reducing pumping losses.

Figure 17: D-EGR Conversion Schematic

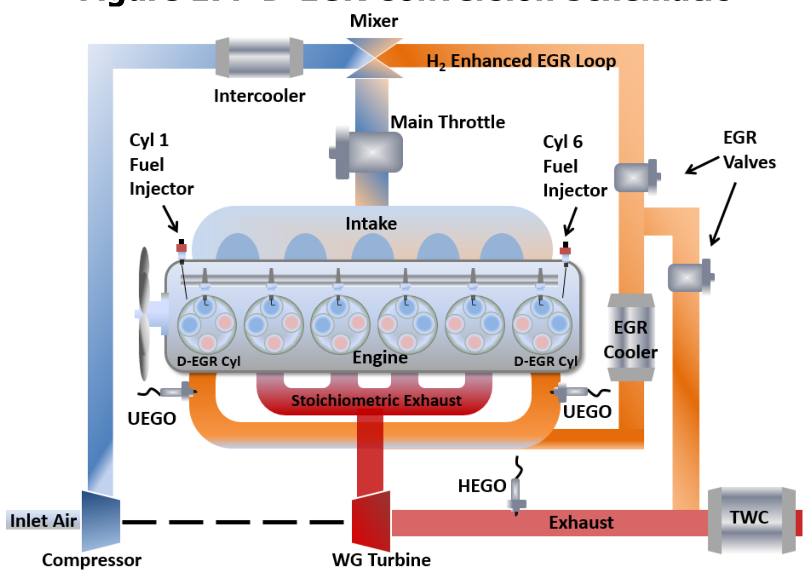

Source: Southwest Research Institute

Table 6: Optimum Engine Configuration

EGR Delivery Method	D-EGR with EGR Bypass (15-25 percent EGR)
Ignition System	Dual Coil Offset (DCO®) (continuous discharge system)
Turbocharger	Garrett prototype Variable Geometry Turbocharger (VNT)
Piston Design	SwRI v2
Bowl Design	Open Bowl
Squish Area Ratio	0.54
Compression Ratio	13.2:1

Source: Southwest Research Institute

Engine Improvement Summary

To ensure that the efficiencies of the baseline and optimal engine configurations can be fairly compared, the overall engine performance must be similar. The high level of EGR dilution desired creates a boosting challenge. The mass flow across the engine is higher with increased EGR (using the intake and exhaust manifolds as the boundary conditions). To maintain a constant load with stoichiometric air fuel ratio, the compressor must be operated at a higher pressure ratio. Further adding to the challenge, the D-EGR configuration removes two cylinders worth of energy and mass flow to the turbine. Using GT-Power model results, a prototype VNT turbocharger was selected to achieve a similar torque curve to the baseline engine. As can be observed in Figure 18, the optimum configuration achieved a similar maximum torque curve to the baseline engine. The ~20 Nm deficiency at the peak torque speed can be overcome with refinement of the turbocharger match and does not impact the ability to fairly compare engine efficiency.

Figure 18: Torque Curve Comparison between the Stock Baseline and Optimum Engine Configuration

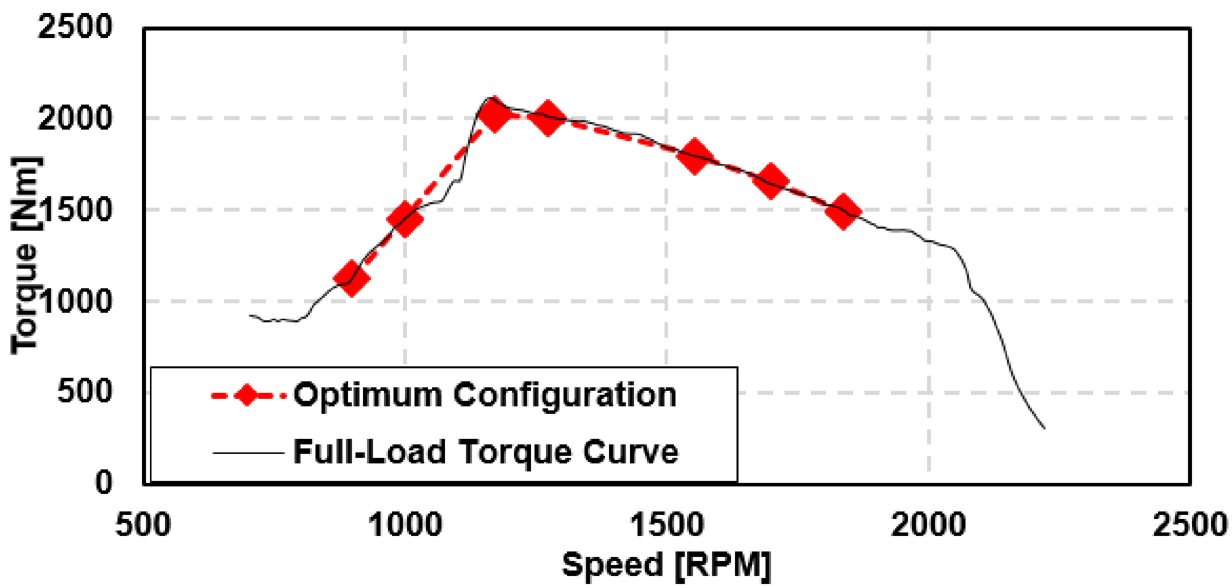

Source: Southwest Research Institute

Figure 19 shows a visual comparison of BTE using the numerical values provided in Table 7. The optimum engine configuration achieved the target BTE at all test points and exceeded the targets in some instances.

Figure 19: BTE Comparison at Test Modal Points Comparing the Baseline and Optimum Configuration with the Program Specified BTE Targets

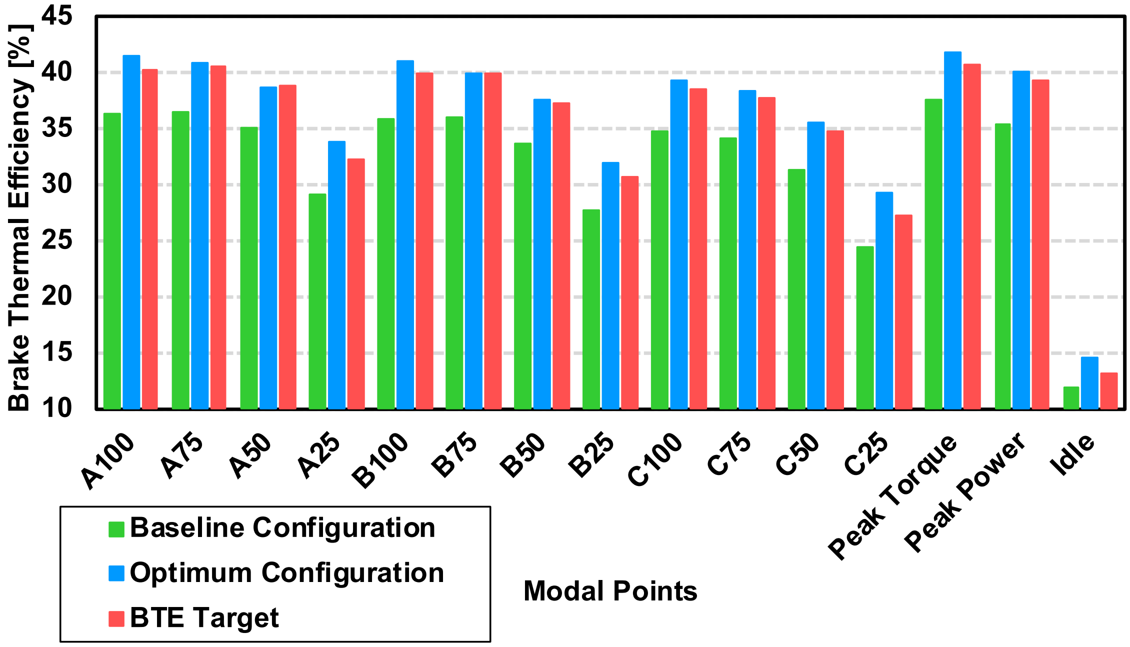

Source: Southwest Research Institute

Table 7: Comparison of Baseline, Optimum Configuration and Target Efficiency

Point	Baseline BTE [%]	Optimum Config. BTE [%]	Target BTE [%]
A100	36.41	41.52	40.3
A75	36.56	40.83	40.5
A50	35.15	38.73	38.9
A25	29.17	33.79	32.3
B100	35.94	41.02	39.9
B75	35.95	39.90	39.9
B50	33.72	37.53	37.3
B25	27.72	31.90	30.7
C100	34.76	39.29	38.5
C75	34.14	38.30	37.8
C50	31.36	35.54	34.7
C25	24.46	29.26	27.2
Peak Torque	37.60	41.73	40.7
Peak Power	35.41	40.15	39.3
Idle	11.92	14.15	13.2

Source: Southwest Research Institute

RMC-SET weighting was applied to the modal points to determine an average overall improvement in the engine BTE over baseline. Table 8 shows the RMC SET weighting factors. Weight A represents the original weights (identical to those of the European Stationary Cycle). Weight B factors were developed to account for the down speeding trend in the heavy-duty engine and are typically used for testing of engine CO_2 emissions for the purpose of

USEPA Phase 2 GHG emission standards. Weight A factors continue to be used for the purpose of criteria pollutant (CO, HC, NO_X, PM) emission testing.

Table 8: RMC SET Weighting Factors

Mode	Speed	Load [percent]	Weight A [percent]	Weight B [percent]
1	idle	0	15	12
2	A	100	8	9
3	A	75	5	12
4	A	50	5	12
5	A	25	5	12
6	B	100	9	9
7	B	75	10	10
8	B	50	10	10
9	B	25	10	9
10	C	100	8	2
11	C	75	5	1
12	C	50	5	1
13	C	25	5	1
		TOTAL	**100**	**100**
		Total A Speed	23	45
		Total B Speed	39	38
		Total C Speed	23	5

Source: DieselNet

Figure 20: RMC SET Cycle Weighted BTE

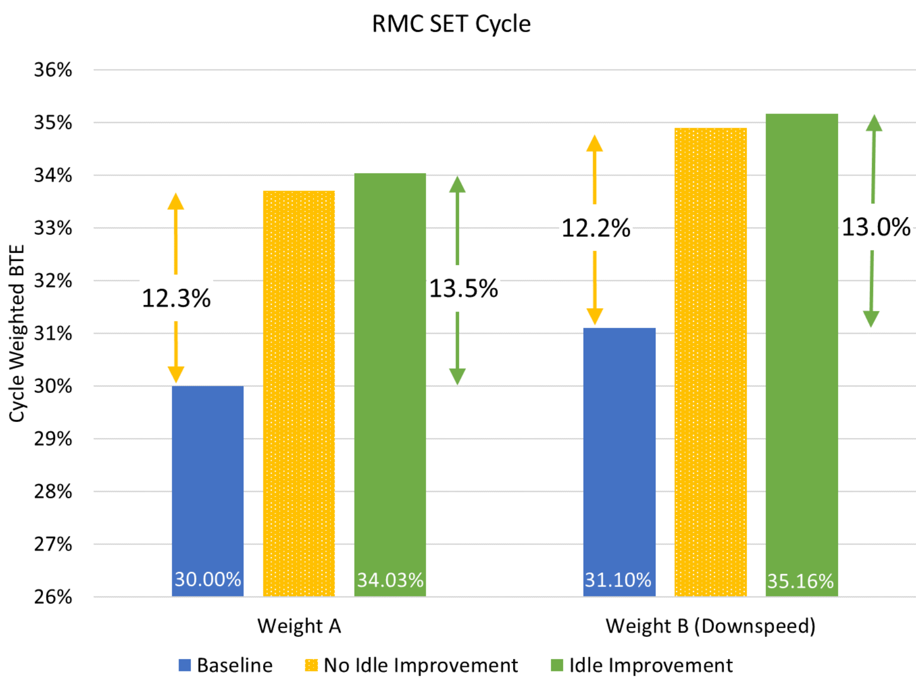

Source: Southwest Research Institute

The optimum engine configuration showed a weighted improvement of 13.5 percent for weight A and 13.0 percent for weight B as shown in Figure 20. In a light-duty gasoline engine, D-EGR can take significant advantage of down speeding owing to the improved combustion phasing allowed by the reformate in addition to the typical down speeding benefits of reduced pumping work and reduced friction. Due to heavy-duty natural gas engines being calibrated for near MBT combustion phasing at peak torque, the D-EGR engine could not provide the additional combustion phasing benefit, hence the lower relative improvement with Weight B. It must be pointed out that the idle point efficiency is sensitive to changes in load and calibration for catalyst performance. SwRI believes that at this load, the engine can exhibit a range of BTE values between the baseline of 11.92 percent and the recorded BTE for the optimized case of 14.15 percent, depending on the calibration strategy used. This factor was taken into consideration by assuming an idle efficiency for the optimum case equal to that of the baseline case (11.92 percent). With that in consideration, the overall adjusted weighted improvement over baseline was 12.3 percent for Weight A and 12.2 percent for Weight B. As can be observed, the idle point is heavily weighted in both approaches A and B, and smaller changes in BTE at the idle point can affect the overall weighted improvement. Assuming the worst-case scenario for idle point efficiency, SwRI was still able to meet the program's efficiency goal. When applied to the CARB Low NO_X baseline data, the RMC SET CO_2 can be reduced from 454 g/bhp-hr to ~390-400 g/bhp-hr. On the Heavy-Duty FTP the efficiency improvement is expected to reduce cycle CO2 from 542 g/bhp-hr to ~470-480 g/bhp-hr.

Sources of Efficiency Improvement

Figure 21 shows the calibrated EGR rate for the optimal configuration, which is significantly higher compared to the baseline configuration.

Figure 21: EGR Comparison between the Baseline and Optimum Configuration

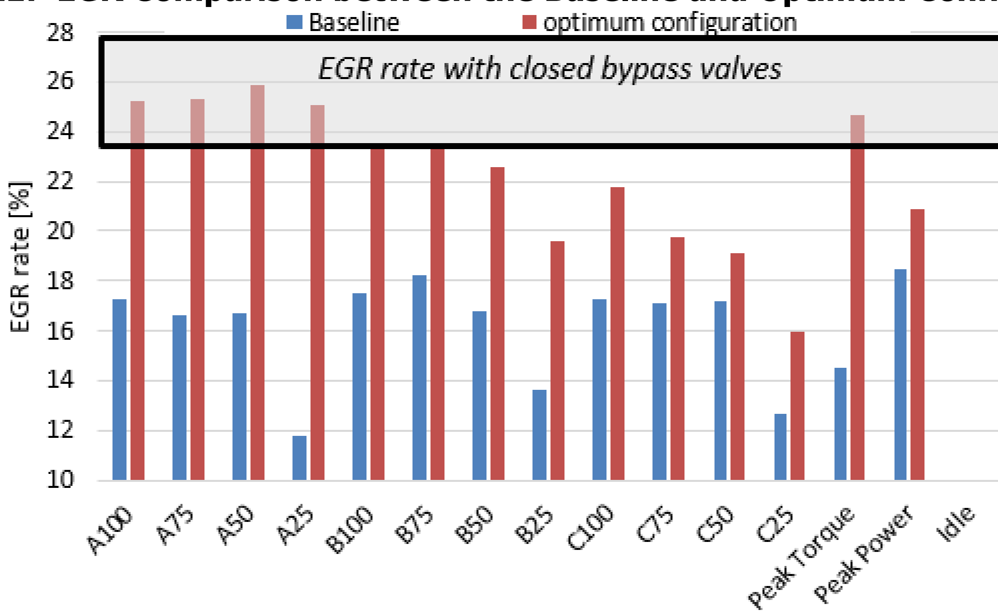

Source: Southwest Research Institute

This was partly due to the EGR delivery method allowing for higher EGR rates, but also due to the increased dilution tolerance provided by the DCO ignition system. As the EGR was below full D-EGR operation at the B and C speeds, no enrichment was used in the dedicated cylinders to allow for stoichiometric conditions at the three-way catalyst. The increased EGR rate and EGR delivery method has many implications for improved engine efficiency, including enabling an increased compression ratio, improvement in pumping efficiency, and reductions in heat transfer losses.

Increased Compression Ratio

The addition of high levels of EGR has the effect of reducing knock in SI combustion by lowering combustion temperatures. This allows the compression ratio to be increased, therefore improving the ideal efficiency of the engine. Results from a GT-Power study suggested that 12.5:1 was an achievable compression ratio when using the baseline combustion phasing. Considering that the baseline calibration was near MBT phasing at peak torque, further drive cycle efficiency improvements could be achieved by increasing compression ratio beyond 12.5:1 and allowing for some spark retard at peak torque. The increase in compression ratio was achieved by reducing the piston bowl depth to 21.2 mm while reducing the squish area ratio to 0.54. The removal of the valve pockets necessary for engine braking resulted in a final compression ratio of 13.2:1. Prior to machining the new pistons (SwRI v2 design), the piston design was simulated using CFD to confirm similar knock characteristics to the baseline piston design to ensure excessive knock would not be present. Engine testing confirmed that 13.2:1 was a feasible compression ratio as the combustion phasing at high loads was near MBT combustion phasing (5-10 °aTDC), Figure 15. By raising the compression ratio 1.5 points, the ideal Otto Cycle efficiency is improved from 54.2 percent to 56.2 percent using an assumed specific heat ratio of 1.32.

The baseline ISX12 G was designed for fuels with a minimum methane number of 75. To ensure that this requirement could still be met with the optimal engine configuration, bottled ethane was fed into the intake system using a separate fuel system. Testing was conducted with up to 20 percent ethane, which resulted in a methane number of approximately 76. Peak torque was able to be achieved with only three degrees of combustion phasing (CA50) retard required to maintain the same knock characteristics. Figure 22 shows that while combustion phasing was only slightly retarded, the ignition timing was retarded significantly. This is due to the faster laminar burning velocity of ethane compared to methane.

Figure 22: Key Locations of Combustion with Varying MN at Peak Torque

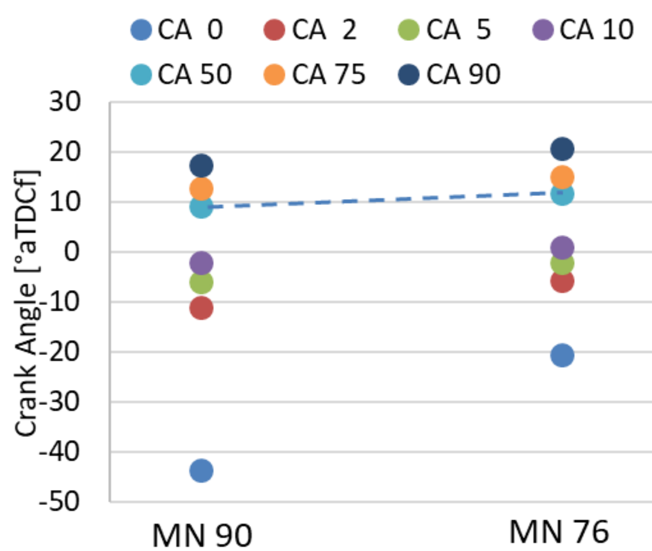

Source: Southwest Research Institute

Pumping Work Improvement

The combination of increased EGR rate, EGR delivery method and VNT turbocharger resulted in significant pumping work improvements. Figure 23 shows that pumping work was reduced at all the modal points. The B100 point shows over a 50 percent reduction.

Figure 23: Pumping Work Differences between Baseline and Optimal Configuration

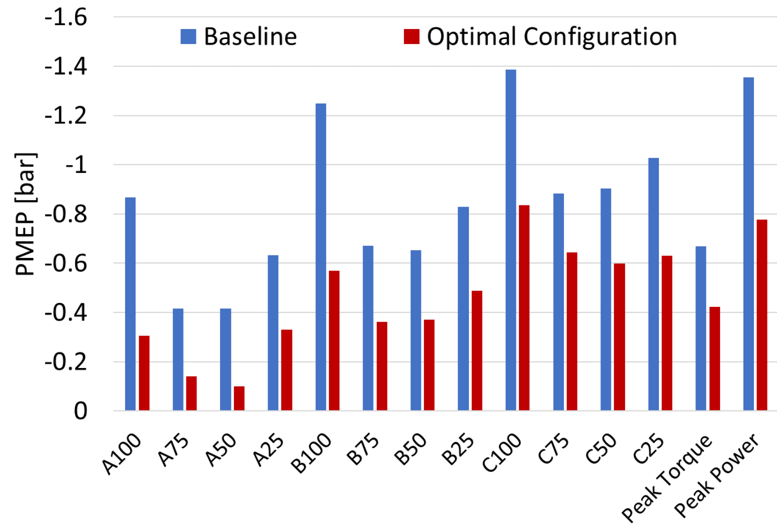

Source: Southwest Research Institute

The D-EGR configuration can deliver EGR more efficiently as the cylinders act as an EGR pump rather than a turbine restriction as is the case with HP-EGR. This is apparent when looking at the engine average pumping work as a function of EGR rate for the two EGR delivery methods, Figure 24, as the D-EGR configuration has ~10 percentage points more EGR at similar (or improved) PMEP.

Figure 24: EGR Delivery Efficiency of HP-EGR Compared to D-EGR for all Modal Points

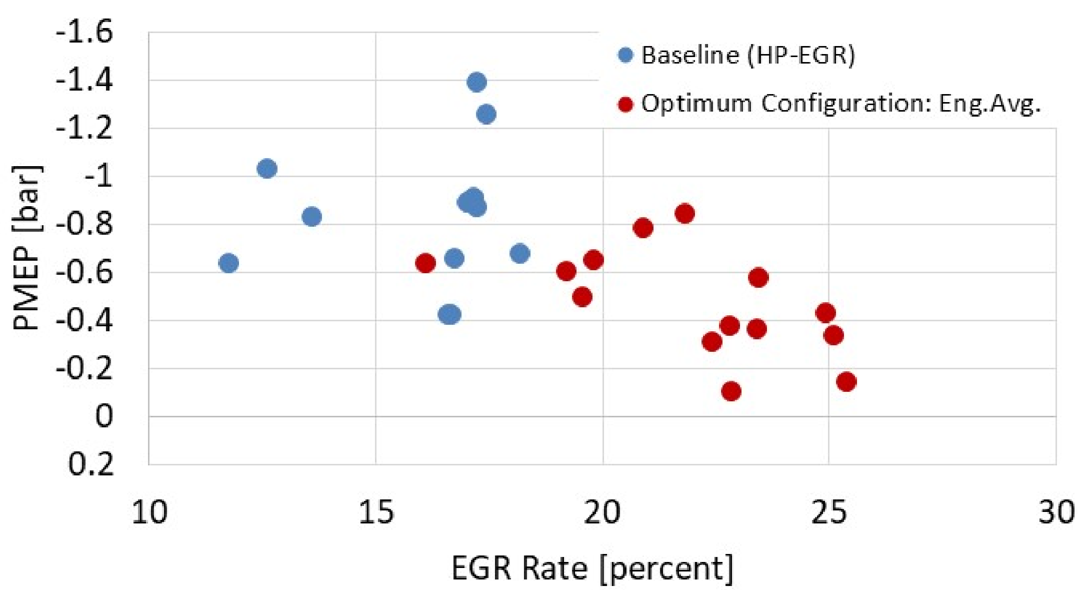

Source: Southwest Research Institute

Looking into the D-EGR configuration in more detail, it is apparent that the main pumping work benefit is due to the ability to re-match the turbine. Figure 25 shows that the pumping work of the dedicated cylinders is similar to the baseline configuration, albeit at a higher EGR rate. The main cylinders, however, show a significant improvement in pumping work, with some modal points achieving positive pumping work. Positive pumping work is impossible to achieve with the traditional HP-EGR configuration.

Figure 25: EGR Delivery Efficiency Comparing Main and Dedicated Cylinders Pumping Work for all Modal Points

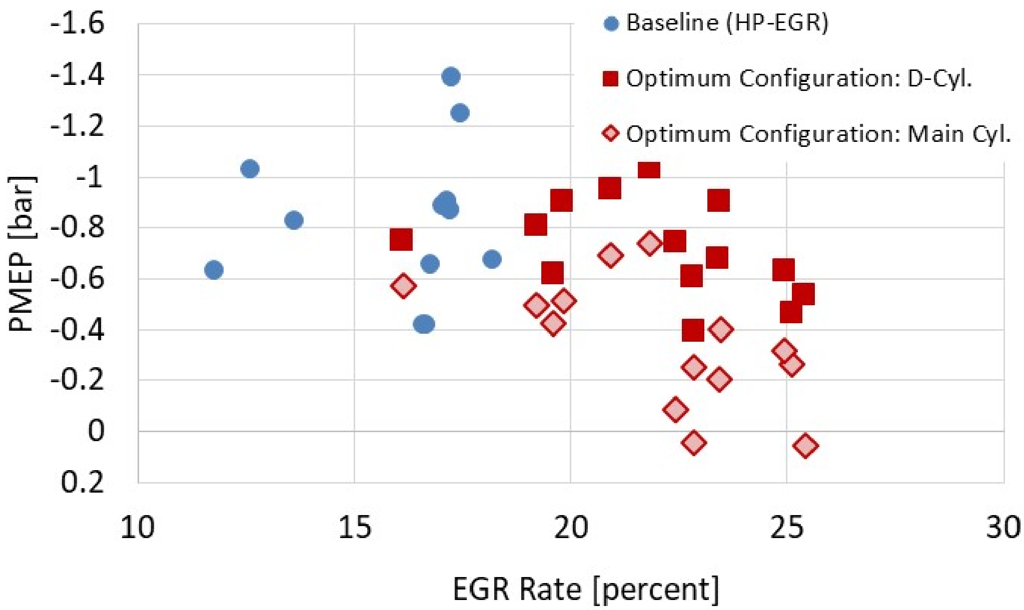

Source: Southwest Research Institute

Heat Transfer Losses

The design of the piston bowl contributed to a significant improvement in the heat transfer losses. The squish ratio was decreased from 0.8 to 0.54. The depth of the bowl was adjusted to increase the compression ratio to the final 13.2:1 used in the optimal engine configuration.

CFD results in Table 9 show that SwRI v1 design had an increase in indicated thermal efficiency (ITE) (calculated from IVC to EVO) of 1.3 ITE points over the stock piston when compared at the same EGR level (HP-EGR).

Table 9: CFD Results for Combustion and Indicated Thermal Efficiency (Closed Cycle) Comparison between Stock and SwRI v1/v2 Pistons

	Stock HP-EGR	SwRI v1 HP-EGR	SwRI v1 D-EGR	SwRI v2 D-EGR
MFB10 (deg.)	6	8	7.5	8.4
MFB50 (deg.)	16.6	16.8	16.9	17.1
MFB90 (deg.)	24.8	25.7	26.3	27.2
MFB10-90 (deg.)	18.8	17.7	18.8	18.7
ITE (percent) IVC –EVO	38.5	39.8	40.6	41.6

Source: Southwest Research Institute

Increasing the compression ratio and EGR rate (SwRI v2) improved ITE by an additional 1.8 ITE points. 0.8 ITE points of that increase was the result of approximately doubling the EGR rate from the stock calibration.

As the 10-90 burn durations for the pistons were similar, the ITE improvement was determined to be a result of reduced wall heat loss for the open bowl piston. The comparison of wall heat losses is shown in Figure 26. The SwRI v2 open bowl piston had a 41 percent reduction in heat loss. This contribution came mainly from the reduced surface area to volume ratio of the piston as the effect on the liner and head heat loss was minimal.

Figure 26: Comparison of Net Heat Transfer to Various Parts of Combustion Chamber with D-EGR

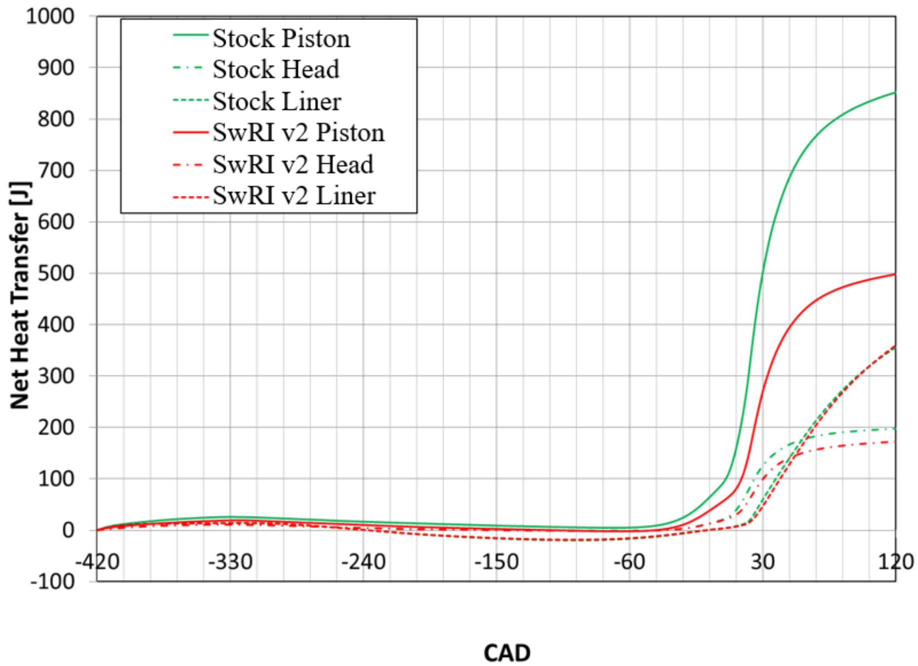

CFD Results

Source: Southwest Research Institute

In Figure 27, 2 percent, 10 percent and 50 percent mass fraction burned (MFB) crank angle locations are shown to assist in understanding the flame evolution; the flame is shown as a 1500 K iso-surface. There was more flame to wall interaction for the re-entrant stock piston which led to higher heat loss. Both pistons resulted in flames that were offset towards the exhaust (left direction), but the flame grew more symmetrically with the SwRI v2 piston.

Figure 27: Piston-Flame Interaction with Baseline and SwRI v2 Piston Design

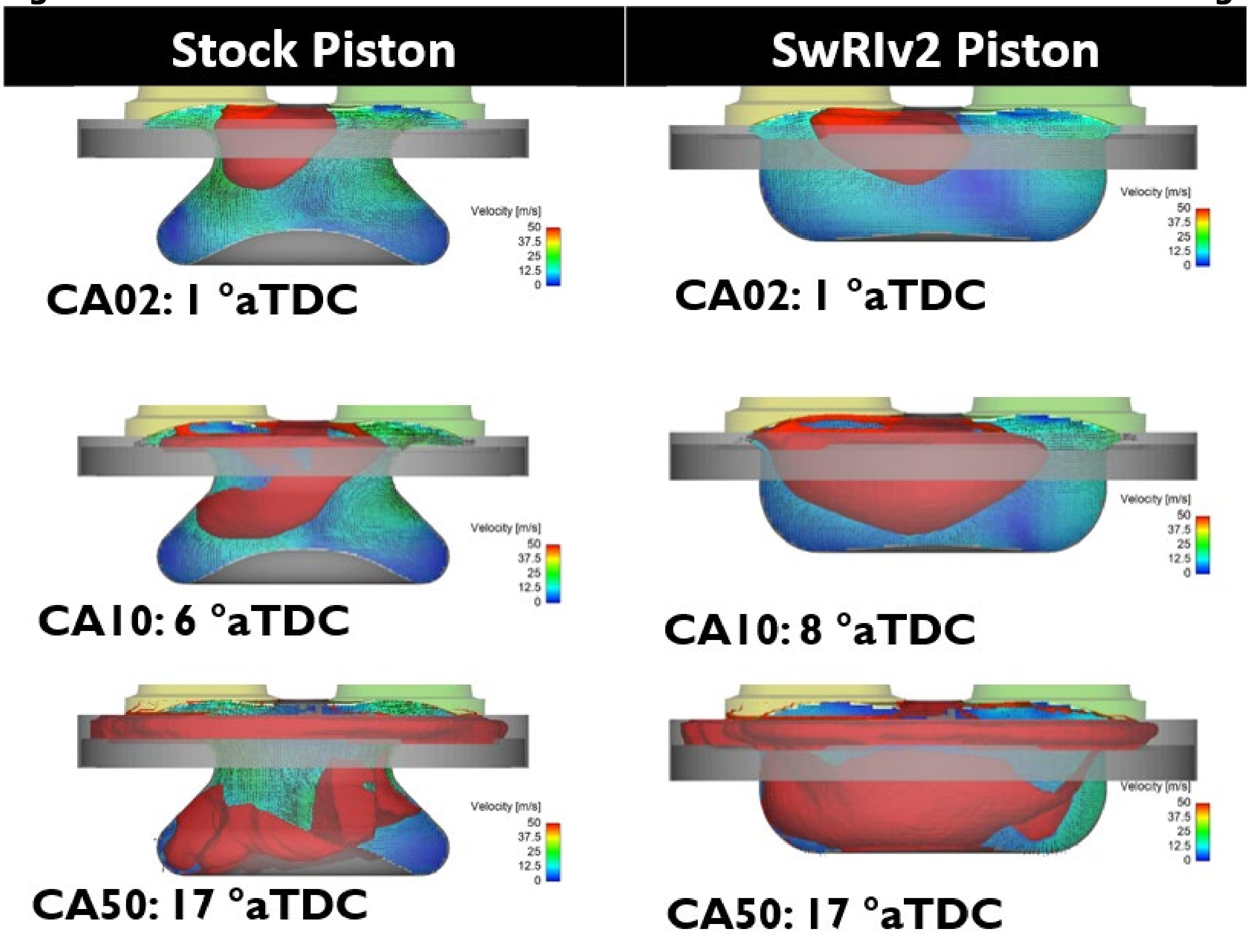

Source: Southwest Research Institute

Engine testing confirmed the significant heat transfer improvement with the reduced squish piston design. Figure 28 shows that the heat transfer was reduced by up to 10 percent of fuel energy. The heat transfer losses were calculated as the remaining sum of quantifiable losses, Equation 1, and therefore includes other losses such as cycle losses. Not all of the heat transfer reduction was converted to useful energy as Figure 29 shows that the exhaust energy increased at some conditions. This is due to the EGR being bled off a location after the turbine, meaning no useful energy was extracted by the gasses being expanded through the turbine.

Eq. 1:

$$Heat\ Transfer = Fuel\ Energy - Brake\ Energy - Combustion\ Inefficiency - Exhaust\ Energy - Friction - Pumping$$

Figure 28: Heat Transfer Losses at Modal Points

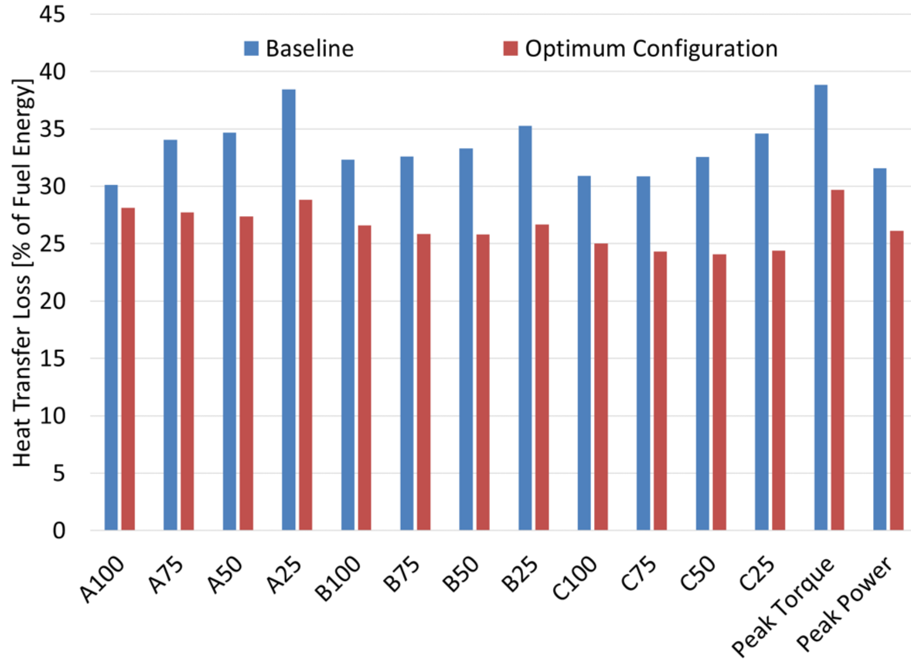

Source: Southwest Research Institute

Figure 29: Post-Turbine Exhaust Energy and Modal Points

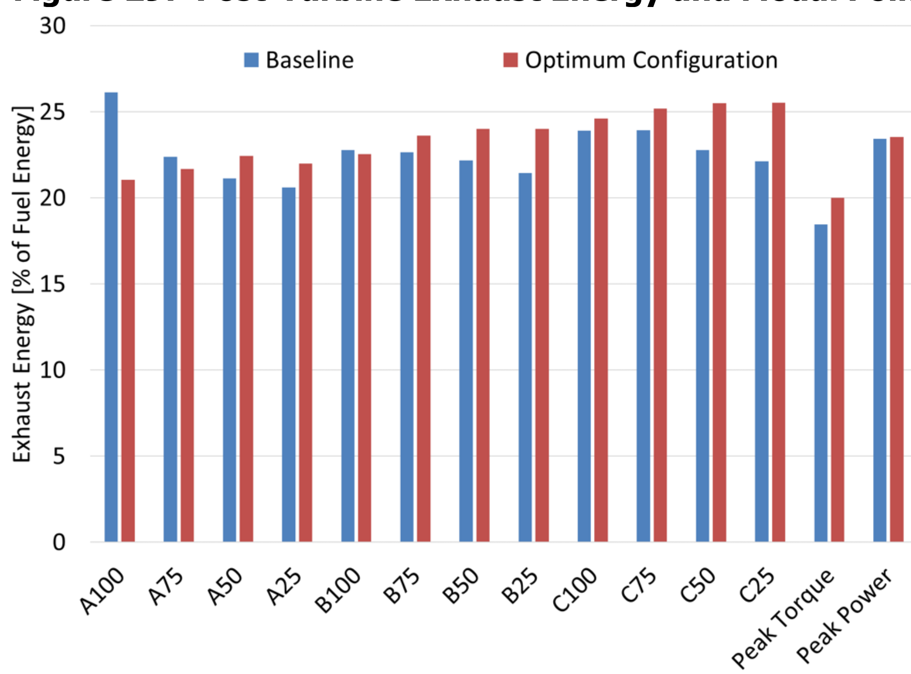

Source: Southwest Research Institute

Ultra-Low NO_X Potential

In addition to achieving at least a 10 percent efficiency improvement, a secondary goal of the project was to achieve 0.02 g/bhp-hr NO_X. This emissions level was previously demonstrated by SwRI in a CARB Low NO_X project (Agreement Number 13-312) utilizing the Cummins Westport ISX12 G. The CARB project utilized a combination of a close-coupled three-way catalyst (TWC) and a conventional under-floor TWC, which is similar to configurations used on Tier 2 gasoline light-duty passenger vehicles. In addition to the TWC arrangement, an advanced engine controller using a model-based control approach and proprietary injection and mixing hardware were utilized. While 0.02 g/bhp-hr NO_X was achieved, there was an increase in CO_2 emissions by about 1 percent due to the impact of the rapid cold-start warm-up strategy.

The engine controller used was not fully capable of transient operation due to the hardware changes necessary for the D-EGR configuration, so the optimal configuration could not be demonstrated over the U.S. Heavy-Duty Federal Test Procedure (FTP) transient cycle. Additionally, after making the required controller changes, a significantly increased calibration effort would be required as there would be no base calibration to start from. Therefore, SwRI developed a quasi-cold start cycle to demonstrate the catalyst warm-up performance compared to the CARB Low NO_X data that worked within the limitations of the controller. The demonstration utilized the same catalyst arrangement as the CARB project. The locations of the close-coupled and under-floor catalyst relative to the turbine outlet were kept as close to the CARB arrangement as possible. The D-EGR configuration should allow similar or improved catalyst warm-up performance due to the fact that two cylinders of exhaust are able to bypass the turbine completely and therefore not lose energy while heating up the turbine.

The quasi-cold start cycle simulated the first 100 seconds of the U.S. Heavy-Duty FTP transient cycle. Figure 30 compares the quasi-cold start cycle to the U.S. Heavy-Duty FTP transient cycle. The engine speed profile was able to be closely matched; however, the torque rise rate was limited which led to a smoothing of the torque profile. Additionally, the engine controller was unable to provide a fuel cut during heavy tip-outs which shows as negative torque in the CARB data. The timing of the first two torque hills were kept relatively similar. The cumulative exhaust energy, measured prior to the close-coupled TWC, was similar over the first 60 seconds. About 800 kJ of additional energy was delivered at 100 seconds due to the large amount of fuel cuts present in the CARB data that could not be replicated.

Figure 30: Quasi-cold Start Cycle Compared to CARB data on U.S. Heavy-Duty FTP Transient Cycle

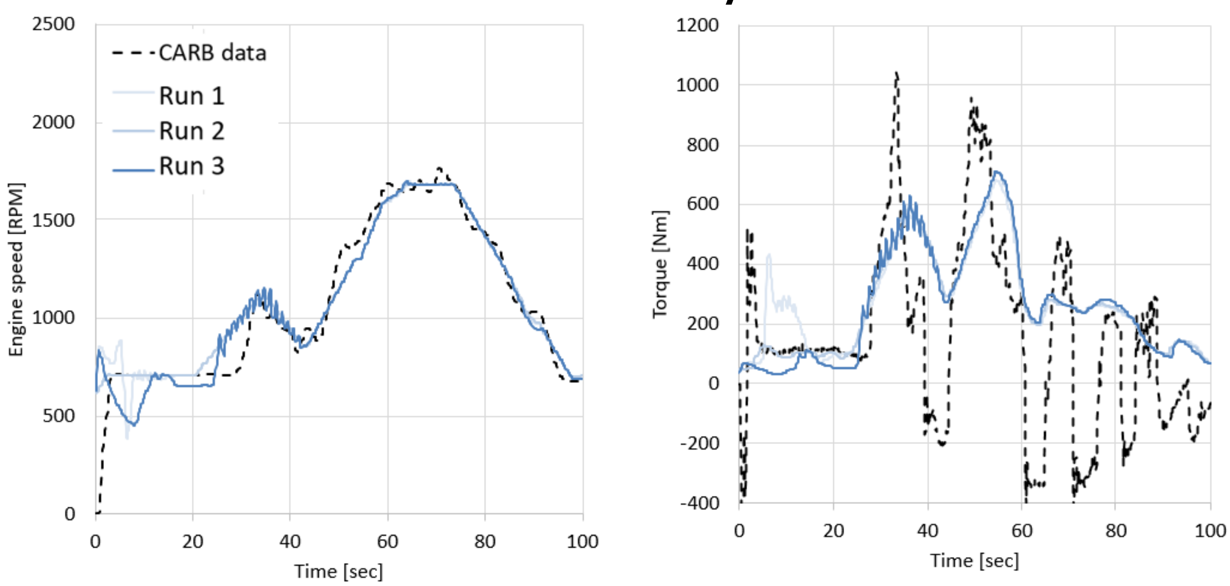

Source: Southwest Research Institute

Figure 31: Cumulative Exhaust Energy of Quasi-Cold Start Cycle Compared to CARB Data on U.S. Heavy-Duty FTP Transient Cycle

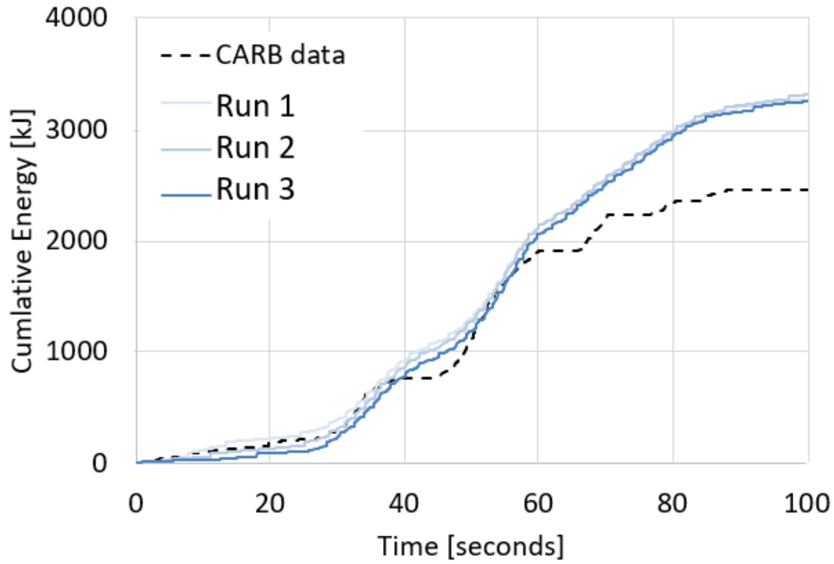

Source: Southwest Research Institute

Testing was conducted from ambient which although not controlled, the starting temperature was usually ~ 22 °C. The catalysts were instrumented with 1/8" thermocouples in the center of the flow with the tip about one inch into the catalyst face which is similar to the instrumentation in the CARB data. 350 °C was used as a reference temperature as an indication of catalyst light-off. The engine was operated with the EGR bypassed before the EGR cooler and operated without EGR during the cycle. The thermostat was blocked open meaning that the coolant would not heat up as fast as a production engine. This was considered insignificant due to the short cycle time. The spark timing was set at 10° aTDCf and was advanced as necessary to meet the load requirements. This mimics the rapid warm-up strategy employed in the CARB project.

Figure 32: Catalyst Inlet Temperature Comparison

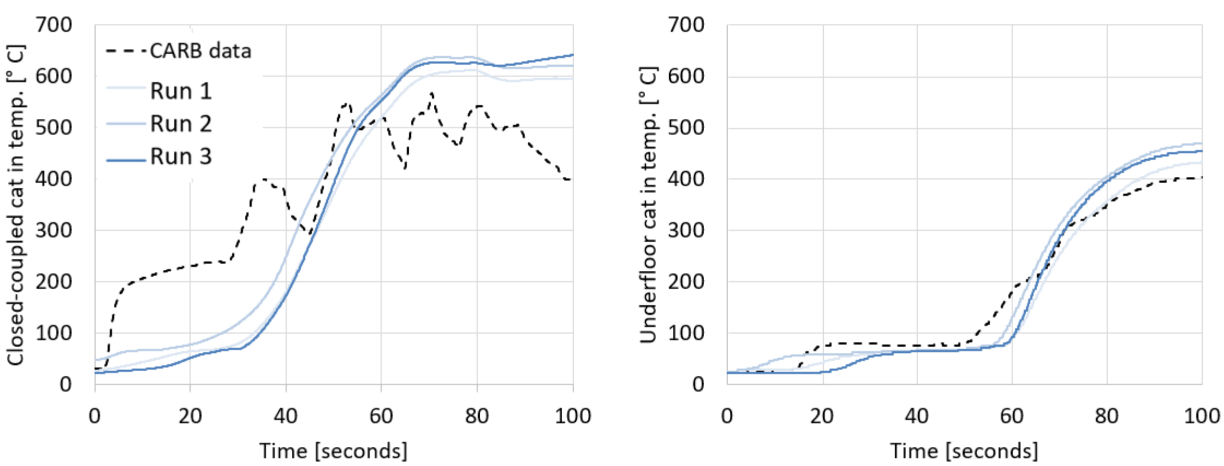

Source: Southwest Research Institute

Figure 32 shows a comparison of the catalyst inlet temperatures for the close-coupled and under-floor catalysts. The close-coupled catalyst achieved 350 °C within ~50 seconds while the CARB results show that temperature being achieved within ~35 seconds. The differences are likely due to the cycle and engine controller. The temperature rise in the first 10 seconds of the cycle was not able to be replicated although the exact source of the initial temperature rise is unknown. Both sets of under-floor catalysts achieved 350° C after ~75 seconds. The similar catalyst warm-up performance shows that the D-EGR configuration is not significantly different than a typical HP-EGR configuration. With a fully functional transient controller and more mature calibration, SwRI expects that the D-EGR engine in the optimum configuration can meet the 0.02 g/bhp-hr NO_X target.

CHAPTER 4: Technology/Knowledge/Market Transfer Activities

Southwest Research Institute (SwRI®) is making the knowledge gained in this project available to the public and promote the technical and economic benefits of this project through a number of technology transfer activities:

- Conference Presentations: SwRI regularly attends and presents at conferences, technology forums and industry events. SwRI plans to include the details of the engine efficiency improvement with ultra-low NO_X potential technology at these events. These presentations include PowerPoint presentations with results conveyed in pictures, charts, graphs and tables. SwRI also makes these presentations publicly available either through the conference organizers or direct request from attendees. Table 10 lists the events where SwRI presentations have occurred or are planned to be presented at.

Table 10: SwRI Planned Presentations and Event Participation

Event	Approximate Date
Natural Gas Vehicle Technology Forum (NGVTF), Downey, CA	February 21-22, 2018
SAE World Congress, Detroit, MI *D-EGR Conversion* *Piston Development*	April 9-11, 2019
SAE Innovations in Mobility, Novi, MI	October 29-31, 2019
Natural Gas Vehicle Technology Forum, Downey, CA	February 4-5, 2020
SAE High Efficiency Engine Symposium	April 19-20, 2020
SAE World Congress, Detroit, MI Project Overview	April 21-23, 2020
Sustainable Fleet Technology Conference, Durham, NC	August 26-27, 2020
COMVEC, Rosemont, IL	September 16-18, 2020
SAE Powertrain, Fuels & Lubricants Meeting, Krakow, Poland *Fuel Quality Effect on NG D-EGR*	September 22-24, 2020

Source: Southwest Research Institute

- Consortium Presentations: SwRI provided updates to the HEDGE-IV consortium members throughout the project at regularly scheduled Technical Advisory Committee meetings. The members of the consortium consist of OEM's and Tier One suppliers from across the globe. These updates included current project results, detailed analysis of engine data and recommendations for further development. An overview of the project results, including final efficiency improvement, was delivered to the consortium member at the October 2019 meeting in San Antonio, TX.
- Technical Papers: SwRI regularly publishes technical papers to convey detailed technical results to the industry. These papers focused on individual technical challenges and/or observations as well as provide a summary of the development process and project

results. The following list shows the papers published to date and planned future papers.

- Moiz, A., Abidin, Z., Mitchell, R., and Kocsis, M., "Development of a Natural Gas Engine with Diesel Engine-like Efficiency Using Computational Fluid Dynamics," SAE Technical Paper 2019-01-0225, 2019.
- Mitchell, R. and Kocsis, M., "Performance Evaluation of Dedicated EGR on a 12 L Natural Gas Engine," SAE Technical Paper 2019-01-1143, 2019.
- Kocsis, M., Briggs, T., Mitchell, R., Moiz, A., Sjovall, S., "Improving Heavy Duty Natural Gas Engine Efficiency: A Systematic Approach to Application of Dedicated EGR," SAE Technical Paper, *Currently under peer review*
- Fuel Quality Effects on HD NG D-EGR Operation, *Manuscript currently being prepared*

- OEM/Supplier Visits: SwRI regularly visits OEMS and suppliers to discuss current challenges and future opportunities for their product line. These visits often include presentations on publicly funded projects such as this current project. While the results of this project are based on a single engine platform, SwRI discusses how the knowledge learned can be transferred to their specific product offerings.

The results of this project presented in the final report and disseminated through technology transfer activities could be used in the following ways:

- Government emissions regulators will be able to use the results to confirm that natural gas engines are capable of delivering a low CO_2 solution with "near-zero" NO_X potential. This provides valuable insight into the potential of future technology in order to make informed decisions on the content and timing of future emissions regulations.
- SwRI is engaged with many of the major vehicle OEMs and engine manufacturers in the on-road heavy duty vehicle market. These entities, if not already aware of the technology, will be informed of the potential of using D-EGR technology along with challenges to implementation. This may alter research and development plans to include similar technologies to the results presented in this report.

CHAPTER 5: Conclusions/Recommendations

Southwest Research Institute (SwRI®) modified a Cummins Westport ISX12 G using a systematic approach towards improved efficiency. One-dimensional simulations were performed to predict the maximum compression ratio and select a prototype VNT turbocharger. Three-dimensional combustion simulations were used to improve the design of the piston by maintaining fast burn rates with a reduced squish design. The optimal configuration consisted the following components:

- Dedicated EGR® (D-EGR®) arrangement with two dedicated EGR generating cylinders
    - Cold side valves to modulate EGR rate where necessary
- Prototype VNT turbocharger
- High energy, continuous discharge ignition system (DCO®)
- SwRI v2 piston
    - Squish area ratio - 0.54
    - Compression ratio - 13.2:1

With this optimal configuration, the program efficiency goal of 10 percent improvement over the baseline case was exceeded by demonstrating a 12.3 percent – 13.5 percent improvement depending on idle calibration strategy. A peak brake thermal efficiency of 41.7 percent was observed at peak torque. These efficiency improvements were achieved by:

- Optimized EGR rate and delivery method through the use of a D-EGR arrangement which was enabled by an advanced ignition system.
- Increased ideal efficiency through increased compression ratio which was enabled by increased EGR rate.
- Reduced pumping work through optimizing EGR delivery method and turbocharger match.
- Reduced heat transfer losses through optimization of the piston design.

The optimal configuration maintained the potential to achieve 0.02 g/bhp-hr NO_X. The development engine controller used was not fully capable of transient operation due to the hardware changes necessary for the D-EGR configuration, preventing the team from conducting emissions testing over the heavy-duty FTP transient cycle. The controller limitations are easily overcome, but require more development effort beyond the scope of this project. Therefore, the ultra-low NO_X potential was demonstrated through a custom quasi-cold start cycle and the catalyst warm-up performance compared to the CARB Low NO_X data.

The demonstration used the same catalyst arrangement as the CARB Low NO_X project. The locations of the close-coupled and under-floor catalyst relative to the turbine outlet were kept as close to the CARB arrangement as possible. The D-EGR configuration should allow similar or improved catalyst warm-up performance due to the fact that two cylinders of exhaust are able to bypass the turbine completely and therefore not lose energy while heating up the turbine. Due to differences in the cycle, the close-coupled catalyst achieved 350 °C within ~50 seconds while the CARB results show that temperature being achieved within ~35 seconds. Both sets of under-floor catalysts achieved 350° C after ~75 seconds. The similar catalyst warm-up performance shows that the D-EGR configuration is not significantly different than a typical HP-EGR configuration. With a fully functional transient controller and more mature calibration, it is expected that the D-EGR engine in the optimum configuration would be able to meet the 0.02 g/bhp-hr NO_X target.

Recommendations

A key limitation in additional efficiency improvements was that the EGR tolerance was lower than expected at the onset of the project. This limited the project from taking the full advantage of the expected benefits of the D-EGR configuration. SwRI recommends that EGR tolerance be improved through the following activities:

- Continue development of advanced ignition systems: More robust ignition systems are required to allow engines to operate at EGR levels above 30 percent. It is expected that future engines will require 30-50 percent EGR rates to achieve future efficiency and emissions standards. As shown in this project, pre-chamber technologies offer potential for high efficiency, but passive pre-chambers are limited due to the high dilution levels within the pre-chamber itself resulting from insufficient scavenging. Further development of an air scavenged and/or fueled pre-chamber should overcome these limitations and provide a pathway to higher dilution tolerance.
- Investigate more favorable flow fields within combustion chamber: This project was limited by the flow field in the combustion chamber that was a result of the swirl designed into diesel head that the ISX12 G was based upon. Squish is used to create the turbulent kinetic energy necessary for fast combustion, however high heat losses result from this sub-optimal design. The use of a pent-roof head and a tumble flow field is more favorable for SI combustion. Tumble naturally breaks down into small scale turbulent kinetic energy through the motion of the piston. This should enable higher EGR rates with a more traditional ignition system.

CHAPTER 6: Benefits to Ratepayers

Natural gas vehicles have long been observed as clean alternatives to their diesel counterparts in the medium and heavy-duty segment by their notable absence of trailing clouds of soot when accelerating away from a stop under a heavy load. As NO_X emission standards became more stringent, natural gas engines have the distinction of being the first to demonstrate the near-zero emissions capability of 0.02 g/bhp-hr with a shift to the pairing of stoichiometric combustion and three-way catalyst. The immediate benefit of the availability of such engines was recently demonstrated in a case study presented by Cummins Westport and a California transit agency, Figure 33. In this study, repowering a fleet of two hundred transit buses with near-zero certified engines resulted in a total reduction of 315,161 lbs/year in NOx emissions; a 90 percent decrease from the previous year [4]. With funding assistance through incentive programs like the California Hybrid and Zero-Emission Truck and Bus Voucher Incentive Program (HVIP), these results will continue to be replicated as more natural gas vehicles are deployed in California fleets. This project has demonstrated that a near-zero NO_X emission level can be maintained while pursuing further improvements in engine efficiency.

Figure 33: Case Study on NOX Reduction with Natural Gas Vehicles

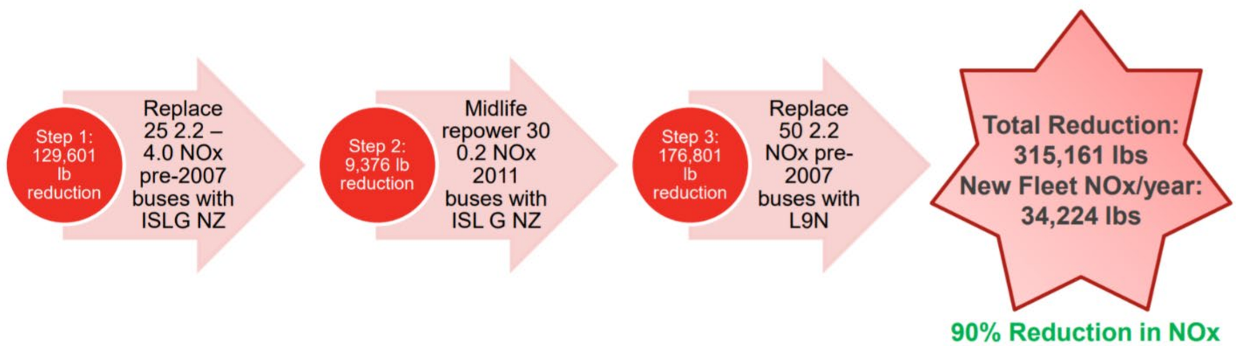

Source: [Southern California Gas Company]

Reductions in criteria pollutants will have a more direct and noticeable impact on the local air quality for stakeholders and ratepayers of the state of California. Facing the increasing effects of global warming and climate change, many world leaders have reached the conclusion that global cooperation is needed for greenhouse gas reduction. California has set very ambitious targets for state-wide greenhouse gas reductions through 2050. Having met the 2020 target of returning to 1990 GHG emissions levels, the next phase requires a further reduction of 40 percent by 2030. Transitioning to sustainable transportation solutions is a key strategy to achieving these targets because the transportation sector is responsible for 41 percent of California's GHG emissions, as shown in Figure 34. This is another area where natural gas has a fundamental advantage over diesel and other petroleum-based fuels. Made up of much simpler and smaller hydrocarbons (primarily methane), the hydrogen to carbon ratio of natural gas is nearly double that of diesel fuel, which results in roughly 25 percent less CO_2 on an energy equivalent basis. [5] Natural gas engines can also use renewable natural gas, a low carbon transportation fuel captured from waste sources such as wastewater treatment plants and dairies, for additional reductions in lifecycle CO_2 emissions.

Figure 34: California's 2017 GHG Emissions by Economic Sector

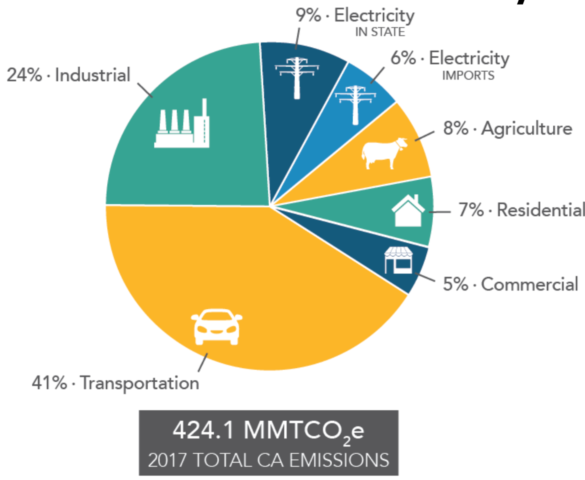

Source: [California Air Resources Board]

Unfortunately, the full extent of this GHG advantage cannot be achieved with a simple engine replacement due to a persistent efficiency deficit between natural gas and diesel engines. Depending on the application, this deficit can range from 10 to 20 percent, which in turn reduces the GHG benefit of the natural gas engine to between 12 and 16 percent [6]. The greater than 10 percent efficiency improvement demonstrated by this project represents a substantial decrease in the efficiency deficit and represents a significant step toward achieving parity with the diesel engine. Under these same assumptions, an engine with the optimal configuration described here would be expected to achieve a total GHG reduction of 16 to 20 percent.

A secondary benefit of the 10 percent efficiency improvement is the reduction in total operating cost for fleets that convert to natural gas vehicles. As described by Dr. Robert Marlay of the Department of Energy's office of Energy Efficiency & Renewable Energy at the 2019 Natural Gas Vehicle Technology Forum [7], a major barrier to broader adoption of natural gas vehicles lies in the incremental cost of the NG engine variant, Figure 35. With little competition in the market, NG engines are often sold at a premium to an equivalent diesel engine with the added cost of the complex fuel storage system which can cost as much as the engine itself. For a fleet owner seeking a 2-year payback period on this incremental cost, the operating cost of the engine must be low enough to quickly recover the initial investment.

In Dr. Marlay's data, an NGV purchased at an incremental cost of $37.5k with and efficiency deficit of 15 percent provides a 2-year cost savings of only $12k; less than half of the incremental cost of the engine. If the efficiency deficit is removed, the 2-year cost savings more than doubles to $25k. While this is still not sufficient to cover the incremental cost, another assumption affects the economics. In this scenario, the cost differential of the CNG fuel is assumed to be roughly one dollar (equivalent to the national average). However, in the state of California where diesel prices are substantially higher than the national average, the CNG fuel differential cost is closer to $1.50 [8]. This price difference results in an additional savings of $14k, added with the $25k savings from the more efficient engine, results in a total cost savings of $39k which is a far more economical prospect.

Figure 35: Cost of Natural Gas Vehicle Ownership

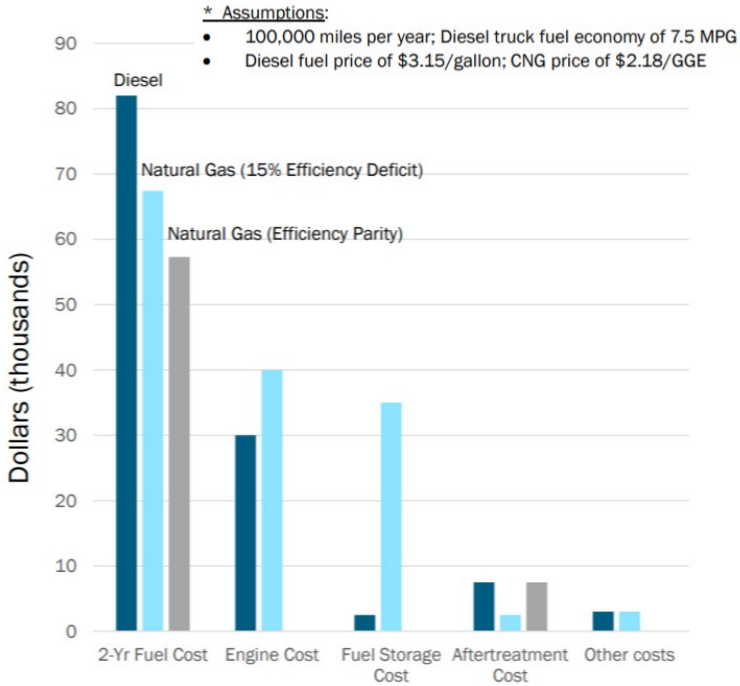

Source: [National Renewable Energy Laboratory]

Figure 36: CNG Price Differential Relative to Diesel across U.S.

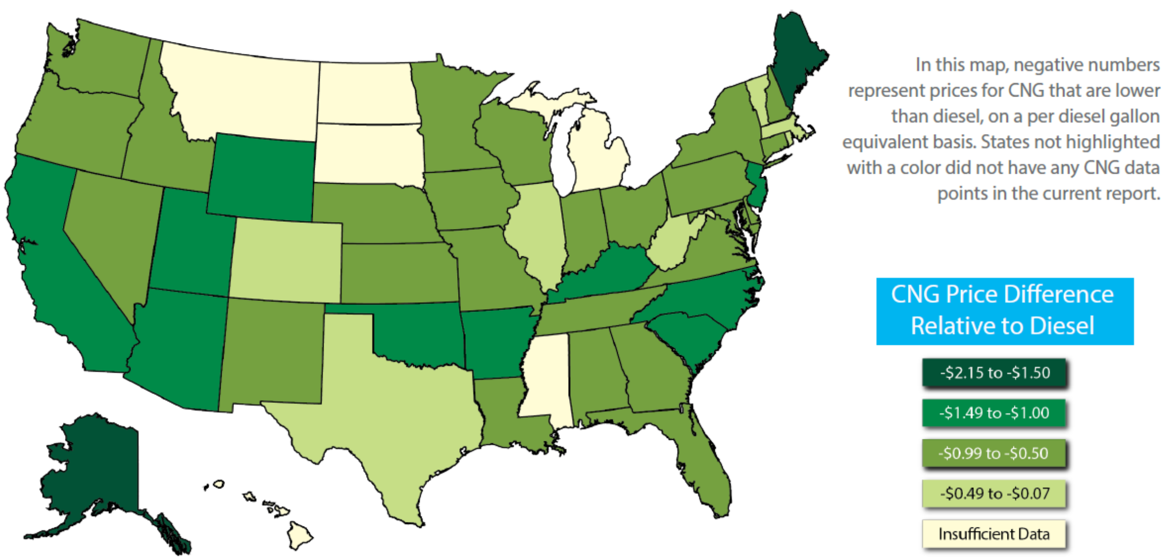

Source: [Alternative Fuels Data Center]

The next phase of GHG reductions laid out in the California Climate Change Scoping Plan will be extremely challenging, and natural gas vehicles hold the potential for significant GHG reduction in the transportation sector. Coupled with the efficiency improvements detailed in this project, the GHG reduction potential further improves and opens the pathway for broader NGV adoption in more commercial applications.

GLOSSARY AND LIST OF ACRONYMS

Term	Definition
AFR	Air-fuel ratio
AKI	Antiknock index
°aTDC	Degrees after top dead center
bhp	Brake horsepower
BMEP	Brake mean effective pressure
BTE	Brake thermal efficiency
CA50	Location of 50 percent mass fraction of fuel burned
CARB	California Air Resources Board
ccTWC	Close-coupled three-way catalyst
CEC	California Energy Commission
CFD	Computational fluid dynamics
CH4	Methane, a greenhouse gas
CNG	Compressed natural gas
CO	Carbon monoxide, a criteria pollutant
CO2	Carbon dioxide, a greenhouse gas
CoV gIMEP	Coefficient of variation of the gross indicated mean effective pressure
CR	Compression ratio
DCO®	Dual Coil Offset, a continuous discharge ignition system
D-Cyl(s)	Dedicated (EGR generating) cylinder(s)
D-EGR®	Dedicated Exhaust Gas Recirculation
ECU	Engine control unit
EGR	Exhaust gas recirculation
EVO	Exhaust valve opening
FTP	Federal Test Procedure
g/bhp-hr	Gram per brake horsepower hour
GHG	Greenhouse gas
GT-Power	One-dimensional engine simulation code
H_2	Hydrogen gas
HC	Hydrocarbons, a regulated emission

Term	Definition
HD	Heavy-duty
HEDGE®	High Efficiency Dilute Gasoline Engine
HEDGE-IV	Fourth iteration of HEDGE research consortium
HP-EGR	High pressure (before turbocharger) EGR
ISX12 G	12 liter heavy-duty natural gas engine produced by Cummins Westport
ISX12N	Low NO_X version of ISX12 G
ITE	Indicated thermal efficiency
IVC	Intake valve closing
L	Liter
LHV	Lower heating value
MBT	Maximum brake torque
MN	Methane number, a measure of knock resistance for gaseous fuels
NG	Natural gas
NH3	Ammonia
NO_X	Nitrogen oxides, a criteria pollutant
OEM	Original Equipment Manufacturer
PM	Particulate matter, a criteria pollutant
PMEP	Pumping mean effective pressure
R&D	Research and Development
RMC SET	Ramped Mode Cycle Supplemental Emissions Test
RON	Research octane number
SAE	Society of Automotive Engineers
SI	Spark ignition, a combustion mode
SwRI®	Southwest Research Institute
SwRI v1	Improved low squish piston design
SwRI v2	High compression ratio version of SwRI v1 piston
TAC	Technical Advisory Committee
TWC	Three-way catalyst
ufTWC	Under-floor three-way catalyst
USEPA	United States Environmental Protection Agency

Term	Definition
VNT	Variable geometry turbine
WG	Wastegate
WHTC	World Harmonized Transient Cycle

REFERENCES

[1] D. Robertson, C. Chadwell, T. Alger, J. Zuehl, R. Gukelberger, B. Denton and I. Smith, "Dedicated EGR Vehicle Demonstration," *SAE Int. J. Engines,* Vols. 10(3):898-907, 2017.

[2] R. Gukelberger, D. Robertson, T. Alger and S. Almaraz, "Alternative Fuel Testing on a Port Fuel Injected LPL EGR and D-EGR® Engine," *SAE Technical Paper 2016-01-2170,* 2016.

[3] C. Sharp, C. Webb, G. Neely and I. Smith, "Evaluating Technologies and Methodologies to Lower Nitrogen Oxide Emissions From Heavy-Duty Vehicles," 2017.

[4] K. Cook, "Cummins Westport Report," October 2017. [Online]. Available: https://www.socalgas.com/1443741246231/CWI---Sacramento-RNG---Oct-2017_Cook.pdf.

[5] California Air Resources Board, "California's 2017 Climate Change Scoping Plan," November 2017. [Online]. Available: https://ww3.arb.ca.gov/cc/scopingplan/scoping_plan_2017_es.pdf.

[6] TIAX, LLC, "https://ww3.arb.ca.gov/cc/scopingplan/scoping_plan_2017_es.pdf," 1 August 2017. [Online]. Available: https://ww2.energy.ca.gov/2007publications/CEC-600-2007-004/CEC-600-2007-004-REV.PDF.

[7] R. Marlay, "Natural Gas as a Transportation Fuel – A Strategic Opportunity for U.S. Energy Security Enabled by Innovation and Advanced Technology," in *Natural Gas Vehicle Technology Forum*, Salisbury, NC, April 16-17, 2019.

[8] U.S. Department of Energy, "Clean Cities Alternative Fuel Price Report," January 2019. [Online]. Available: https://afdc.energy.gov/files/u/publication/alternative_fuel_price_report_jan_2019.pdf.

[9] C. Chadwell, T. Alger, J. Zuehl and R. Gukelberger, "A Demonstration of Dedicated EGR on a 2.0 L GDI Engine," *SAE Int. J. Engines,* Vols. 7(1):434-447, 2014.

[10] B. Denton, C. Chadwell, R. Gukelberger and T. Alger, "Design and Implementation of a D-EGR® Mixer for Improved Dilution and Reformate Distribution," *SAE Int. J. Engines,* Vols. 10(3):892-897, 2017.

[11] Holset Turbo, [Online]. Available: http://www.myholsetturbo.com/resources/holsetturbo_productionspecs.pdf.

[12] T. Alger, J. Gingrich, C. Roberts, B. Mangold and M. Sellnau, "A High-Energy Continuous Discharge Ingition System for Dilute Engine Applications," *SAE Technical paper 2013-01-1628,* no. doi:10.4271/2013-01-1628, 2013.

[13] R. Gukelberger, T. Alger, J. Gingrich and B. Mangold, "Impact of Operating Parameters on Ignition System Energy Consumption," *SAE Technical Paper 2014-01-1233,* no. doi:10.4271/2014-01-1233, 2014.

[14] A. A. Moiz, Z. Abidin, R. Mitchell and M. Kocsis, "Development of a Natural Gas Engine with Diesel Engine-like Efficiency Using Computation Fluid Dynamics," *SAE Technical Paper 2019-01-0225,* 2019.

APPENDIX A: Dedicated Exhaust Gas Recirculation Conversion

Careful selection of what cylinders will be used as the EGR generating cylinder is required to enable D-EGR operation of this engine. As shown in Figure A-1, the outermost intake valve of cylinder 1 and cylinder 6 have dedicated intake ports whereas all other cylinders share intake ports with the adjoining cylinder known as a Siamese configuration. Due to the head design (integrated intake manifold with Siamese intake ports), cylinder 1 and cylinder 6 were selected as the dedicated EGR cylinders. These two cylinders were selected as they do not share an intake port with the adjoining cylinder. The use of these two outer cylinders gives individual control of fuel enrichment for each dedicated cylinder thereby allowing for separate fuel injector trimming should one of the cylinders have slightly different breathing characteristics than the other. Cylinders 3 and 4 were an option as well for the dedicated cylinders, but would not have the advantage of individual cylinder fueling and modifying the exhaust manifold would have been more difficult.

Figure A-1: Integrated Intake Manifold and Head

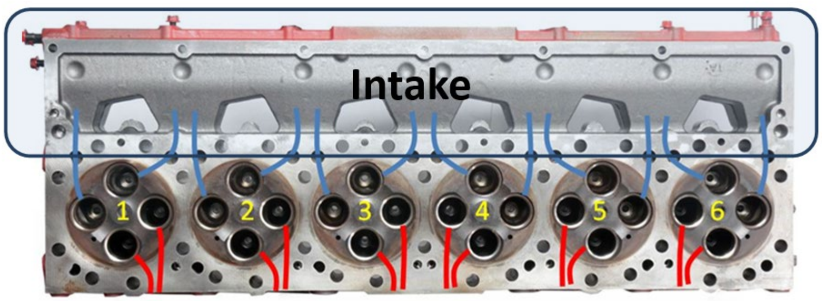

Source: Southwest Research Institute

The exhaust manifold was a three-piece design with a sealed slip-joint between cylinders one and two and between cylinders five and six, allowing for thermal expansion. To segregate exhaust from cylinders one and six from the other cylinders the three pieces were separated at the slip-joints and welded closed, Figure A-2. The exhaust from cylinders one and six were then combined and routed into the EGR cooler.

Figure A-2: Exhaust Manifold

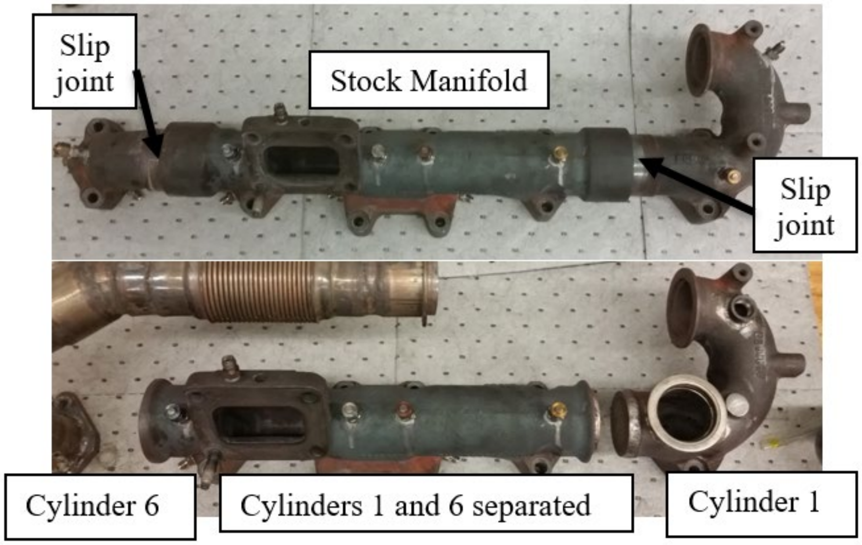

Source: Southwest Research Institute

Starting the engine with 33 percent EGR can be difficult and therefore a bypass valve was installed, Figure A-3. This allows the EGR to bypass the turbine and enter the main exhaust stream before the catalyst. An EGR valve is also installed in the EGR stream and can be closed if there is not sufficient pressure differential to fully bypass the EGR. When D-EGR mode is required, the bypass valve is closed and EGR valve is opened fully. While installed with the intention of being used for cold-start purposes only, this arrangement also allows the EGR rate to be optimized at reduced levels if necessary.

Figure A-3: D-EGR Route

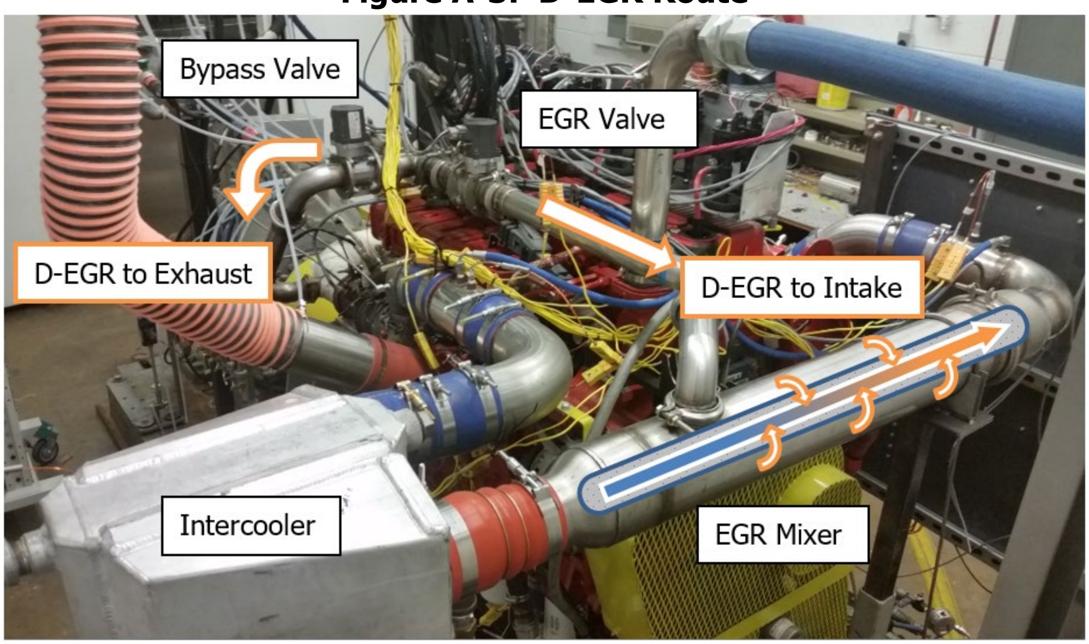

Source: Southwest Research Institute

When the engine operates in D-EGR mode, the exhaust gas produced by cylinders 1 and 6 is routed back into the engine's intake. However, because of the pulsed nature the D-EGR configuration, an EGR mixer is needed to ensure that each cylinder receives similar dilution [9] [10]. The mixer, shown in Figure A-4 with the insert removed, was designed as a spatial and temporal mixer to address the pulses from the two dedicated cylinders. The general design criteria for the mixer is such that the ratio of insert volume (through which the fresh air flows) to outer shell volume (through which the EGR flows) equals the ratio of dedicated cylinder volume to total engine volume. The total flow area of the lateral holes along the wall of the insert is equal to the flow area of the exhaust ports, allowing minimum back pressure on the dedicated cylinder(s). Given the firing sequence of this engine, 1-5-3-6-2-4, spaces the combustion event of the dedicated cylinders by 360°, the mixer could be sized for half the total engine displacement. The mixer insert volume was approximately 6 L.

Figure A-4: D-EGR Mixer

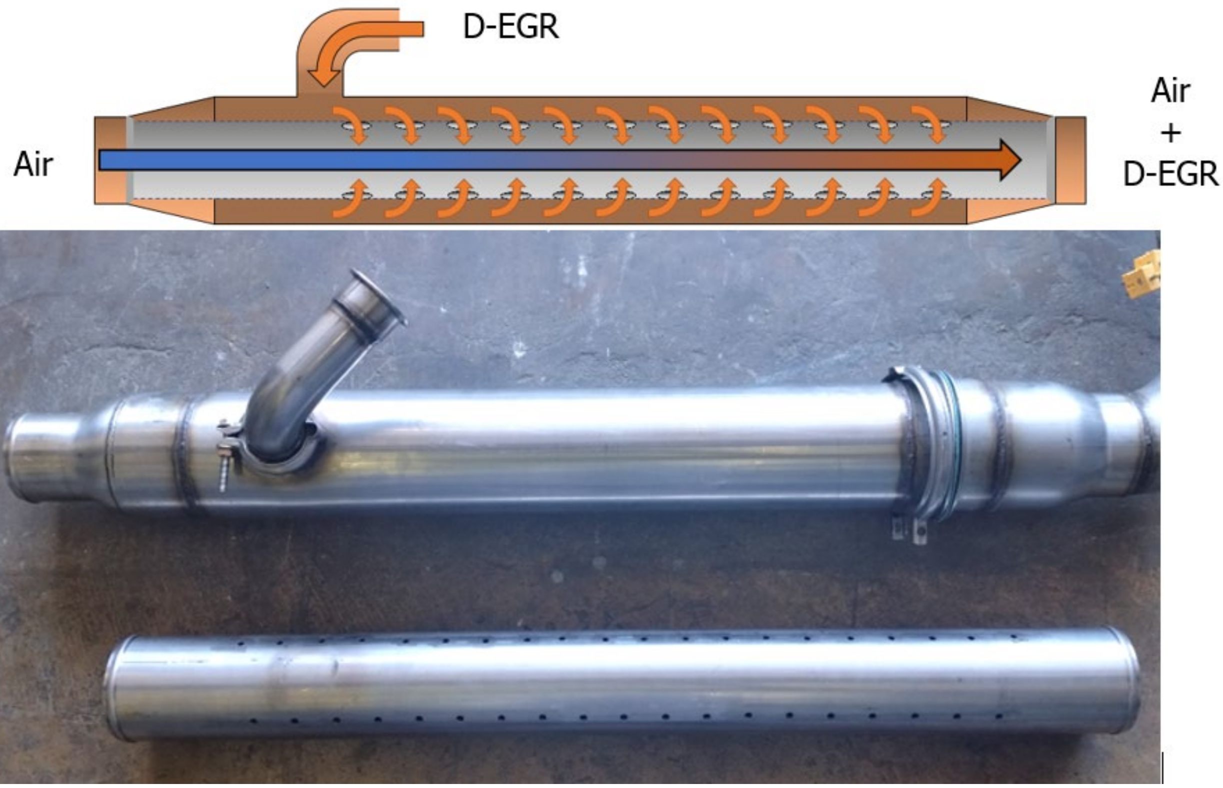

Source: Southwest Research Institute

To be able to optimize the air-fuel ratio of the dedicated cylinders, (typically to produce reformate), two Bosch PFI fuel injectors were installed into the cylinder head through freeze plug inserts located near cylinder 1 and cylinder 6, Figure A-5. A stainless-steel tube extension at the end of the injector was directed towards the intake port for each cylinder to prevent reverse flow of the additional fuel to adjoining cylinders. The injectors were supplied 100 psi of natural gas by adding a tee into the main supply line prior to the injector fuel block.

An additional feature of the D-EGR setup was the installation of wide-band UEGO sensors in the dedicated exhaust stream for fueling feedback and control. The Woodward ECU software was modified to control injector pulse-width of each injector using the UEGO feedback, giving the user full authority of enrichment of the two cylinders. As the primary fueling system was a single point fumigated system, the dedicated cylinder air-fuel ratio could only be optimized from stoichiometric to rich.

Figure A-5: Fuel Injectors for Dedicated Cylinder Enrichment

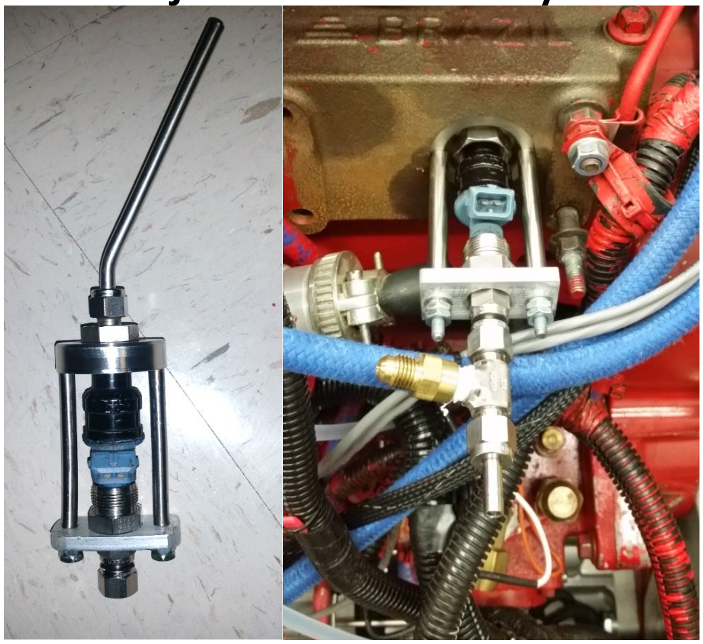

Source: Southwest Research Institute

APPENDIX B: Performance Prediction Using One-Dimensional Modeling

To aid in the development of the optimal engine configuration, the Cummins Westport ISX12 G was simulated using the one-dimensional modeling tool GT-Power.

Baseline Model

Baseline Model Development

A model of a Cummins Westport ISX12-G engine was developed in GT-Power version 2017. The baseline engine is an in-line six-cylinder natural gas engine with a displacement of 11.95 L. The engine utilizes a wastegate turbocharger and a fumigated fuel delivery system. The torque curve in Figure B-1 was determined during the baseline testing by SwRI.

Figure B-1: Baseline Torque Curve

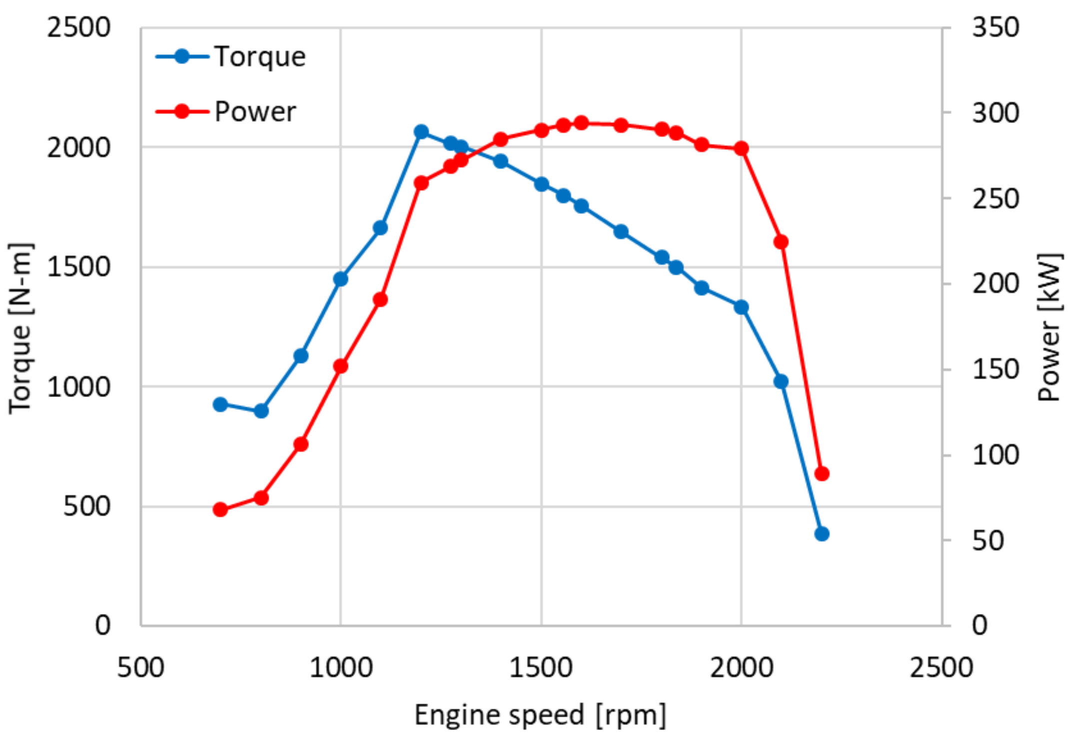

Source: Southwest Research Institute

Measurement of the engine components were taken during an engine benchmarking program performed at SwRI previously. Using these measurements, the one-dimensional model was created as shown in Figure B-2. The model was then tuned by adjusting some key tuning factors. A list of these factors and typical ranges is shown in Table B-1.

Figure B-2: GT Power Model Layout of the Stock Engine Configuration

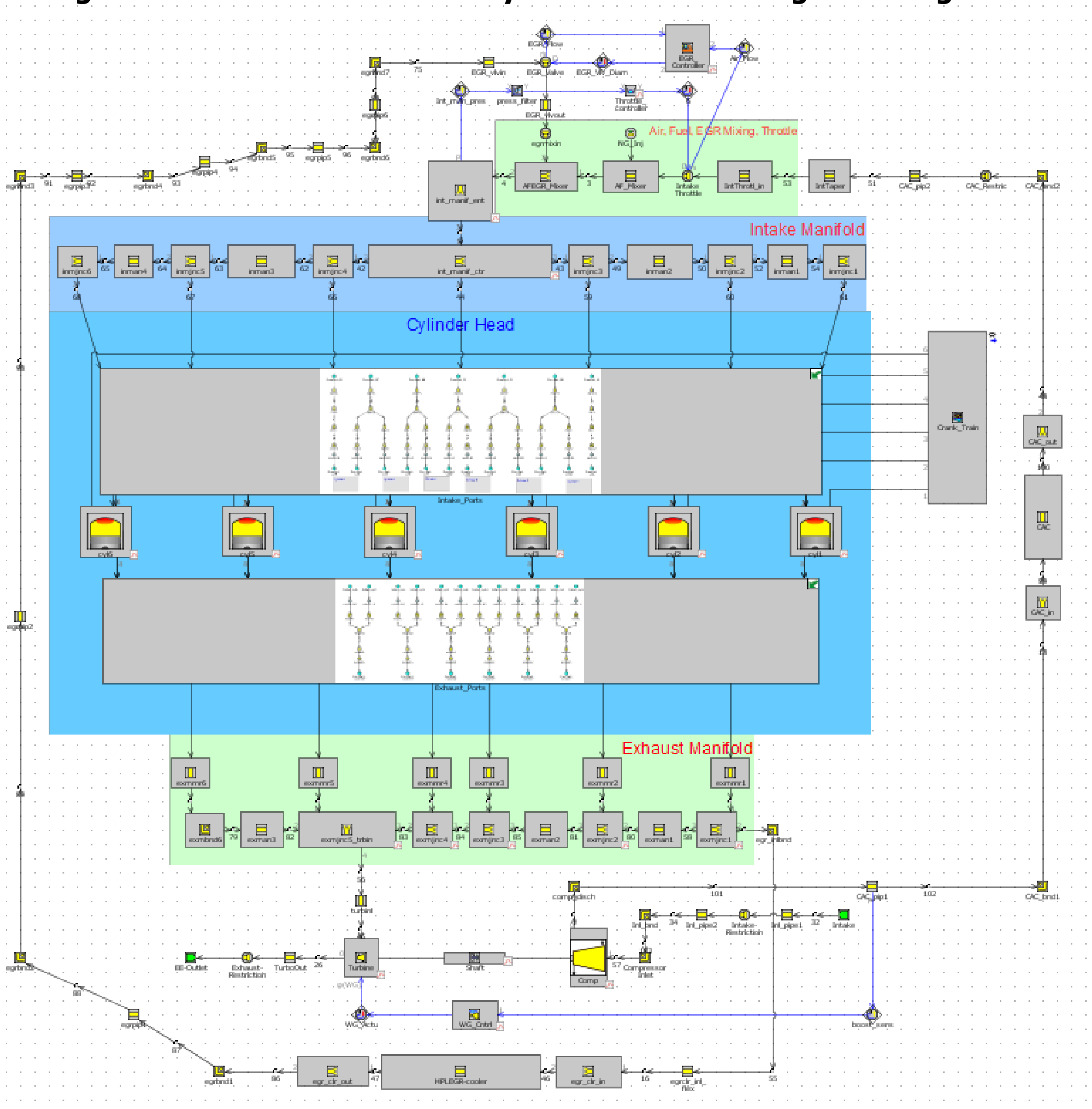

Source: Southwest Research Institute

Table B-1: Tuning Factors and Typical Values

Tuning Factors	Typical Value
In-cylinder heat transfer multiplier	0.9-1.1
Compressor mass multiplier	0.85-1.15
Compressor efficiency multiplier	0.9-1.1
Turbine mass multiplier	0.75-1.25
Turbine efficiency multiplier	0.9-1.1
Fraction of fuel burned	0.92- 0.99

Source: Southwest Research Institute

For this work, detailed compressor and turbine maps were not available for the Holset HE300WG turbocharger. The approximate pressure ratio and mass flow rates for the turbocharger were found on Holset's website [11]. Another turbocharger with similar pressure ratios and mass flow rates was used to input the compressor and turbine maps. The maps were adjusted by tuning mass and efficiency multipliers to match collected data.

The baseline model uses a throttle controller, WG controller and EGR controller. The throttle controller and WG controller are set to control to the measured intake manifold pressure. The EGR controller senses the air flow rate and targets the measured EGR rate.

A Chen-Flynn model was used for friction estimation. This estimates the friction based on mean piston speed, mean piston speed squared and max in-cylinder pressure. Heat transfer coefficients are assigned for coolant to the cylinder and to the head as well as oil to the cylinder and piston. The in-cylinder heat transfer is modeled with the Woschni swirl mechanism and uses a convection multiplier for tuning to collected data.

The model uses an "engcylcombprofile" object for specifying the heat release. Collected in-cylinder pressure data was analyzed for its apparent heat release rate (AHRR) and cumulative heat release (CHR). The CHR was input directly as the combustion rate in the "engcylcombprofile" object. The CHR for all six cylinders are shown in Figure B-3 for the baseline A100 point. The engine exhibits poor air distribution to the different cylinders as shown by the large variation in the CHR for each cylinder. The CHR was input from each respective cylinder to account for the large differences.

Figure B-3: Cumulative Heat Release for 1270 rpm, Full Load 17 percent EGR

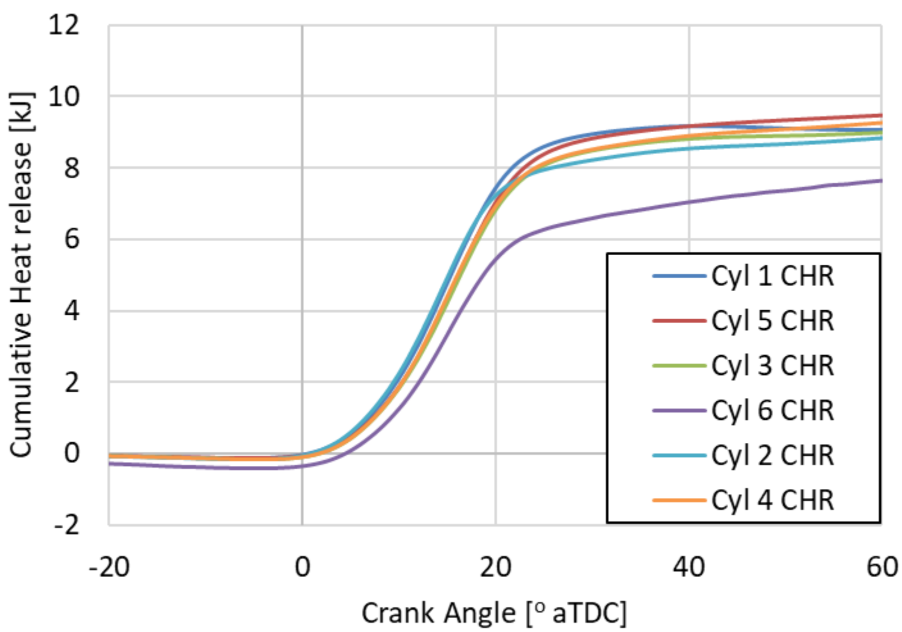

Source: Southwest Research Institute

The turbine and compressor were tuned by mass and efficiency multipliers. In general, the mass multipliers adjusted the mass flow rate at a given compressor power. This primarily adjusted the turbine in and compressor out pressures. The efficiency multipliers mainly adjusted the compressor out temperatures. The final multipliers for the turbocharger are presented in Table B-2. Then the combustion and heat transfer models were tuned after the air flows were matched.

Table B-2: Turbocharger Mass and Efficiency Multipliers Used to Match Test Data

	Mass multiplier	Efficiency multiplier
Compressor	0.87	0.95
Turbine	0.75	0.9

Source: Southwest Research Institute

Initially, fraction of fuel burned was set at 0.98 and the in-cylinder heat transfer was adjusted. This was able to match the test data within 5 percent. Then the fraction of fuel burned was adjusted while maintaining the in-cylinder heat transfer multiplier constant at 1. The fraction of fuel burned was adjusted as a way to lower the combustion efficiency. The simulation matched torque and BSFC within the typical 3 percent error targeted for GT power models. A comparison of simulation and test data for the baseline engine configuration was shown in Table B-3.

Table B-3: Baseline Comparison Between Simulation and Engine Data at A75 Point

Parameter	Units	Simulation	Test Data	Percent Difference
Speed	Rpm	1272	1272	0
Brake Torque	Nm	1525	1509	-1.1
Brake Power	kW	203	201	-1.1
BSFC	g/kW-h	195.9	195.9	0.54
BTE	percent	37.0	37.2	0.32
Fuel Flow	kg/h	39.8	39.6	-0.61
EGR rate	percent	16.6	16.6	0.38
Peak Pressure	Bar	101	106	4.72
Location of Peak Pressure	^{o}aTDC	17.4	17.6	1.13
MAP	Bar	2.17	2.19	0.64
MAT	^{o}C	44	46	5.17
Pre-turbine P	Bar	2.34	2.44	4.07
Pre-turbine T	^{o}C	667	704	5.26

Source: Southwest Research Institute

Knock Prediction

The dilution tolerance testing showed the engine was knock limited at 0 percent EGR at 75 percent load. The baseline GT model was simulated at these conditions and tuned to have the GT Kinetics Fit Natural Gas knock model predict the onset of knock when an unburned fuel fraction of 0.11 was left in the cylinder. Previous engine testing at SwRI has shown this to be a condition with incipient knock. A sweep of knock induction time multipliers was performed on a few of the A75 points from the dilution tolerance testing at incipient knock. The results from the sweep showed a multiplier of 0.42 predicted knock at a mass fraction burned of 0.89, Figure B-4. This multiplier was used in further simulations investigating potential compression ratio increases.

Figure B-4: Knock Induction Time Multiplier Sweep Results at A75 with 0 percent EGR

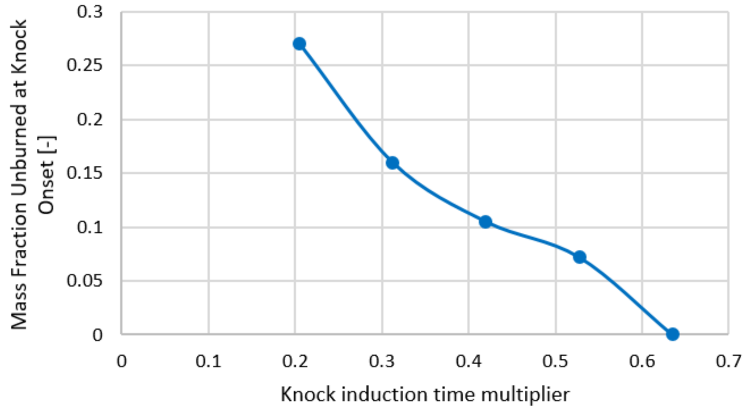

Source: Southwest Research Institute

D-EGR Conversion of Baseline Model

The baseline model was converted to D-EGR operation to aid in analysis of engine results and performance prediction. Most of the baseline model was re-used, but there were some significant changes that were needed. These changes are detailed in the following section.

Major Model Changes

The major model changes made for the conversion to D-EGR for the simulation were in the EGR routing. First, the exhaust manifold was changed to match the modified exhaust manifold detailed in Appendix A. The overall model is shown in Figure B-5 with a zoomed in view of the exhaust manifold in Figure B-6. For comparison, the baseline exhaust piping is presented in Figure B-7. The exhaust manifold for these cylinders are separated from the main exhaust manifold providing a nominal 33 percent EGR. The EGR cooler remained the same as the HP-EGR configuration. A D-EGR mixer was added that was not explicitly modeled in the baseline model. The runner geometries remained the same, but the manifold flow split geometries to cylinders one and six were capped. Cylinders two through five are then the only ones flowing through the turbine. The dedicated cylinders are connected to a separate exhaust pipe routed to the EGR cooler parts. For the stock engine, the EGR valve and mixer are downstream of the throttle.

Because the D-EGR configuration does not deliver a consistent EGR rate intra-cycles, it needs a specially designed mixer, which was discussed in Appendix A. The mixer is modeled as a series of volumes and orifices that approximate the actual mixer design and is located downstream of the charge air cooler but upstream of the throttle. The modeled mixer assembly is shown in Figure B-8. The EGR valve and control parts were removed so the dedicated cylinder breathing controls the EGR rate.

The baseline model and the converted model used test data to target intake manifold pressure (MAP). Additional PFI injectors were added for the dedicated cylinders. The total fuel flow rate was known from test data and could be directly input through the fuel injector for the fumigation system. The air flow is determined by the manifold pressure and temperature as controlled to values from test data. The cumulative heat release (CHR) from test data was imported directly for each cylinder to determine burn rates.

Figure B-5: GT Power Model of the D-EGR Engine Configuration

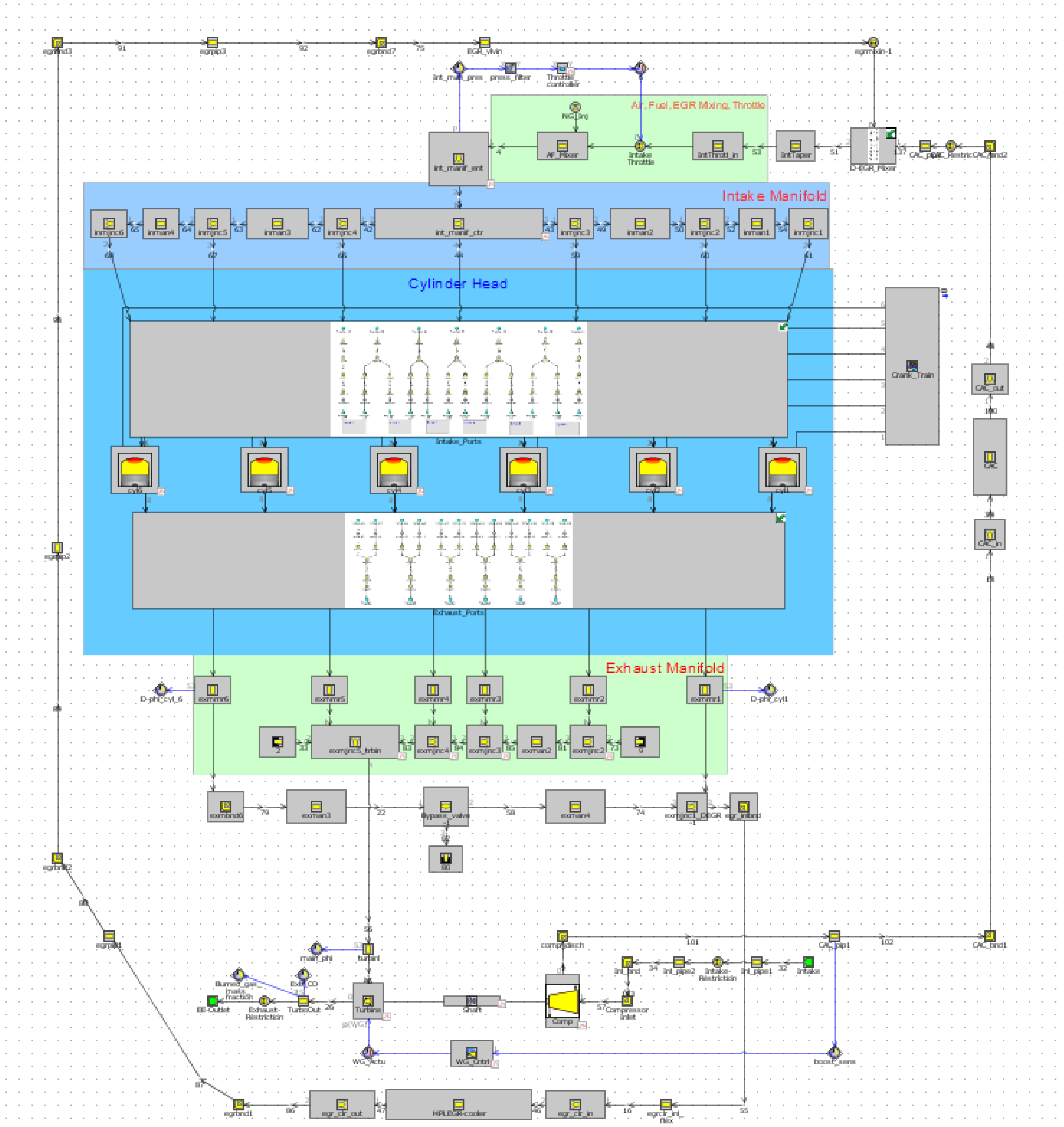

Source: Southwest Research Institute

Figure B-6: Exhaust Manifold Model Modified for Main and Dedicated Cylinders

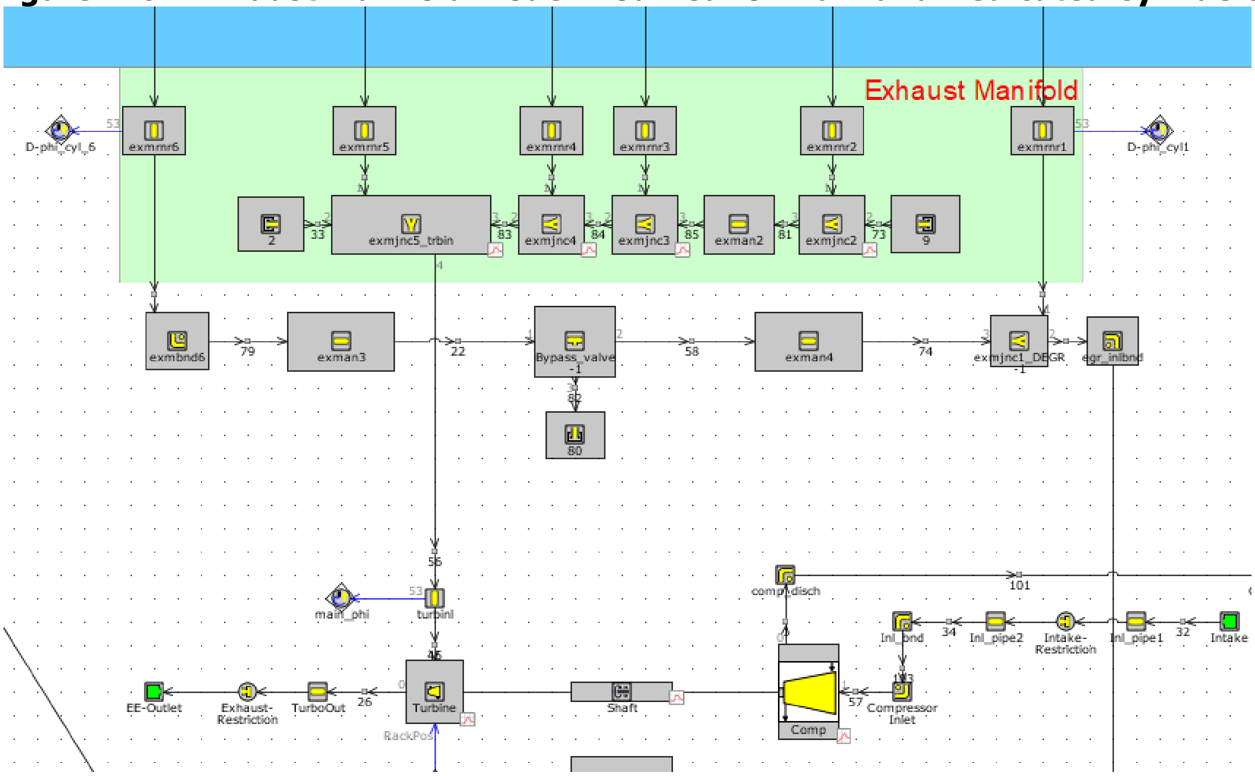

Source: Southwest Research Institute

Figure B-7: Stock Exhaust Manifold Model

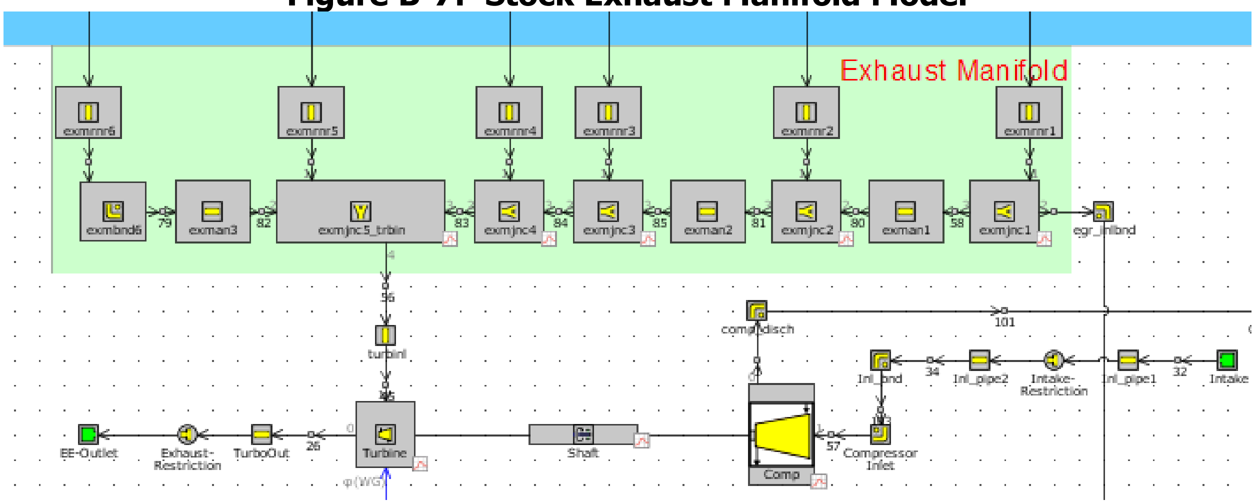

Source: Southwest Research Institute

Figure B-8: Sub-model of D-EGR Mixer

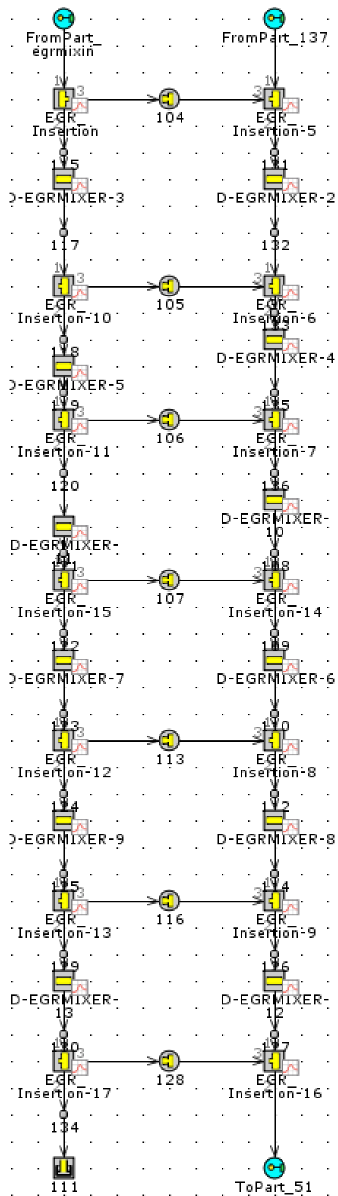

Source: Southwest Research Institute

D-EGR Model Calibration

The D-EGR model was calibrated to initial engine data in D-EGR configuration. The only modification made to the base engine was the EGR configuration and addition of high energy ignition system. The simulation to test data comparison is shown in
Table B-4. The power and BSFC error were less than 5 percent between the simulation in the model. This was acceptable for having tuned the model without the actual turbine and compressor maps.

Table B-4: A75 Data Comparison Between Simulation and Test Data in D-EGR Configuration (Stock Turbocharger and Piston)

Parameter	Units	Simulation	Test Data	Percent Difference
Speed	Rpm	1270	1269	-.1
Brake Torque	Nm	1556	1504	-3.4
Brake Power	kW	207	200	-3.5
BSFC	g/kW-h	187	192	2.6
BTE	percent	39.1	38.1	-2.7
Fuel Flow	kg/h	38.6	38.2	-0.77
Air flow	Kg/h	641	648	1.1
Peak Pressure	Bar	124	126	1.6
Location of Peak Pressure	°aTDC	11.9	11.7	-1.7
MAP	Bar	2.52	2.56	1.6
MAT	°C	55	56	1.8
Pre-turbine P	Bar	2.62	2.68	2.2
Pre-turbine T	°C	562	610	7.9

Source: Southwest Research Institute

The logP-logV diagrams for a main and a dedicated cylinder are shown in Figure B-9 and Figure B-10. The simulation was able to predict the blow-down and gas exchange events. The compression and expansion strokes also have the correct slopes to signify the trapped mass was representative of test data. The valve timing and port heat transfer were unchanged from the baseline engine simulation. The exhaust runner conditions can also affect the residuals and cause differences in the compression slope. The two figures demonstrate the model was able to account for the correct exhaust pressures for a dedicated versus a main cylinder. The dedicated cylinders had greater exhaust pressures than main cylinders because they are providing the pumping work for the EGR loop.

Figure B-9: Dedicated Cylinder Pressure Comparison (A75)

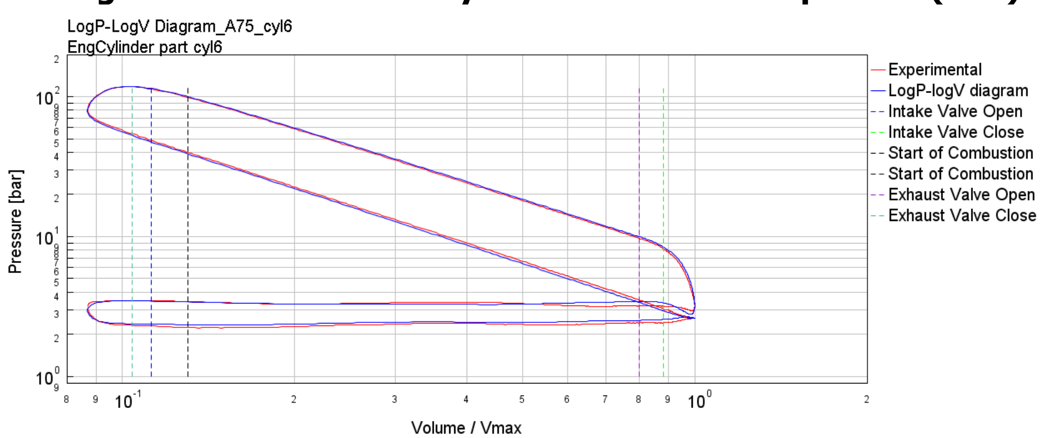

Source: Southwest Research Institute

Figure B-10: Main Cylinder Pressure Comparison (A75)

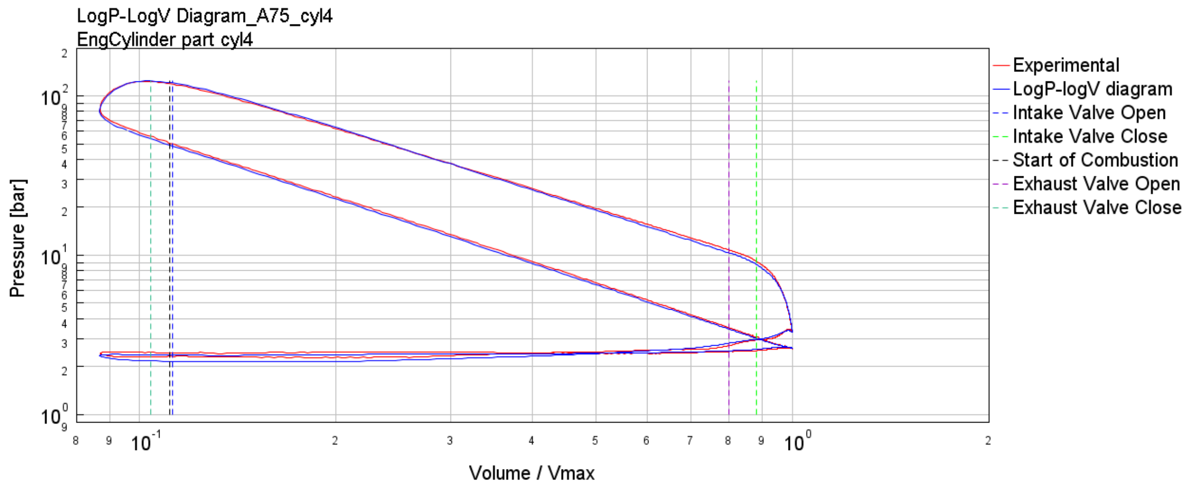

Source: Southwest Research Institute

Hardware Selection

Compression Ratio Prediction

The initial compression ratio increase was determined by modeling increased compression ratios using the knock model previously discussed to predict the onset of knock. A Wiebe model was generated to match the CHR from cylinder 1 for a prediction of knock tolerance at increased compression ratios in the D-EGR configuration. This was performed with the CHR from cylinder 1 because it is the fastest burning of the cylinders and most likely to knock. A design of experiments run was performed on the D-EGR model with the knock induction time multiplier at 0.42 while varying the compression ratio from 11.5 to 12.5 and the CA50 from 8 to 20 ^{o}aTDC. The results from the DOE are shown in Figure B-11 and can compare that to the baseline combustion phasing in Figure B-12.

Figure B-11: Mass Fraction Unburned at Knock Onset for Compression Ratio and Combustion Phasing Sweep

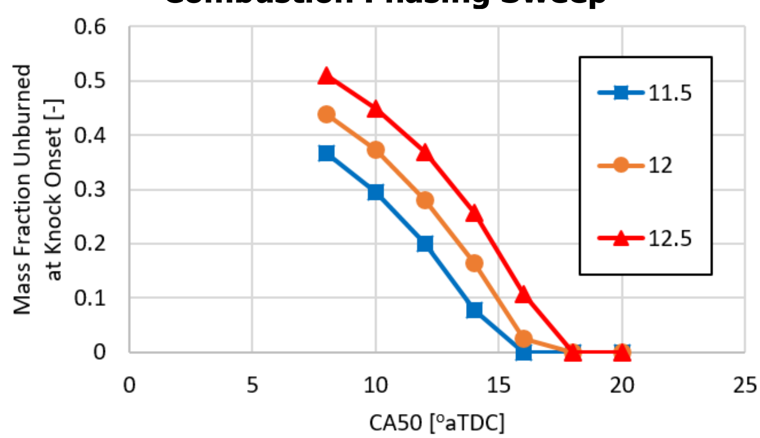

Source: Southwest Research Institute

Figure B-12: Combustion Phasing (CA50) for the Baseline Engine

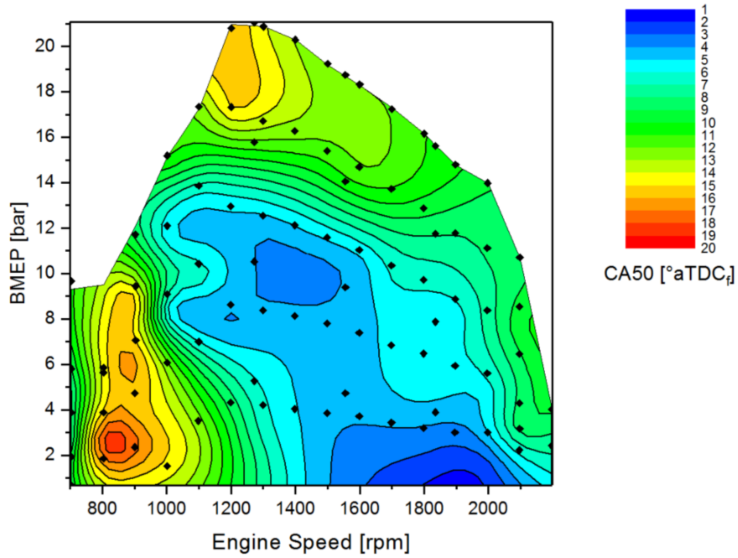

Source: Southwest Research Institute

The stock combustion phasing at 1270 rpm full load is approximately 16 °aTDC. The simulation showed that with the increased dilution level of D-EGR, the combustion phasing can be advanced to 14 °aTDC with the compression ratio maintained at 11.5. Increasing the compression ratio to 12.5 required approximately 2 degrees of combustion retard to avoid knocking. This allowed the combustion phasing to be the same as the baseline with one point of compression ratio increase. 13.0:1 is possible with slight combustion phasing retard, but increased combustion phasing retard across a larger area of the operating range may not have provided the desired efficiency improvement. A compression ratio of 12.5 was selected for the turbocharger matching exercise as it was the more conservative for air flow requirements.

Turbocharger Selection

Airflow Requirement Prediction

As there was a long lead time associated with procuring a prototype turbocharger, the initial airflow requirements were predicted using the D-EGR GT-Power model before the model could be calibrated to engine data in D-EGR configuration. Additionally, the stock turbocharger maps were replaced with simple compressor and turbine models. The assumed compressor and turbine efficiencies were determined based upon SwRI's and Garrett's (formerly Honeywell) experience with next generation turbocharging hardware. Combustion was assumed to be at maximum brake torque (MBT) phasing and a constant duration consistent with advanced ignition systems. The compression ratio was increased to 12.5:1 and the MBT phasing assumption was later validated once the calibrated knock model was available. Details of the model assumptions are provided in Table B-5. The model was run targeting the stock torque curve and the results were consolidated into a data reduction spreadsheet, Table B-6, and provided to Garrett for initial map selection.

Table B-5: Airflow Prediction Model Assumptions

Item	Assumption
Combustion Phasing	10 deg aTDCf
Combustion Duration	20 degCA
Compression Ratio	12.5:1
Compressor Efficiency	72 percent
Turbine Efficiency	68 percent
Model Calibration Stage	Baseline engine data
Knock Model	Not active

Source: Southwest Research Institute

Table B-6: Data Provided Garrett to Select a Turbocharger for the D-EGR Configuration

		****************************** INPUT DATA ******************************							
AIR FLOW (Wa)	g/s	79.9	150.3	239.6	273.1	298.3	298.5	308.1	246.1
ENGINE SPEED (ERPM)	RPM	800	1000	1200	1400	1600	1800	2000	2100
POWER (P)	kW	75.3	151.9	259.4	284.7	294.1	290.4	279.3	224.8
FUEL FLOW (Wf)	kg/h	17.3	32.5	51.8	59.0	64.4	64.5	66.6	53.2
(alternatively BSFC)	g/kWh	229.0	213.9	199.6	207.4	219.0	222.0	238.3	236.6
AIR+EGR FLOW (Wa)	g/s	122.8	232.4	372.0	422.9	461.9	461.3	478.0	380.0
SMOKE INDEX	UB								
TURBO SPEED (N)	rpm								
COMPRESSOR INLET TEMP (T1c)	°C	25	25	25	25	25	25	25	25
COMPRESSOR OUTLET TEMP (T2c)	°C	106	175	232	234	234	217	208	158
CHARGE COOLER OUTLET TEMP (T2cac)	°C	47	50	54	54	55	54	54	50
ENGINE INLET TEMP (T1e)	°C	69	71	73	73	72	72	72	70
TURBINE INLET TEMP (T1t)	°C	487	559	639	623	648	669	658	643
TURBINE OUTLET TEMP (T2t) T1_EGR	°C	426	445	479	460	485	520	516	540
CHARGE COOLER COOLANT TEMP (T1x)	°C								
AMBIENT PRESSURE (P0)	kPa abs	101.3	101.3	101.3	101.3	101.3	101.3	101.3	101.3
COMPRESSOR INLET PRESS (P1c)	kPa abs	98.3	97.0	94.2	92.8	91.5	91.5	91.0	93.9
COMPRESSOR OUTLET PRESS (P2c)	kPa abs	183.9	288.0	397.1	397.2	392.6	353.9	334.3	251.8
ENGINE INLET PRESS (P1e)	kPa abs	180.4	280.3	383.4	379.8	371.9	331.0	308.3	229.4
TURBINE INLET PRESS (P1t)	kPa abs	175.6	317.9	518.8	579.5	614.7	577.2	574.7	401.6
TURBINE OUTLET PRESS (P2t)	kPa abs	100.1	102.8	109.1	111.7	114.8	115.5	116.6	110.5
EGR Rate	%	34.95	35.29	35.57	35.40	35.42	35.27	35.52	35.21

Source: Southwest Research Institute

Turbocharger Selection

Garrett used the provided airflow data to screen available turbine and compressor maps that can be assembled into a new unit. It was not expected that an off-the-shelf unit would be able to achieve the performance requirements as the turbine is missing two cylinders worth of flow in D-EGR configuration. Two solutions were identified that had the potential to achieve the desired torque with both requiring prototype wheels to be manufactured. Garrett provided the map data to be input into GT-Power to select the primary unit choice. These maps are shown in Figure B-13 and Figure B-14. The GT3571V unit uses a VNT mechanism to control the power produced by the turbine while the GT3067 unit uses a traditional wastegate mechanism.

Figure B-13: VNT Turbocharger (GT3571V) Turbine and Compressor Map

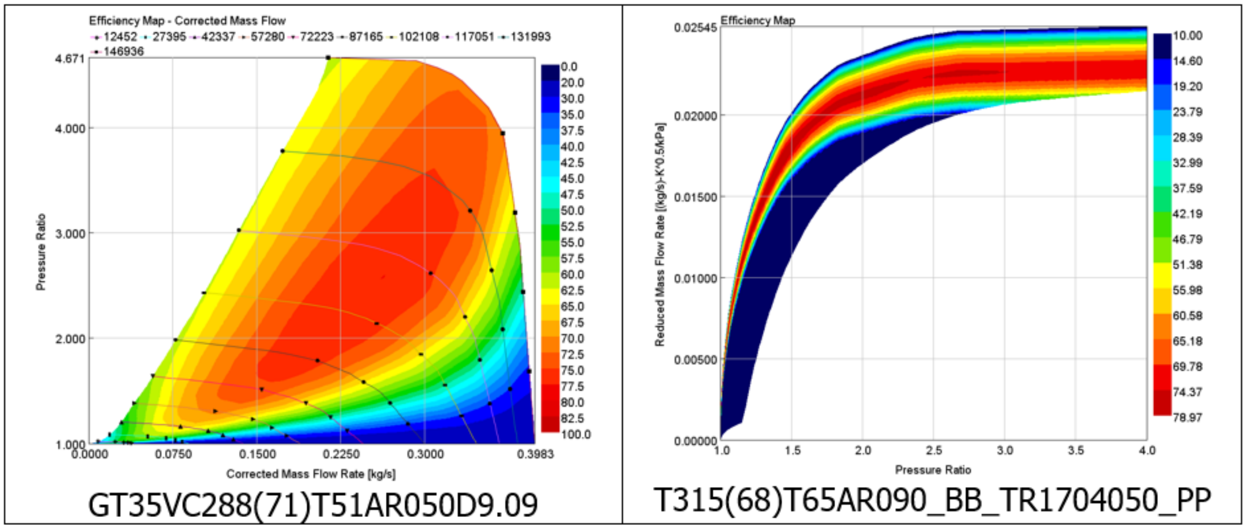

Source: Southwest Research Institute

Figure B-14: Wastegate Turbocharger (GT3067) Turbine and Compressor Map

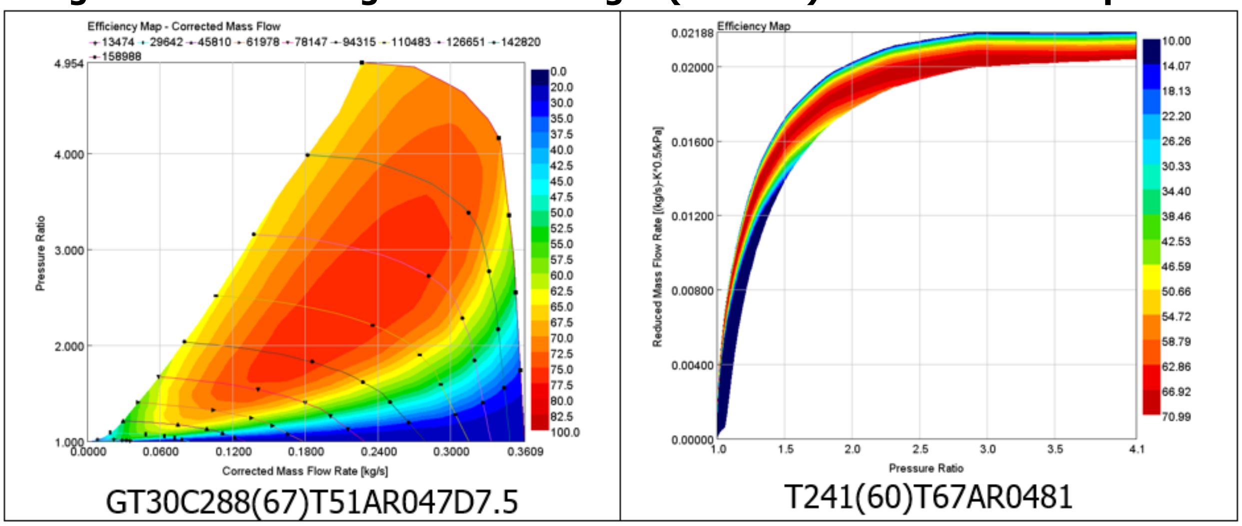

Source: Southwest Research Institute

The map data was input into GT-Power to replace the simple turbine and compressor models. All other input data remained the same as shown in Table B-5. Additional scaling of the turbine and compressor maps, via mass and efficiency multipliers, were not used as the data came directly from Garrett. Figure B-15 shows the predicted performance of the two turbochargers along the torque curve. The VNT turbocharger was able to achieve the desired torque at all the engine speeds whereas the wastegate turbocharger was only able to achieve the desired load at speeds above 1200 rpm. The VNT turbocharger had some operational margin with the VNT mechanism at lower engine speeds while the wastegate was fully closed below the peak torque speed, Figure B-16.

Figure B-15: Predicted Torque Curve Performance with VNT and Wastegate Turbochargers

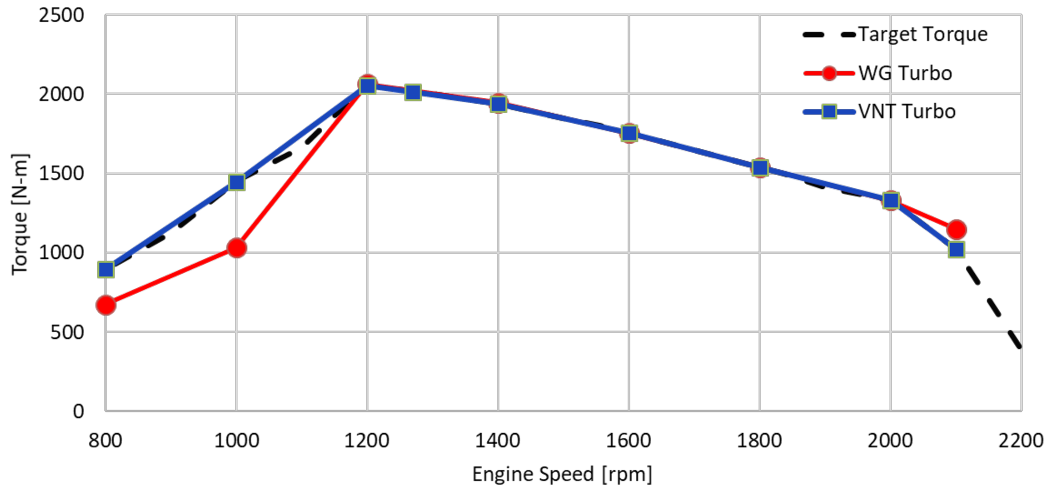

Source: Southwest Research Institute

Figure B-16: VNT Rack Position and Wastegate Diameter at Torque Curve Operation

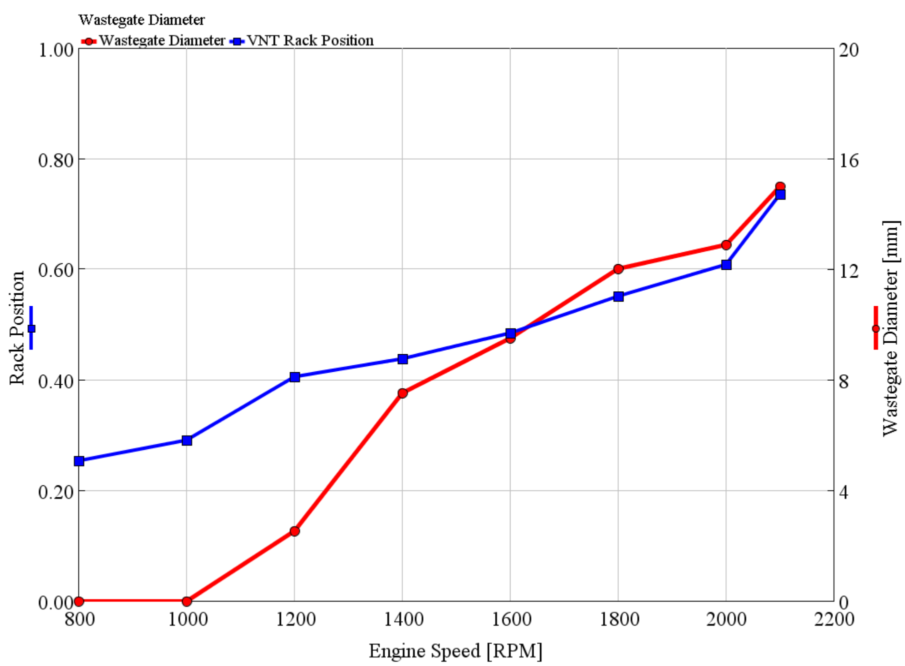

Source: Southwest Research Institute

The fuel consumption was lower for the VNT turbocharger across all engine speeds (Figure B-17). This is primarily from the lower pumping work from the VNT turbocharger (Figure B-18). At 1000 rpm and below, despite higher pumping work from the VNT, the fuel consumption was lower than the wastegate case because the overall thermal efficiency was higher for the higher low-speed torque achieved with the VNT. As the VNT turbocharger has wider operational margin and lower fuel consumption, the VNT turbocharger was chosen as the primary turbocharger for physical engine testing.

Figure B-17: BSFC Comparison for VNT and Wastegate Turbocharger

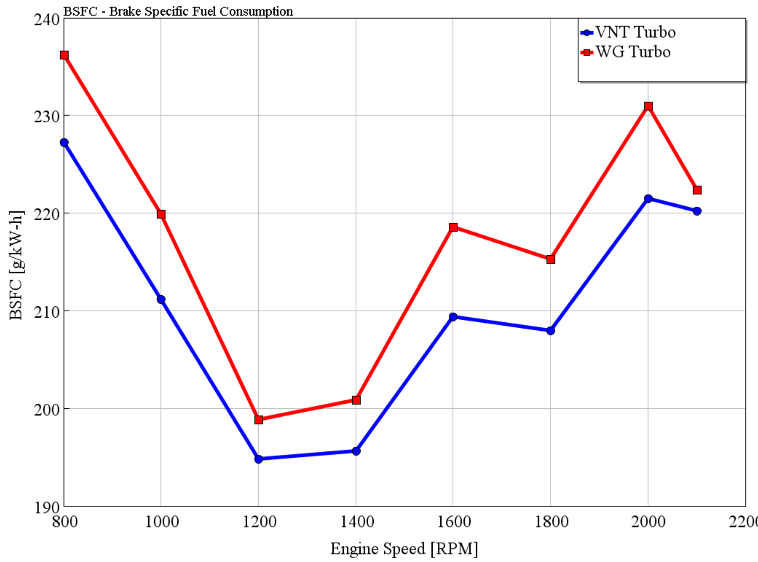

Source: Southwest Research Institute

Figure B-18: PMEP Comparison for VNT and Wastegate Turbocharger

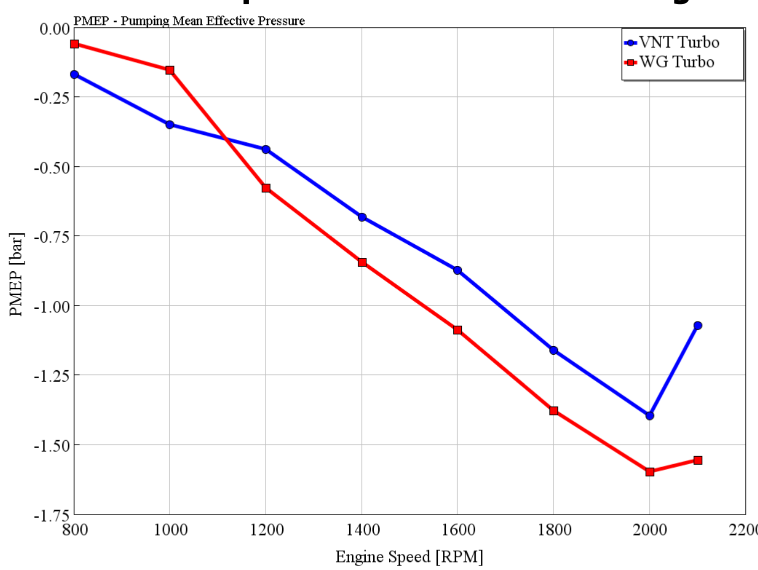

Source: Southwest Research Institute

Summary

A GT-Power model of the Cummins Westport ISX12 G was calibrated to baseline engine data. Multipliers were used to tune the compressor and turbine maps to match engine inlet and outlet manifold conditions. Then in-cylinder heat transfer and fraction of fuel burned values were adjusted to match test data within three percent. The model was updated to match the D-EGR modifications, including splitting the main and dedicated exhaust manifolds and adding in a D-EGR mixer representative of the on-engine hardware. This was first tuned to match the test data with the stock turbocharger. Without the actual compressor and turbine maps the simulations match test data values within five percent.

A dilution tolerance study was conducted on the engine before the engine was converted to its D-EGR configuration. At low EGR rates and high loads the engine was knock limited. A few of these points were used to tune the kinetics-fit-natural-gas knock model provided by GT-Power. The knock model was used early on in the project to start the long lead time task of iterating and procuring high compression ratio pistons. The knock model predicted a one point CR increase was reasonable and a more aggressive CR around 13:1 could also be investigated.

Using assumed turbine and compressor efficiencies, air flow requirements were predicted for the engine in D-EGR configuration. This data was reviewed by Garrett to select potential turbochargers that would allow for the stock torque curve to be maintained. Two prototype options were presented, a VNT turbocharger and a wastegate turbocharger. The VNT option was preferred as it had the capability to achieve the desired torque curve at all engine speeds while the wastegate turbocharger was predicted to be deficient at lower engine speeds.

APPENDIX C: Piston Development Using Computation Fluid Dynamics

Computational Fluid Dynamics (CFD) was used to aid in the development of the improved piston design. The computational setup of the CFD simulations is provided in Table C-1. A well-mixed reactor with chemical kinetics in each computational cell was used (mechanism consisting of 53 species and 325 reactions) to simulate both the flame propagation and knocking events.

Table C-1: Computational Setup for Combustion CFD Simulations

Modeling Tool	CONVERGE v2.4
Dimensionality, and type of grid	3D, Cut-cell, Adaptive Mesh Resolution
Smallest and largest grid size	Base grid size: 6 mm Fixed embedding near spark: 0.1875 mm Gradient base AMR on velocity and temperature fields: 0.75 mm
Time-step size	Variable (1e-8 to 2.5e-5 sec)
Combustion model	Detailed chemistry combustion model (53 species and 325 reactions)
Turbulence model	RANS (RNG k-ε model)
Peak Cell count	~1 million at BDC

Source: Southwest Research Institute

Figure C-1 shows the CAD geometry as modeled in CFD. The cylinder model had two split intake ports with two manifolds upstream and two exhaust ports with one manifold downstream. The re-entrant stock piston bowl is also shown in the figure. Experiments were done on the stock piston at various EGR levels and speed-load operating points.

Figure C-1: CAD Geometry Used in the CFD Engine Modeling

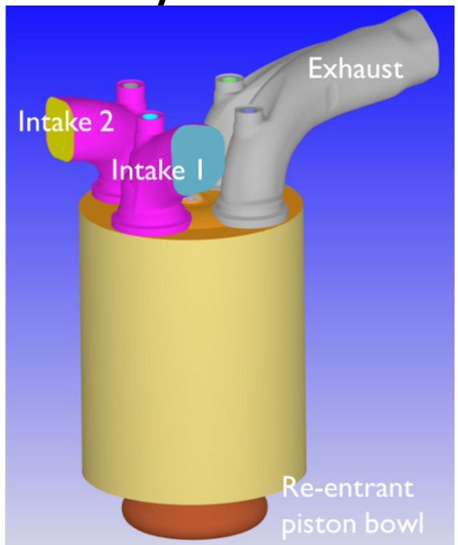

Source: Southwest Research Institute

Table C-2 shows the operating conditions used for CFD validation. The experiment used a DCO® high energy ignition system which is designed to create a pseudo-continuous discharge to improve ignition and flame development in dilute fuel-air mixtures. This was simulated with 0.01 J of energy during breakdown phase for 0.1 CAD and then 0.07 J of energy during the glow phase for the next 15 CAD. The energy was comparable to a typical DCO ignition event. The EGR rate was set at ~20 percent in the boundary conditions.

Table C-2: Engine Operating Point for CFD Validation

Item	Measurement
Bore	130 mm
Stroke	150 mm
Compression Ratio	11.5
Speed	1272 RPM
Load	23.58 bar nIMEP
EGR	20.45 percent
AFR	18.1
Spark timing	-10.5 deg.
EVO, EVC, IVO, IVC timing	-581,-363,-360,-129 deg.

Source: Southwest Research Institute

Figure C-2 shows the in-cylinder pressure from the experimental data. Cylinder pressure variability was seen clearly, and peak cylinder pressure ranged from 110 to 150 bar.

Figure C-2: Cycle-to-Cycle Variation Observed in Experiments for Pressure Traces

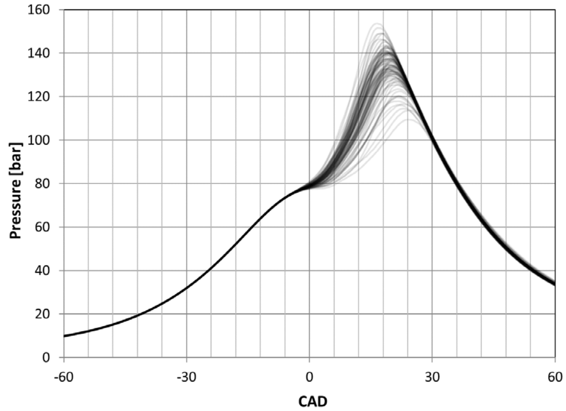

Source: Southwest Research Institute

As RANS CFD simulations represent an “average” cycle, the most appropriate comparison between the experimental results and the CFD results is to use the mean cycle from the cylinder pressure spread as the equivalent cycle for comparison. Using this approach, the impacts of D-EGR, piston bowl shape, and compression ratio can be evaluated with respect to the baseline engine configuration.

Piston Bowl Modifications

The stock piston was a re-entrant bowl design with a very high squish area ratio of 0.8. The port geometry for the Cummins-Westport ISX12G was designed for diesel combustion and generates swirl rather than tumble, which means the turbulence isn’t very high. The squish breaks up the swirl to try and regain the right kind of flow motion for spark ignited combustion. The high swirl also results in high heat transfer to the walls of the cylinder. In a spark ignited system where flame propagation is dominant, the increase of wall heat transfer might be more dominant than the flame speed improvement that is a result of the turbulence generated by squish. While reduction of the swirl ratio was desired, it was expected that it would require a level of effort that was outside the scope of this project to achieve. To reduce the heat transfer losses, an open bowl piston with lower surface area (SwRI v1) was designed. The SwRI v1 piston design reduced the squish area ratio to 0.54. The compression ratio and the squish height were kept the same between the stock piston and SwRI v1, so the bowl depth was adjusted to maintain the production compression ratio. Figure C-3 shows the CAD geometry of the stock and the SwRI v1 pistons.

Figure C-3: Piston Bowl Differences Between the Stock (Top) and SwRI V1 (Bottom) Pistons

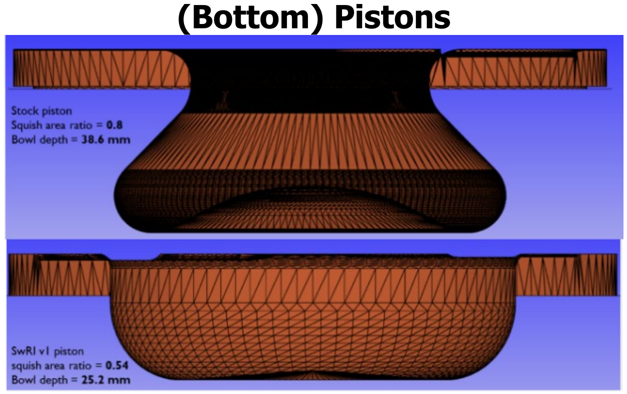

Source: Southwest Research Institute

Combustion simulations were performed for these two pistons at the same operating conditions as shown in Table C-2. Boundary conditions were kept the same between these two sets of simulations. Ignition timing for the SwRI v1 piston was advanced by 5 deg. to maintain the same combustion phasing (MFB50) as that of the stock piston. Figure C-4 shows the in-cylinder pressure and apparent heat release rate (AHRR) profiles with the stock and SwRI v1 pistons. The pressure and apparent heat release rate for maximum and minimum traces are overlaid along with the scatter of MFB50 timing and peak cylinder pressure to get an idea of where the CFD traces lie with respect to the experimental data.

Figure C-4: Pressure and Apparent Heat Release Rate Profiles between the Stock Experiments and Stock and SwRI V1 CFD Along with Experimental Spreads.

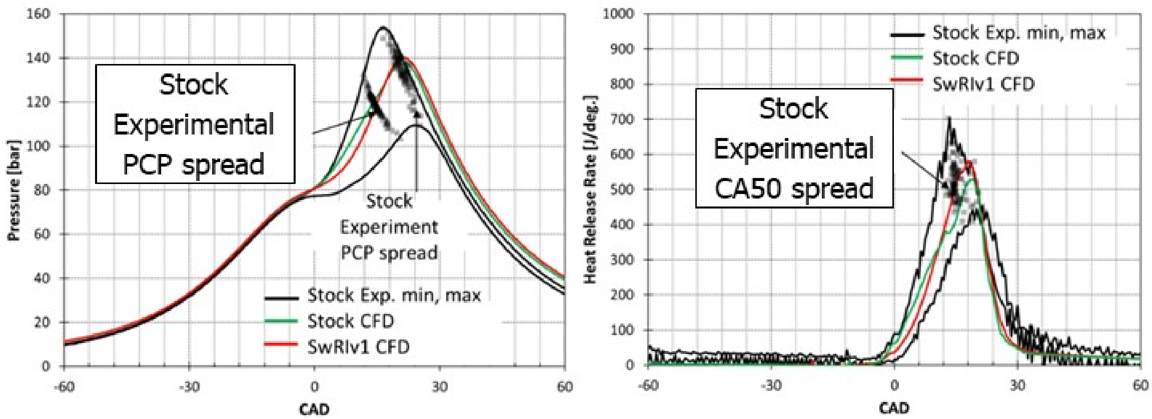

Source: Southwest Research Institute

Combustion phasing of the experimental results (stock piston), and the two CFD cases with stock and SwRI v1 pistons are shown in Table C-3 along with calculated closed cycle (IVC to EVO) indicated thermal efficiency (ITE) for the CFD cases. It is to be noted that the CA50 timing of the CFD stock case was around 1.5 CAD later than the experimental average MFB50 timing (but was within the total CA50 spread). The main objective of these initial simulations was to show a good correlation of the model to experimental data and show no significant impact to combustion performance with the revised piston design. This provided a good baseline point with the stock piston simulation for evaluation of efficiency improvements from further changes.

Table C-3: Combustion Phasing and ITE Comparisons

	Experiment	Stock Piston	SwRI v1 Piston
CA10 (deg.)	6.3	6	8
CA50 (deg.)	15.1	16.6	16.8
CA90 (deg.)	22.7	24.8	25.7
MFB10-90 (deg.)	16.4	18.8	17.7
ITE (percent) IVC – EVO		38.5	39.8

Source: Southwest Research Institute

Table C-3 shows that SwRI v1 piston had an increase in ITE (calculated from IVC to EVO) of 1.3 ITE points over the stock piston. The MFB10-90 burn durations for the two pistons were similar. Therefore, the ITE improvement was determined to be a result of reduced wall heat loss for the SwRI v1 open bowl piston. The comparison of wall heat losses is shown in Figure C-5. The SwRI v1 open bowl piston had a 41 percent reduction in heat loss. This contribution came mainly from the reduced surface area to volume ratio of the piston as the effect on the liner and head heat loss was minimal.

Figure C-5: Heat Transfer Benefit of Using an Open Bowl Piston (SwRI v1 Piston) Over a Re-Entrant Bowl (Stock Piston)

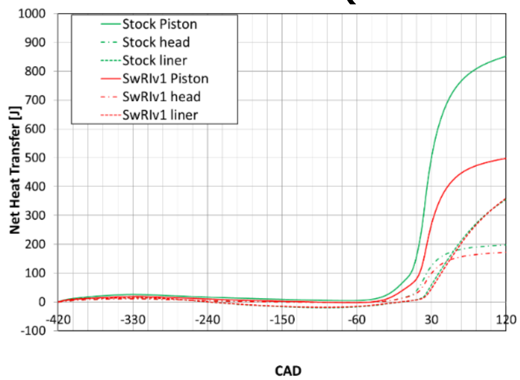

Source: Southwest Research Institute

Figure C-6 shows averaged turbulent kinetic energy (TKE) values for the two pistons in three regions: the squish zone around the top of the piston, the piston bowl and in a 15 mm diameter sphere around the spark center, as illustrated in the inset figure. Due to the reduced squish for the SwRI v1 piston, the TKE values were lower in the squish zone and in the spark plug zone. This slowed the initial flame kernel formation such that the spark timing was advanced to maintain the same combustion phasing as the stock piston. The SwRI v1 piston had a shorter bowl depth, which meant the fluid flow exiting from the squish was constrained in a shorter length of vertical travel before it touched the piston base. This induced more mixing in the bowl region and was evident in higher TKE values for the SwRI v1 piston bowl bottom region relative to the stock piston, in addition to lower turbulence dissipation rates. The SwRI v1 piston had a faster MFB10-50 burn duration by about 2.1 degrees (from Table C-3).

Figure C-6: TKE Comparisons between the Stock and SwRI v1 Pistons in Three Zones: Spark Plug 15 mm Diameter Sphere, In-Bowl and Out-of-Bowl Regions

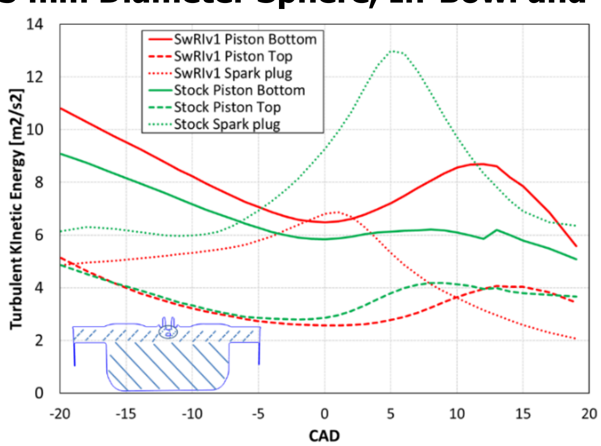

Source: Southwest Research Institute

The SwRI v1 piston design showed an overall improvement in closed cycle efficiency due primarily to reduced heat transfer. Further, the main combustion duration, as measured by MFB10-90, was maintained at the stock level, even with reduced squish. The reduction of TKE around the spark plug increased the duration of early flame kernel formation which may negatively impact dilution tolerance. However, the presence of H_2 from enriched D-EGR operation was expected to help recover the initial flame kernel formation duration. The SwRI v1 piston design showed sufficient efficiency improvement potential and was used as the base design for further simulation studies.

D-EGR Simulations

Simulations were carried out with the D-EGR concept where the enrichment in the dedicated cylinder was set to a phi of 1.34 and the main cylinder was stoichiometric. The EGR rate with D-EGR was increased to 30 percent. With D-EGR, the intake concentration included Hydrogen (H_2) and carbon monoxide (CO), which were directed from the exhaust of the dedicated cylinder into the intake manifold and on to the cylinders. The intake manifold pressure was higher due to the higher dilution. Equilibrium calculations and GT-power models were utilized to obtain the intake concentrations and pressures respectively, such that the net fuel energy going to the cylinder was kept constant between the D-EGR and the HP-EGR cases. Due to H_2 and CO being in the intake stream, the flow rate of natural gas was reduced slightly. These boundary conditions were updated in the CFD model of the stock and SwRI v1 pistons. Simulations were performed at the same compression ratio to evaluate the effect of the D-EGR on burn durations and efficiency. Figure C-7 shows the pressure and apparent heat release rate comparisons between D-EGR and HP-EGR cases at EGR levels of 30 percent and 20 percent respectively.

Figure C-7: Cylinder Pressure and Heat Release Rate Comparison between D-EGR and HP-EGR Cases for Stock and SwRI V1 Pistons

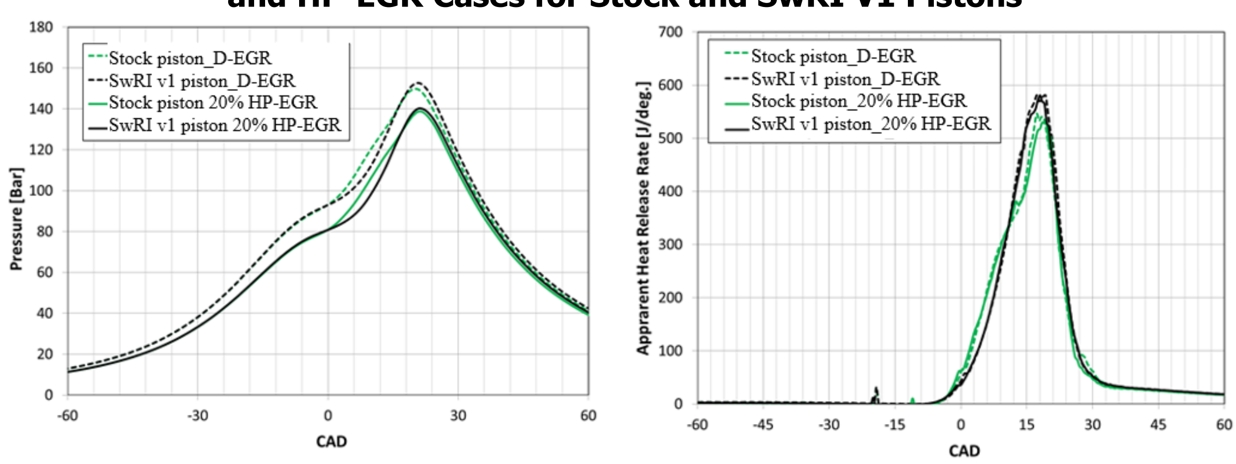

Source: Southwest Research Institute

The CA50 timings for the D-EGR simulation cases were adjusted to maintain the same combustion phasing as the HPL-EGR case. The effect of increased intake pressure can be seen as increased compression pressure in the compression stage of the cycle, but the overall trend of the pressure trace was similar for the two pistons with these two EGR cases. The AHRR traces were also similar but there was a slight increase in the burn duration with the D-EGR case, since it had a higher EGR fraction (30 percent vs. 20 percent). As shown in Table C-4, the burn durations increased by 1.6 deg. for the stock piston and by 1.1 deg. for the SwRI v1 piston. Despite the increase in burn duration, there was an ITE benefit observed with the use of D-EGR.

Table C-4: Combustion Phasing and ITE Comparisons Between HPL-EGR and D-EGR Cases

	Stock HP-EGR	SwRI v1 HP-EGR	Stock D-EGR	SwRI v1 D-EGR
CA10 (deg.)	6	8	5.7	7.5
CA50 (deg.)	16.6	16.8	16.5	16.9
CA90 (deg.)	24.8	25.7	26.1	26.3
MFB10-90 (deg.)	18.8	17.7	20.4	18.8
ITE (percent) IVC –EVO	38.5	39.8	39.3	40.6

Source: Southwest Research Institute

The intake stream of D-EGR had H_2 and CO which are fuels. H_2 has an LHV value of 120 MJ/kg and CO has an LHV of 10 MJ/kg, whereas the natural gas fuel had an LHV value of 49.63 MJ/kg. Due to the requirement of higher EGR fraction in the 30 percent D-EGR mixture, the intake stream had a higher intake pressure but the in-cylinder equivalence ratio of the 30 percent D-EGR could still be maintained at the same level as that of 20 percent LPL-EGR mixture without increasing the fueling. This led to an ITE benefit along with better combustion characteristics for the H_2-CO blended natural gas fuel as part of the D-EGR system. A 2 percent increase in ITE was observed when upgrading from 20 percent LPL-EGR to a 30 percent D-EGR for both the piston bowls.

Knock Analysis

Knock is a limiting factor in the efficiency potential of SI engines. Low to medium engine speeds are the most effected by knock due to higher residence times available for the fuel-air mixture, which effects the temperature history of the charge. Retarding spark timing influences the temperature history of the charge and helps in lowering the end-gas temperature (increasing the ignition delay), thus mitigating knock. Spark retard has negative effects on efficiency and leads to higher exhaust gas temperatures. Increasing spark retard also negatively impacts engine stability. The traditional way to overcome the knock and stability problem is to reduce the compression ratio, which also has a negative effect on efficiency. EGR helps reduce knock by reducing the temperature rise of the end gas via lower adiabatic flame temperature and increased heat capacity of the working fluid. With the higher EGR rate from D-EGR and improved flame kernel formation from the presence of H_2, there is a pathway to increase the compression ratio of the engine while maintaining comparable knock characteristics to the baseline configuration. The SwRI v1 design was modified to increase the compression ratio by 1.5 points while keeping the squish ratio the same. This was accomplished by reducing the piston bowl depth. Figure C-8 shows the modified piston (SwRI v2) along with the original SwRI v1 piston.

Figure C-8: SwRI v1 and SwRI v2 Piston Designs. SwRI v2 Bowl Depth Reduced to Increase CR

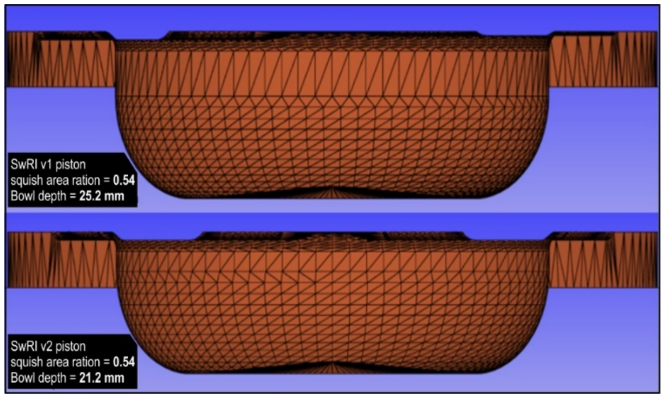

Source: Southwest Research Institute

The SwRI v2 piston (SwRI v1 + 1.5 CR) was simulated at the same CA50 as that of the SwRI v1 piston simulations from the previous section. All simulations had same the fuel energy input. Figure C-9 shows the pressures and AHRR as the CR was increased from 11.65:1 to 13.15:1 (+1.5). The effect of increased CR led to increased compression work and increased the ITE. Table C-5 shows combustion phasing and ITE benefits as the CR was increased for the SwRI v1 piston. Increasing the compression ratio increased the ITE of the SwRI v1 piston (with D-EGR) by 1 ITE percentage point. The final increase in the ITE of the SwRI v2 piston over the baseline stock piston (with 20 percent HP-EGR) is 3.1 ITE points.

Figure C-9: Cylinder Pressure and Heat Release Rate Comparisons between SwRI v1 and SwRI v2 with D-EGR

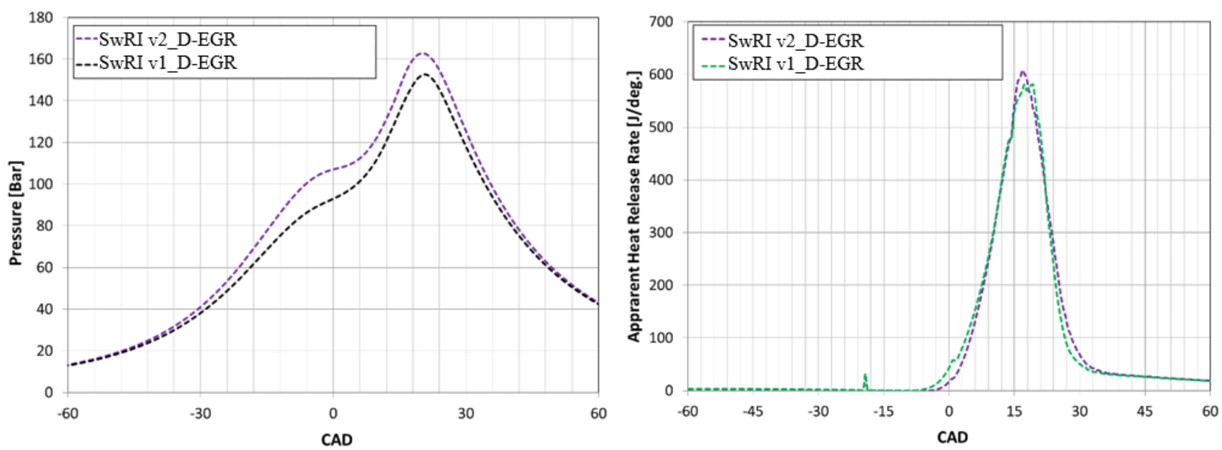

Source: Southwest Research Institute

Table C-5: Combustion and Indicated Thermal Efficiency (Closed Cycle) Comparison Between Stock (HP-EGR) and SwRI v1/v2 with D-EGR

	Stock HPL-EGR	SwRI v1 D-EGR	SwRI v2 D-EGR
CA10 (deg.)	6	7.5	8.5
CA50 (deg.)	16.6	16.9	17.1
CA90 (deg.)	24.8	26.3	27.2
MFB10-90 (deg.)	18.8	18.8	18.7
ITE (percent) IVC – EVO	38.5	40.6	41.6

Source: Southwest Research Institute

The SwRI v2 piston was later analyzed for its knock index to confirm previous GT-Power knock predictions. To perform the knock analysis, a low temperature combustion species, such as formaldehyde, was visualized as the flame kernel compressed the charge inside the combustion chamber. The low temperature combustion specie generation signified auto-ignition related combustion activity which would eventually lead to knocking. The temperature of this low temperature species was higher than the rest of the surrounding charge (by almost 300 K), presumably due to the heat release associated with its existence. Figure C-10 shows the development of the low temperature combustion specie (here formaldehyde: CH_2O) as the flame kernel grew towards it.

Figure C-10: Development of Formaldehyde (a Low Temperature Species) Near the Exhaust Side as the Flame Kernel Grew Towards it

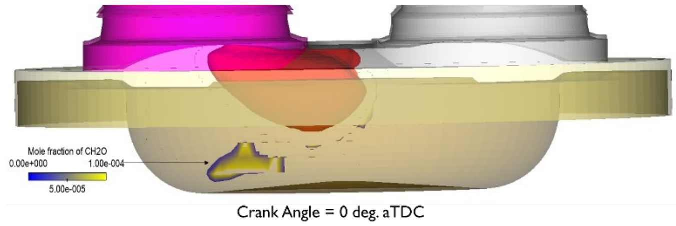

Source: Southwest Research Institute

To perform a knock analysis, a scatter of monitor/interrogation points were placed inside the combustion chamber. Since knock usually occurs near the exhaust side, the interrogation point closer to the piston and liner zones on (one of) the exhaust side was considered as the primary knock interrogation point in this study. Pressure information at this point was monitored and stored. Figure C-11 shows the monitor point location in the present geometry when the piston was at TDC. This point also gave the highest fluctuation of pressure among the other points placed in various locations inside the combustion chamber and so was chosen to be considered for knock analysis.

Figure C-11: Primary Interrogation Point Location for Knock Analysis

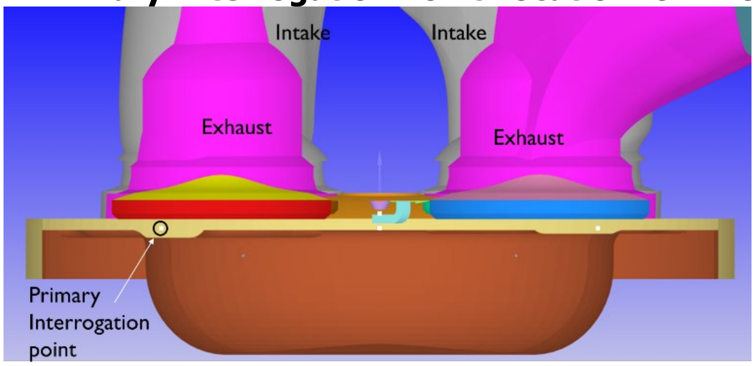

Source: Southwest Research Institute

A fast Fourier transform (FFT) of the monitor point pressure was performed with the Hann window function over the knock target interval of -20 to 30 CAD. This window was wide enough to capture a knock event. An inverse of this FFT was obtained by applying a band-pass filter from 4 kHz to 8 kHz. This gave a fluctuation pressure signifying the ringing of pressure observed during knock, as shown in Figure C-12. The magnitude of this ringing pressure (called Maximum Amplitude of Pressure Oscillation or MAPO) and knock intensity (KI) are common methods for gauging knock strength. MAPO was obtained by measuring the amplitude of the frequency resolved ringing pressure and KI was calculated by performing a crank angle integration of the absolute value of the fluctuation pressure over the target knock interval (-20 to 30 CAD).

Figure C-12: Knocking Pressure from Knock Analysis

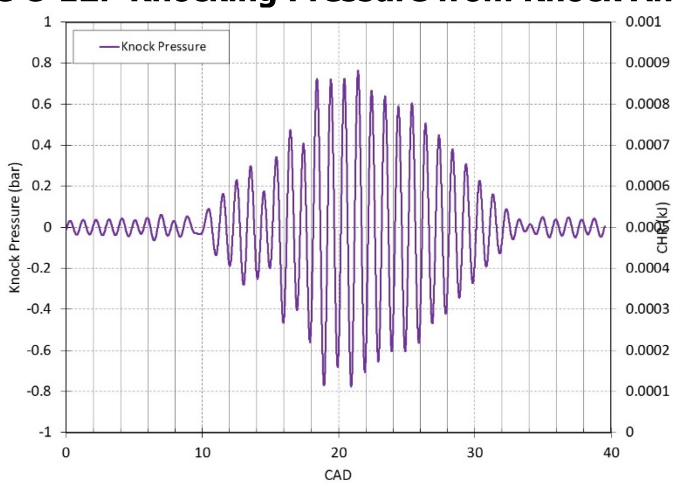

Source: Southwest Research Institute

A KI of 6.8 bar*deg was obtained this way with a MAPO of 1.55 bar. The experimental KI value was 9 bar*deg and MAPO was 1.8 bar for this operating point (with the stock piston). These values were greater than predicted for the SwRI v2 piston. This gave an indication that a 1.5 CR increase did not lead to excessive knock and there may be further opportunity to increase CR for more efficiency gains.

Swirl Evaluation

The primary mechanism of intake flow in the Cummins Westport ISX 12-G is swirl, which is created by the intake port design. To improve burn rates, the swirl motion is broken down into

TKE by the tangentially acting squish flow when the piston is near top dead center. In a diesel engine, swirl is used to promote mixing of the fuel-air mixture. As the ISX12 G is a fumigated fueling system, fuel-air mixing does not need strong swirl to support mixing. Since swirl flow occurs along the circumference of the piston-liner-head regions, it causes increased heat loss. A reduction in swirl can be expected to help reduce heat losses and thus increase ITE.

To evaluate the effect of swirl reduction on improvements to heat transfer losses, and to understand the overall impact on ITE, simulations at various swirl levels were performed. Typically, the intake port geometry must be changed to simulate different swirl levels. This is an iterative process, requiring much time. To reduce the level of effort, this study utilized simulations that were started at IVC (-137 CAD) with swirl being artificially modified by varying the x and y components of velocity (z-axis being along the cylinder axis). The SwRI v2 piston (increased compression ratio) and D-EGR was used, since it performed better than other system designs evaluated.

Figure C-13: Swirl Ratio Sweeps with Baseline Swirl Being 1.44 for the Stock Intake Ports

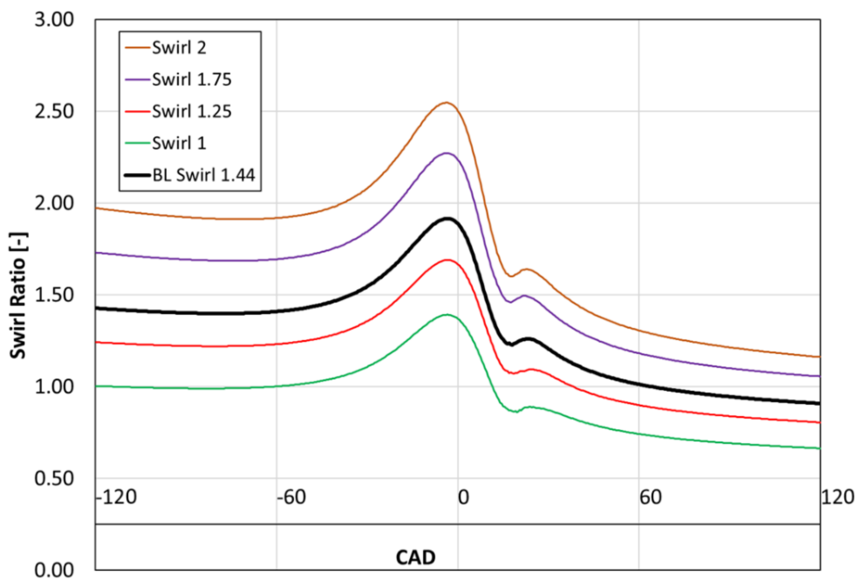

Source: Southwest Research Institute

Figure C-13 shows the swirl ratios obtained at IVC for each of the swirl ratio sweep cases. For each of these cases, MFB50 was targeted to be around the baseline MFB50. Figure C-14 shows the pressure and heat release rate profiles of the swirl sweep cases.

Figure C-14: Pressure and Heat Release Rate Profiles for Different Swirls

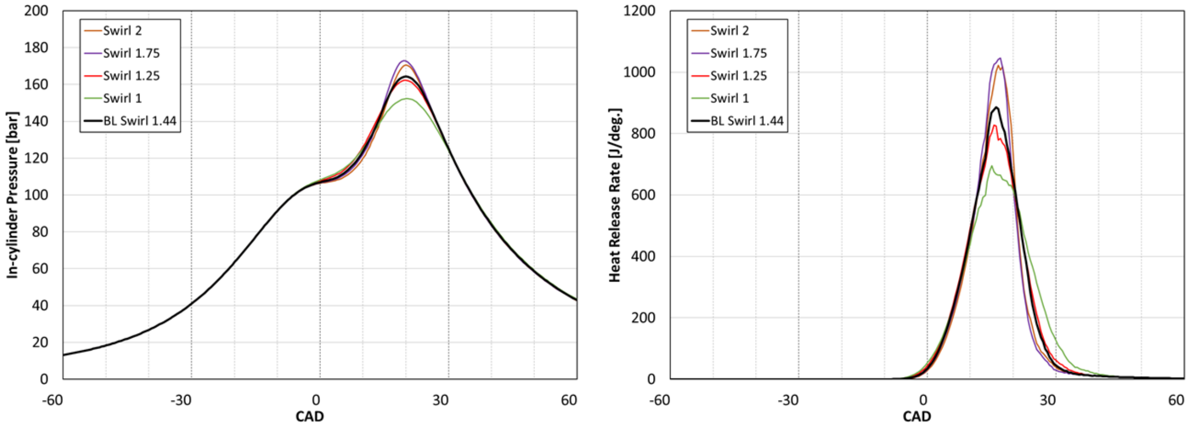

Source: Southwest Research Institute

To evaluate the benefits of heat transfer and work output, they were plotted as percentages of the baseline swirl case in Figure C-15. Note that a swirl ratio of 1.25 gave almost equal work output as that of the baseline swirl case of 1.44 but yielded heat transfer savings of about 3 percent.

Figure C-15: Evaluating Percentage Changes in Wall Heat Loss (WHT) and Work Output with Respect to the Baseline Swirl Case

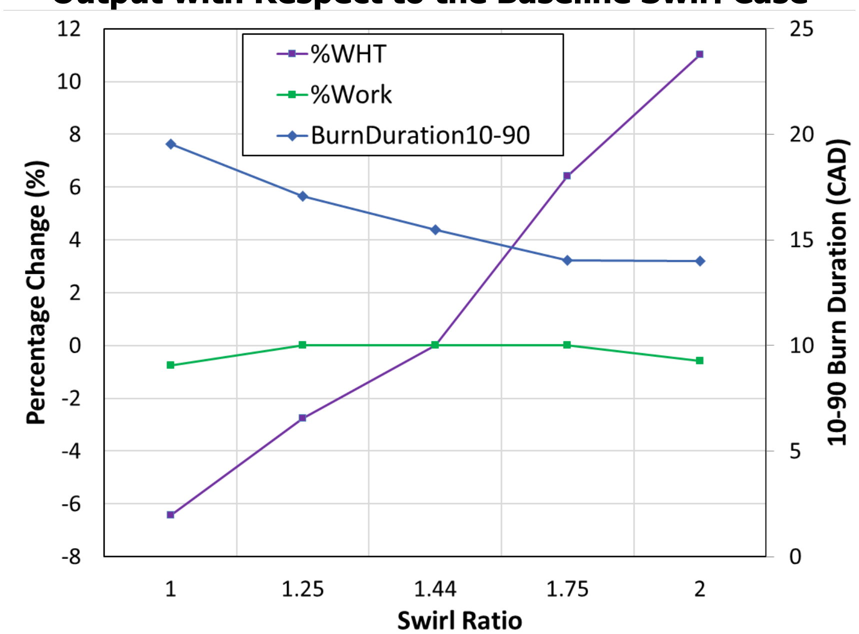

(10-90 Burn Duration are Plotted on Secondary Y-Axis)

Source: Southwest Research Institute

Swirl ratios below 1.25 (for e.g. swirl of 1 in Figure C-15) caused further reduction in heat loss, but also negatively impacted the work output. In addition, a major reduction in swirl level would not be easy to achieve given the physical restrictions around the intake port region (cooling galleries etc.) in the cylinder head design. Swirl ratios above the baseline swirl value increased the heat loss at a faster rate and there were no benefits in increased work output either.

Figure C-16: Energy Balance with Reduced Swirl Level

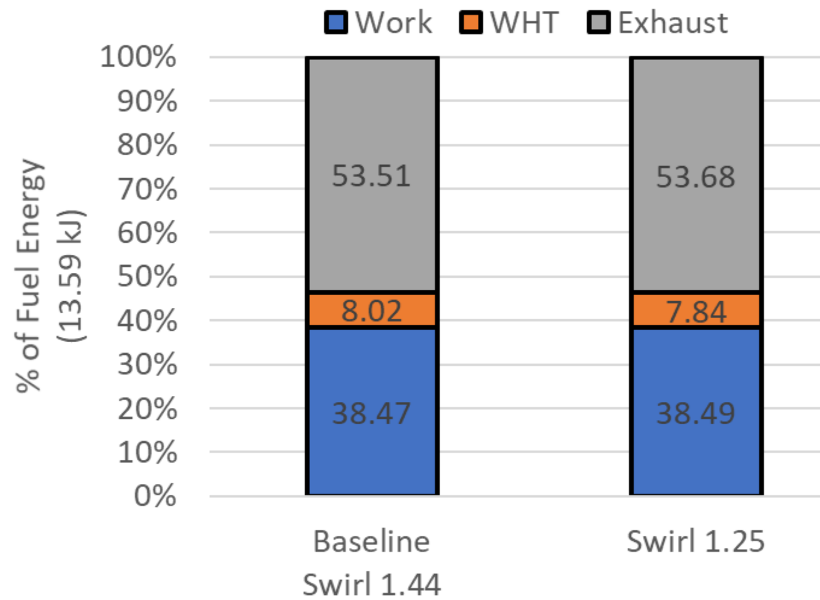

Source: Southwest Research Institute

A swirl ratio of 1.25 signified a 13.2 percent reduction from the current baseline swirl value and was deemed to provide benefits in terms of increased work output and reduced heat loss. Figure C-16 shows an energy balance (evaluating Q=W+PdV) analysis on the case with swirl of 1.25 and comparing it to the baseline swirl level with a constant 13.59 kJ of fuel energy between the two cases. 92 percent of the reduction in heat loss is converted to an increase in the exhaust energy which may help the turbocharger performance. 8 percent of the reduction in heat loss went to a slight increase in work output (2.15 J). The slight increase is work output is not sufficient to warrant complex changes to the head casting.

Summary

CFD simulations were performed on a Cummins Westport ISX12 G engine to optimize the flow field within the combustion chamber for D-EGR operation through modifying the piston design and evaluating the potential for a port re-design. The stock re-entrant type piston bowl resulted in high heat loss from the flame propagation event, which led to design of an open-bowl piston (SwRI v1). TKE values for the SwRI v1 piston bowl (in the bowl region) were higher than the stock piston. This led to faster MFB10-50 burn durations for the SwRI v1 piston by about 2 degrees. With application of D-EGR technology, better thermal efficiencies were observed over conventional high-pressure loop EGR. Due to the knock benefits that come with D-EGR technology, the SwRI v1 piston bowl was modified to increase its compression ratio by 1.5 points (SwRI v2) and analyzed for knock intensity. Figure C-17 shows efficiency gains observed for the various stage-wise developments performed over the baseline stock 20 percent HPL-EGR configuration. Switching to an open-bowl contributed to a 1.3 percent point increases in ITE; using 30 percent D-EGR vs. 20 percent LPL-EGR increased the ITE by about 2.1 percent points. A further 3.1 percent point ITE increase was obtained from the CR increase. All of these translated to an 8.1 percent increase over the base design ITE. Knock was still at acceptable levels with the increased CR for the open bowl type SwRI v2 piston with 30 percent D-EGR. A swirl ratio sweep showed further potential in heat loss reduction by reducing the baseline swirl ratio by about 13 percent which resulted in a 3 percent reduction in heat transfer. As the reduction of swirl ratio on the physical engine would require a high level of effort, this was not pursued for physical engine testing.

Figure C-17: Efficiency Gains Observed as Various Features of Piston Bowl, D-EGR and CR were Added Starting from the Baseline HP-EGR Configuration

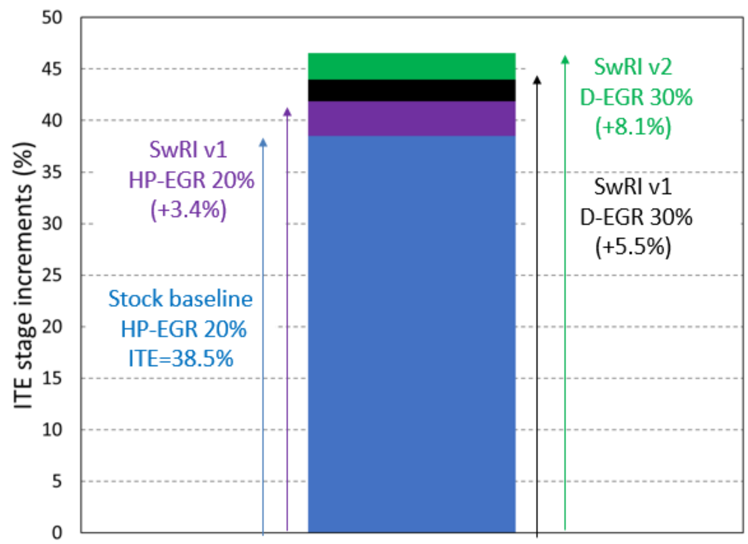

Source: Southwest Research Institute

APPENDIX D: Ignition System Evaluation

Stable combustion at high levels of EGR dilution is a key factor of success of this project. As such, advanced ignition systems were screened as part of this project to find a robust ignition system for Dedicated EGR® (D-EGR®) operation.

Methodology

Engine Configurations

The results in the ignition system evaluation task were recorded with the engine in various configurations due to varying lead times of several key components. The most notable changes to the configuration are the EGR loop, the turbocharger and the piston design. The stock ISX12 G engine uses a high-pressure (HP) EGR system with a wastegate turbocharger. The baseline results used the stock ECU and HP-EGR system. Then the engine was modified for a D-EGR configuration to evaluate the varying ignition systems. The D-EGR system was either plumbed directly to the mixer for a full 33 percent D-EGR or with a bypass valve to bleed off EGR to the exhaust stack.

To fully realize the potential of the D-EGR configuration, additional hardware changes were made. The piston was redesigned to increase compression ratio and reduce heat losses through the reduction of squish area. The revised piston design is shown in Figure D-1. Detail of the piston design are provided in the Flow Field Evaluation report. The compression ratio was increased from 11.5:1 to 13.2:1. Due to the increased EGR rate, the combustion phasing was similar to the baseline. The 13.2:1 CR is referred to as the SwRI v2 configuration throughout the appendix.

Figure D-1: Stock and SwRI v2 Pistons

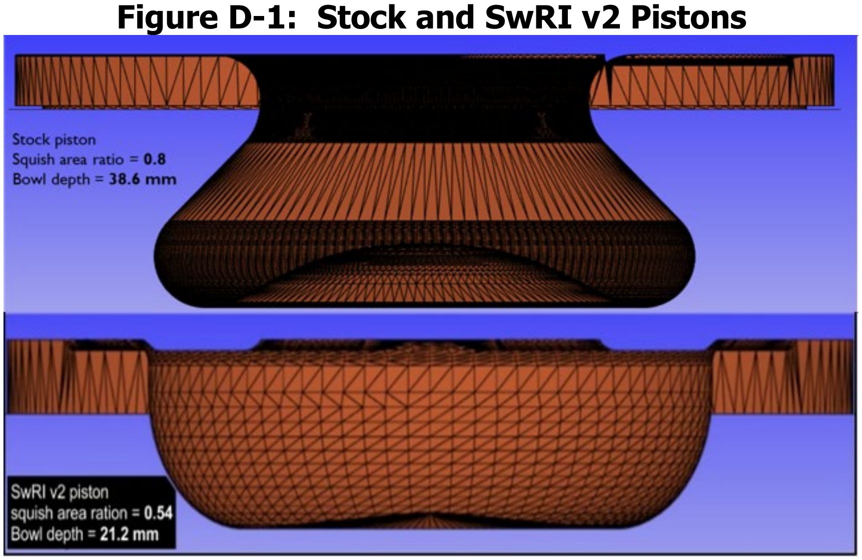

Source: Southwest Research Institute

Stability Limits

D-EGR, D-Cyl Enrichment Sweep

Each ignition system was tested for the ability to extend the dilution tolerance of the engine. In general, the engine was first tested without the EGR bypass to achieve true D-EGR operation at all conditions. If the engine was able to operate with full D-EGR, enrichment sweeps of the dedicated cylinders were performed. In all cases unless specifically noted, the combusting phasing was maintained at MBT timing with the ignition timing being adjusted for individual cylinders. Typically, during an enrichment sweep the ignition timing of the main cylinders was retarded to maintain combustion phasing due to the improved laminar burning velocity of hydrogen. The ignition timing of the dedicated cylinders was generally advanced to maintain combustion phasing or stability. The earliest ignition timing was set at -60° aTDC as ignition earlier than this would not provide any further improvements in the stability of the engine. For research purposes, the stability limit was determined by a coefficient of variation (COV) of gIMEP greater than five percent. The stability limit could be reached from combustion phasing occurring too late or from partial/complete misfires. Once the ignition timing was advanced to its practical limit, more enrichment would slow burn rates increasing the likelihood of late combustion phasing or misfire.

EGR Sweep

In the full D-EGR configuration the EGR bypass loop was capped to eliminate the possibility of a leak through the bypass valve reducing the EGR rate. Without the bypass valve, the measured EGR rate was around 28 percent rather than the nominal 33 percent due to airflow imbalances between cylinders. The tests with this configuration are referred to as EGR capped. If the engine could not operate in the full D-EGR configuration, the EGR bypass loop was installed. In the bypass loop there was a butterfly valve that was used for metering the EGR rate. With the bypass valve fully closed, the measured EGR rate was typically 25 percent due to leakage around the butterfly. The tests in this configuration are referred to as testing with bypass closed. If a test condition was able to operate with the bypass valve fully closed, an enrichment sweep could be performed with minimal hydrocarbons leaking into the tailpipe. Otherwise, an EGR sweep was performed by adjusting the butterfly valve while targeting MBT combustion phasing, denoted by EGR bypassed.

Dual Coil Offset Ignition System, SwRI V2, Bypassed Closed

SwRI's Dual Coil Offset (DCO®) system has proven to extend the dilution limit in EGR and D-EGR engines [12]. Previous research has shown the dilution tolerance improves as the number of restrikes and dissipated energy increases [13]. For this testing, the DCO system was operated with 4 restrikes, delivering approximately 1280 mJ of primary energy. An example of the current discharge from a DCO discharge with four restrikes is shown in Figure D-2. This is generally the number of useful restrikes that has been observed in previous testing. The stock spark plugs were used with a gap of 0.3 mm.

Figure D-2: Example Primary and Secondary Currents from a DCO Discharge [12]

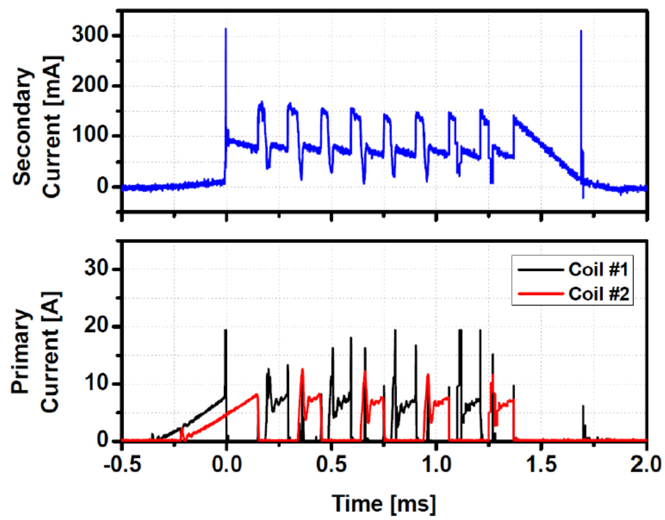

Source: Southwest Research Institute

The DCO system was tested with the SwRI v2 piston and EGR bypass installed but closed, resulting in an EGR rate of ~25 percent. The increase in EGR rate and compression ratio over the baseline provided a BTE improvement. The BTE from this testing and the baseline are compared in Figure D-3. All test points that could be reached with the stock turbocharger showed a BTE improvement. The largest improvement was observed at the 25 percent load condition for each speed.

Figure D-3: BTE Results for the Baseline and D-EGR Engine Configuration with DCO Coils

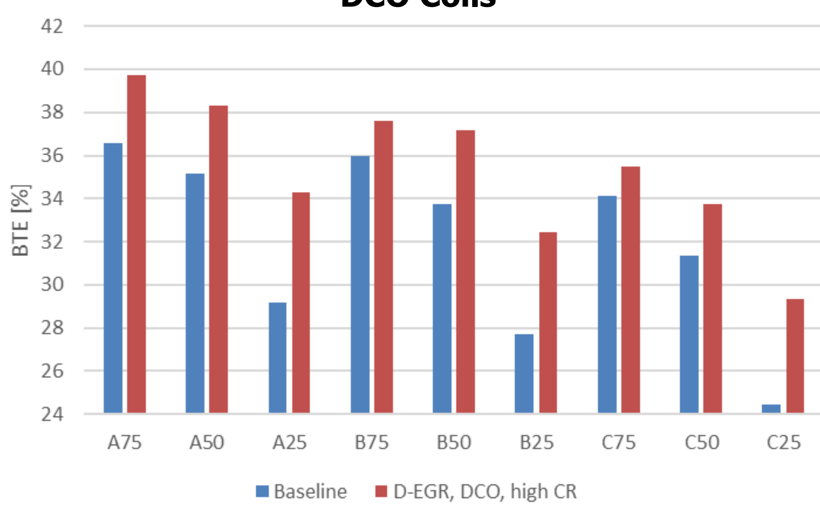

Source: Southwest Research Institute

The maximum cylinder enrichment achieved in the D-EGR configuration with the stock turbocharger for each modal point is shown in Figure D-4. Technically, the maximum enrichment level was beyond the stability limit defined in the methodology section, however, the limit was neglected in this case because the rise in CoV was the result of individual misfire events rather than a greater spread in the gIMEP. The misfires skew the CoV of gIMEP number to higher values depending on the load set point and are less indicative of the quality of the combustion. Therefore, when finding the maximum dedicated cylinder enrichment, the equivalence ratio was increased until the engine CoV was too severe to maintain the torque set point. The general trend that can be observed from Figure D-4 are that more enrichment can be achieved at lower speeds and at higher loads.

Figure D-4: Maximum Dedicated Cylinder Equivalence Ratio in the D-EGR Configuration for the Stock Plugs with the DCO Ignition System

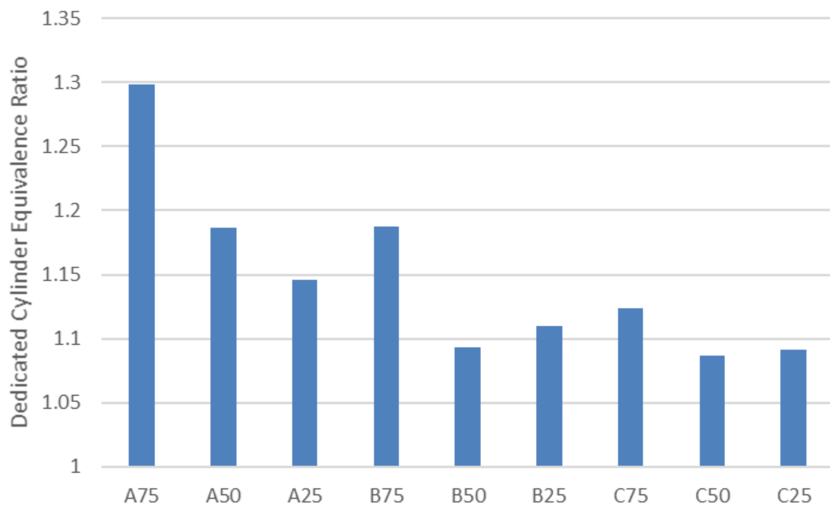

Source: Southwest Research Institute

The combustion stability (CoV gIMEP) does not show a typical gradual development with increased enrichment. Instead, all of the cylinders are stable until the dedicated cylinders become unstable. Misfires become more frequent between -50 and -60° aTDC due to early ignition timing. The ignition timing was held within a small margin from this point. Further increase in the enrichment slowed the MFB 0-2, pushing the combustion phasing further from MBT. From experience, the latest combustion phasing this engine could operate under in a stable manor was 20° aTDC. The combustion was stable up to a dedicated cylinder equivalence ratio of 1.35, as shown in Figure D-5. With more enrichment, the sharper drop in LBV pushes the combustion phasing too late and the engine was unable to maintain the load due to the instability in the dedicated cylinders.

Figure D-5: CoV of gIMEP for an Enrichment Sweep at A75

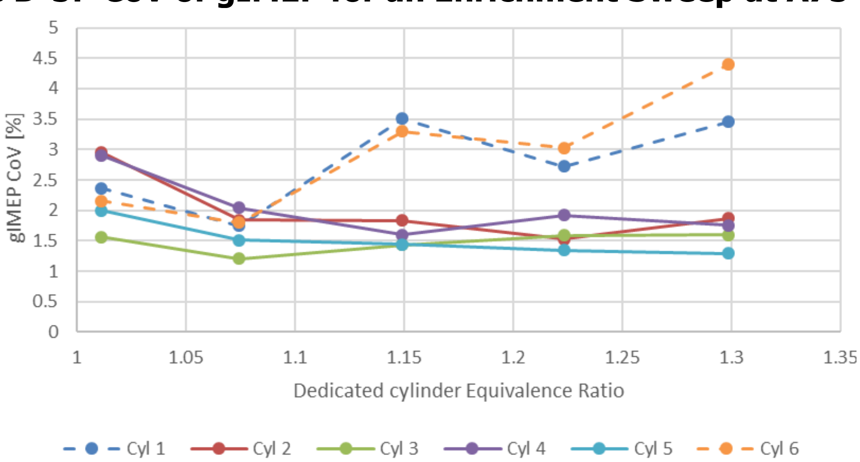

Source: Southwest Research Institute

At higher speeds all cylinders were unstable without any enrichment. Enrichment improved the main cylinders but made the dedicated cylinders less stable. This was most noticeable for the

C75 test condition shown in Figure D-6. There was no level of enrichment tested where all the cylinders were running stable. A dedicated cylinder equivalence ratio of about 1.08 improved ignitibility of the main cylinders enough to become stable. The spark timing for each test point across the sweep was -51° aTDC. This was the earliest spark timing where compression provided enough pressure and temperature for consistent ignition. There was no margin to advance timing on the dedicated cylinders; the dedicated cylinders started out unstable and increased in CoV as equivalence ratio was increased.

Figure D-6: CoV of gIMEP for an Enrichment Sweep at C75

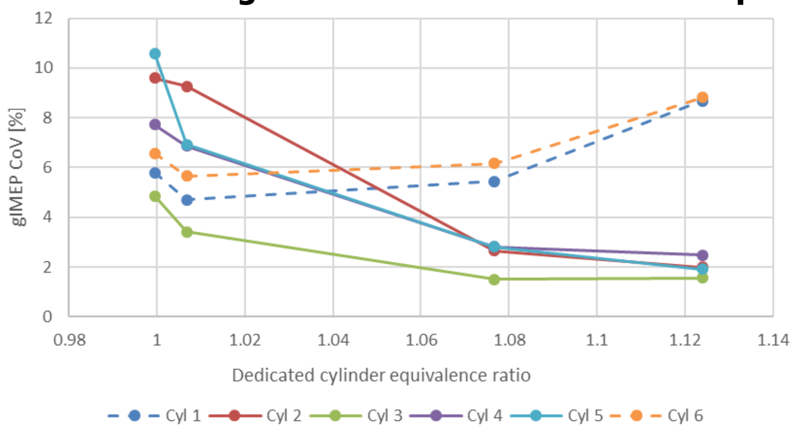

Source: Southwest Research Institute

Pre-chamber Plug, Stock CR, EGR Bypassed

A pre-chamber plug was tested with the stock piston design and EGR bypass installed. The pre-chamber separates the spark and flame kernel from the charge motion variability of the main chamber. The pre-chamber design concept is to (a) protect the flame kernel from main chamber turbulence that tends to “blow it out” and (b) to burn a small volume of the charge very rapidly such that high velocity flame jets are emitted from the pre-chamber which generate turbulence and increase the number of ignition points in the main chamber, resulting in much shorter ignition delay and faster initial heat release rise. The pre-chamber plug was developed and tested with a traditional EGR configuration at moderate dilution levels, and the intent of this testing was to explore the synergistic benefits of pre-chamber combustion in the presence of reformate products from D-EGR.

The pre-chamber plugs were installed in all six cylinders with spacers to control the insertion depth. The EGR was bled off to a controlled set point using the bypass loop, and an EGR sweep was performed at the A25 condition to compare to the baseline dilution tolerance. The CoV of gIMEP for the D-EGR configuration with pre-chamber plugs and the baseline engine configuration with the stock spark plugs are shown in Figure D-7 and Figure D-8 respectively. With the exception of cylinder 4, the pre-chamber plugs showed similar performance to the baseline configuration, reaching a stability limit around 20 percent EGR. The behavior of cylinder 4 can be better understood by examining the cycle-by-cycle variation in gIMEP shown in Figure D-9. It is evident that combustion was very stable with six distinct misfire events, resulting in the higher CoV. It should be noted, however, that the presence of misfire cycles is generally not acceptable for proper catalyst operation.

Figure D-7: CoV of gIMEP for an EGR Sweep at A25 with the Woodward Pre-Chamber Plugs with the Standard Insertion Depth

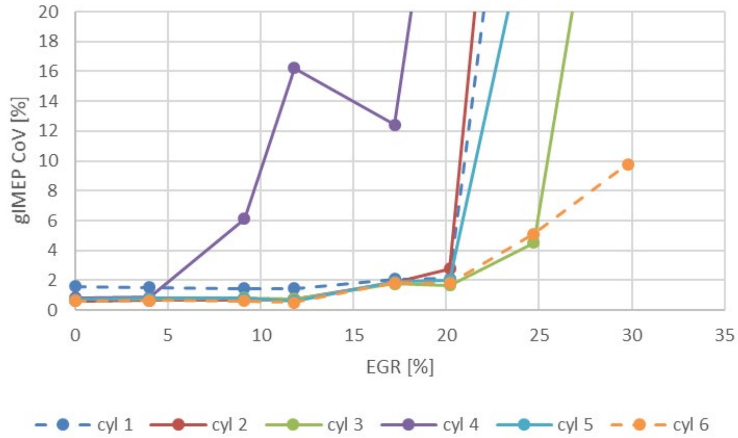

Source: Southwest Research Institute

Figure D-8: CoV of gIMEP for an EGR Sweep at A25 in the Baseline Configuration with the Stock Spark Plugs

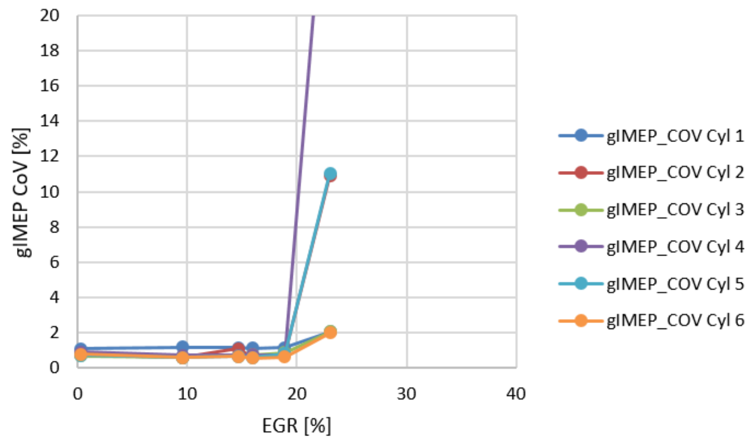

Source: Southwest Research Institute

Figure D-9: gIMEP of Cylinder 4 for Each Cycle at 12 percent EGR (left) and of Cylinder 2 at 25 percent EGR (Right) with the Pre-Chamber Spark Plugs

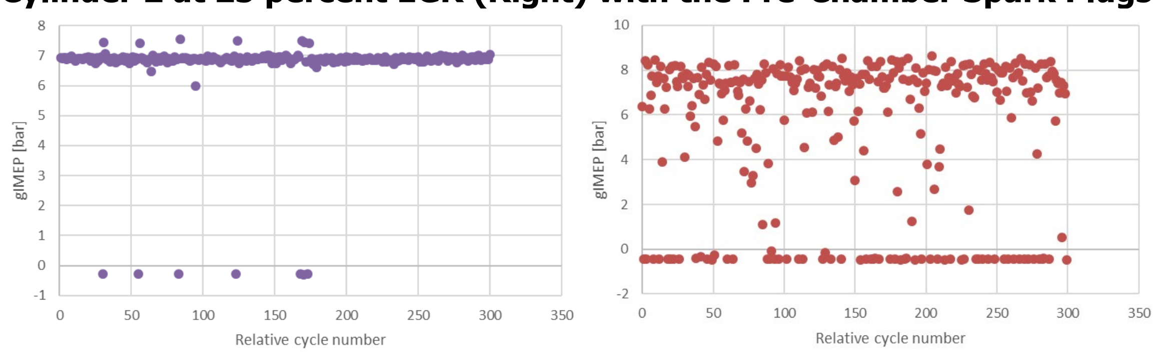

Source: Southwest Research Institute

The mass fraction burn locations for the EGR sweep are presented in Figure D-10. At EGR rates greater than 15 percent, the combustion data is strongly influenced by the misfire events. Misfires occurred at EGR rates lower than the baseline EGR rate at A25. When stable combustion is present, the MFB 10-90 duration is fast at around 20° CA.

Figure D-10: Mass Fraction Burn Development at A25 with the Woodward Pre-Chamber Spark Plugs with the SwRI V2 and Stock Turbocharger

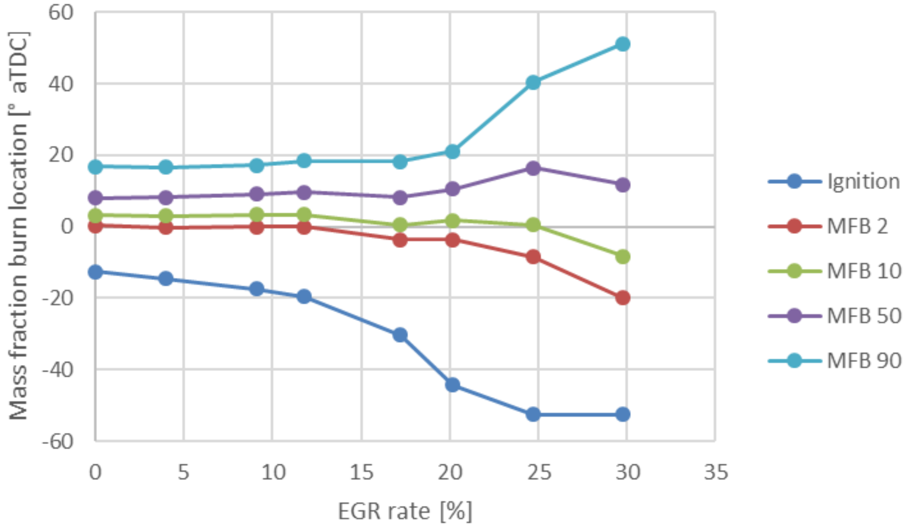

Source: Southwest Research Institute

Maximum Insertion Depth

The pre-chamber plugs were designed with extra-long reach to allow for adjustment of the insertion depth through the use of gasket spacers. As mentioned previously, the pre-chamber plugs were initially installed with the spacers that reduced the insertion depth to a minimum. For the final test, the spacers were removed and the spark plugs were re-installed to position the pre-chambers at the maximum insertion depth. Without the spacers, the pre-chamber was sitting 0.25" further into the main combustion chamber. Increasing the insertion depth increases the metal surface temperatures of the pre-chamber to reduce the quenching effect of heat losses through the walls of the pre-chamber. As expected, this improved the dilution tolerance at the A25 point beyond 20 percent EGR with the notable elimination of misfire in cylinder 4. The gIMEP of CoV for the pre-chamber at the standard and maximum insertion depths are shown in

Figure D-11.

Figure D-11: CoV of gIEMP for an EGR Sweep at A25 with the Woodward Pre-Chamber Spark Plugs at Maximum Insertion Depth

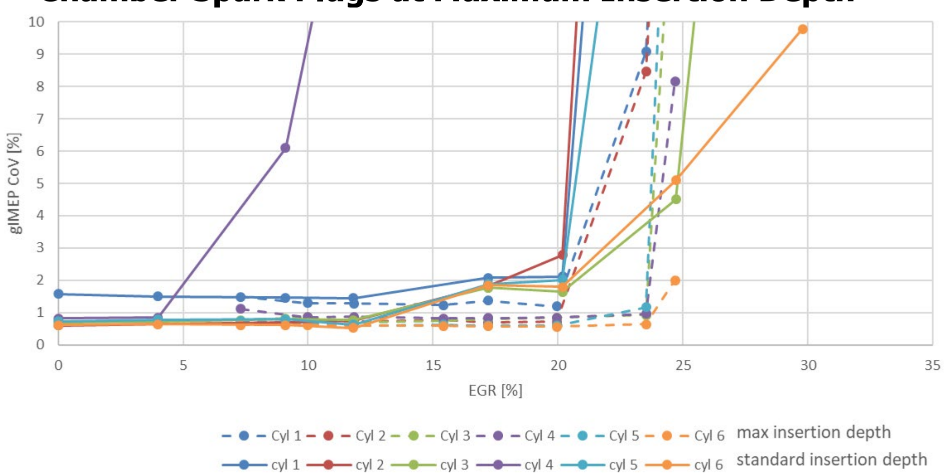

Source: Southwest Research Institute

The trade-off with increasing metal temperatures at maximum insertion depth is the increased potential for pre-ignition (combustion occurring prior to the spark event) from higher internal temperatures or hot spots on the outer surface of the pre-chamber exposed to the main chamber combustion. Examples of pressure traces showing pre-ignition are shown in Figure D-12. Pre-ignition was observed at A75 with 25 percent EGR, A25 with no EGR and at C25 with less than 18 percent EGR. Hot spot pre-ignition is a challenge as the combustion phasing is no longer controlled by the spark event, and in most cases results in excessive knocking.

Figure D-12: In-Cylinder Pressure Traces Showing Pre-I ignition at with the Pre-Chamber Spark Plugs at A75

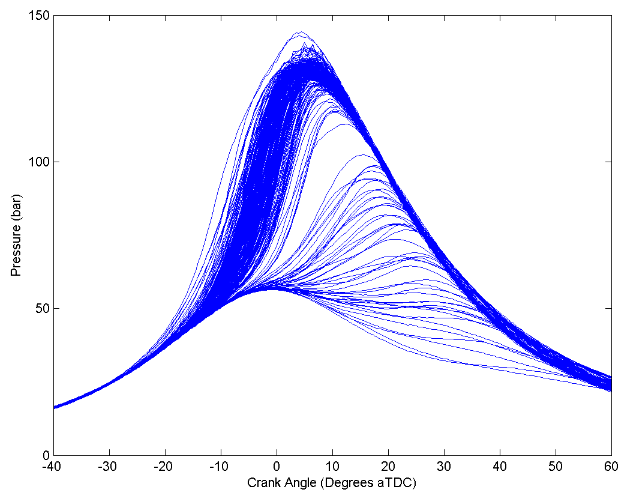

Source: Southwest Research Institute

An ignition timing sweep was performed at the A25 point with a constant EGR rate to determine optimal conditions for ignition. The CoV of gIMEP versus ignition timing and MFB50 for this sweep are shown in Figure D-13 and Figure D-14. The CoV of gIMEP versus ignition timing shows that there is an optimum spark timing window between -37 and -32° aTDC. Early in the compression stroke the pressure is not sufficient to scavenge the pre-chamber. For reference, the pressure near the time of spark is presented in Figure D-15. Woodward confirmed the earliest the spark timing can typically be set for the pre-chamber plugs is around -30° aTDC. It was observed that MFB50 was not affected as spark timing was advanced beyond this point, but the CoV increased. The combustion phasing did respond to later spark timing, however the combustion duration became excessive at later combustion phasing resulting in higher CoV values.

Figure D-13: CoV of gIMEP for an Ignition Timing Sweep at A25 with 25 percent EGR using the Pre-Chamber Spark Plugs

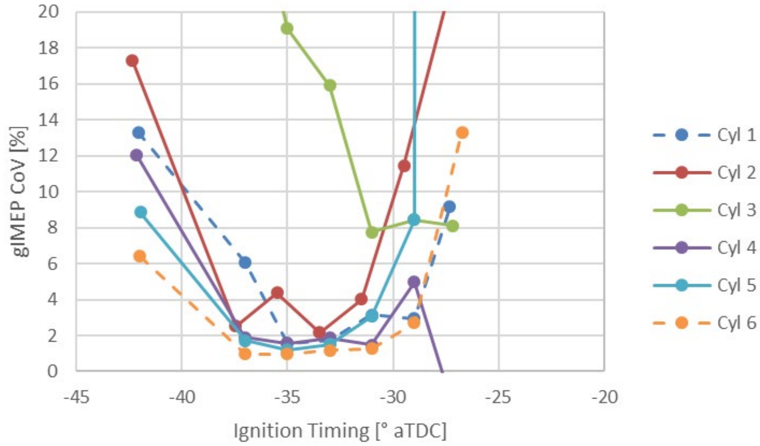

Source: Southwest Research Institute

Figure D-14: CoV of gIMEP vs MFB50 for an Ignition Timing Sweep at A25 with 25 percent EGR using the Pre-Chamber Spark Plugs

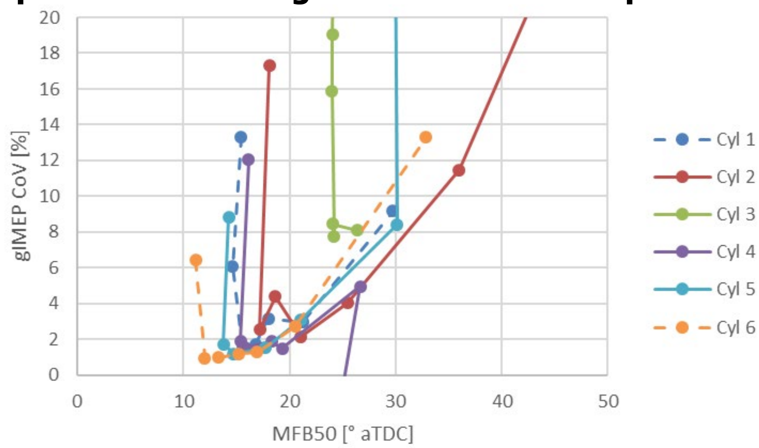

Source: Southwest Research Institute

Figure D-15: Cylinder Pressure during the Spark Window at the A25 Point

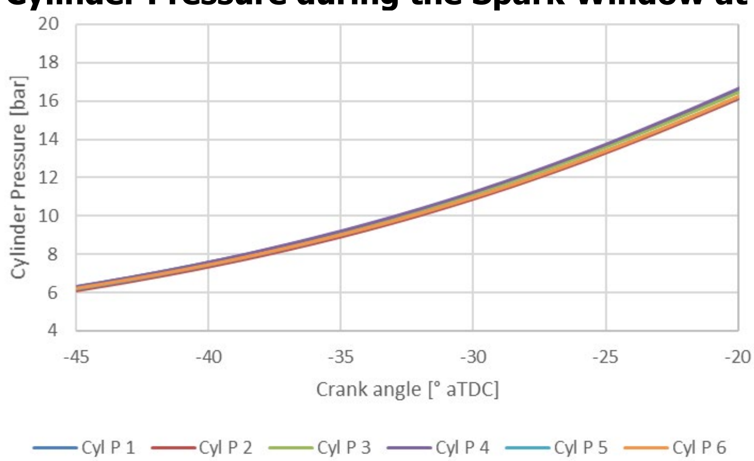

Source: Southwest Research Institute

Figure D-16: Mass Fraction Burn Development with the Pre-Chamber Plugs at the Maximum Insertion Depth for a Spark Timing Sweep at A25 with 25 percent EGR

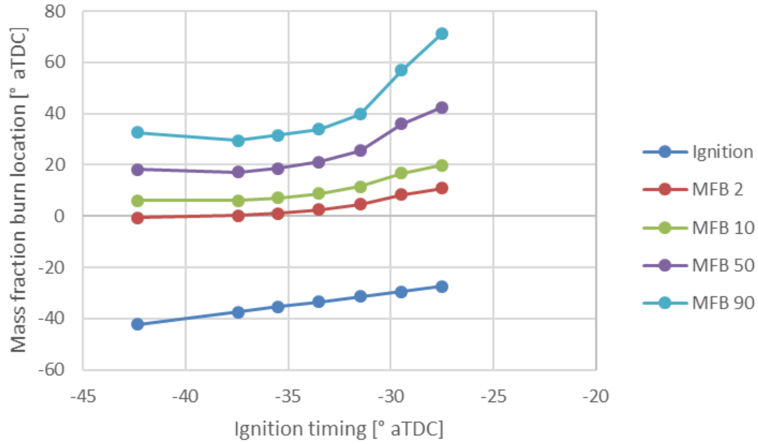

Source: Southwest Research Institute

Advanced Fast Ignitor, SwRI V2, EGR Bypassed

The Woodward Advanced Fast Ignitor system is a further optimized pre-chamber design that consists of an insert that is threaded into the cylinder head replacing the water jacket sleeve that forms the spark plug well. The top of the insert is designed to accept a spark plug which can be driven by a conventional ignition coil and high-tension lead. The Advanced Fast Ignitor was tested with the high compression ratio pistons and the stock waste-gated turbocharger. The higher compression ratio increased the pressure during the compression stroke, improving the scavenging of the pre-chamber. The DCO system was used with four restrikes to improve ignitibility of the mixture within the pre-chamber at high burned gas residual fractions.

The performance of the Advance Fast Ignitor was similar to the pre-chamber plug for EGR tolerance, reaching a stability limit at EGR rates above 20 percent. EGR sweeps were performed at several modal points to define stability limits. Rather than cover the individual EGR sweeps in detail, the EGR limit for each modal point is presented in Figure D-17. The EGR limit is highest for the A speeds and decreases with increasing engine speed. BTE and mass fraction burn results are presented in Figure D-18 for the A75 and A50 cases. Results from the EGR sweeps show that BTE increased as the EGR rate was increased until the engine became unstable. The BTE trends suggest the potential to meet or exceed the DCO BTE if the EGR limit could be extended to the full D-EGR rate. It is believed that this could be accomplished with another design iteration of the Advanced Fast Ignitor, but this was outside the scope of the current evaluation.

Figure D-17: Maximum EGR Rates with the Advanced Fast Ignitor Ignition System

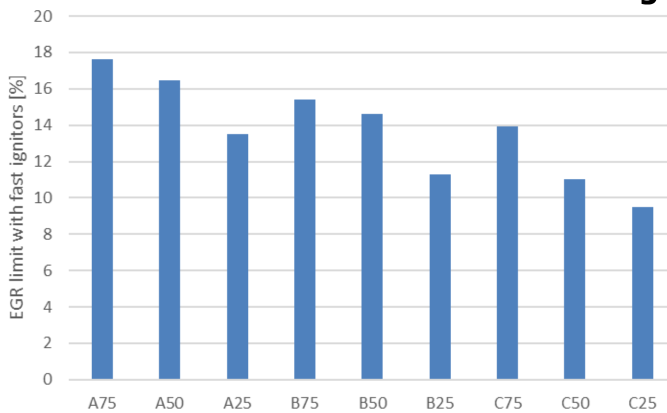

Source: Southwest Research Institute

Figure D-18: BTE and Mass Fraction Burn Development vs EGR Rates for A75 (Left Plots) and A50 (Right Plots). The DCO Points are the from the J-Gap Spark Plugs using Enrichment for the Best BTE

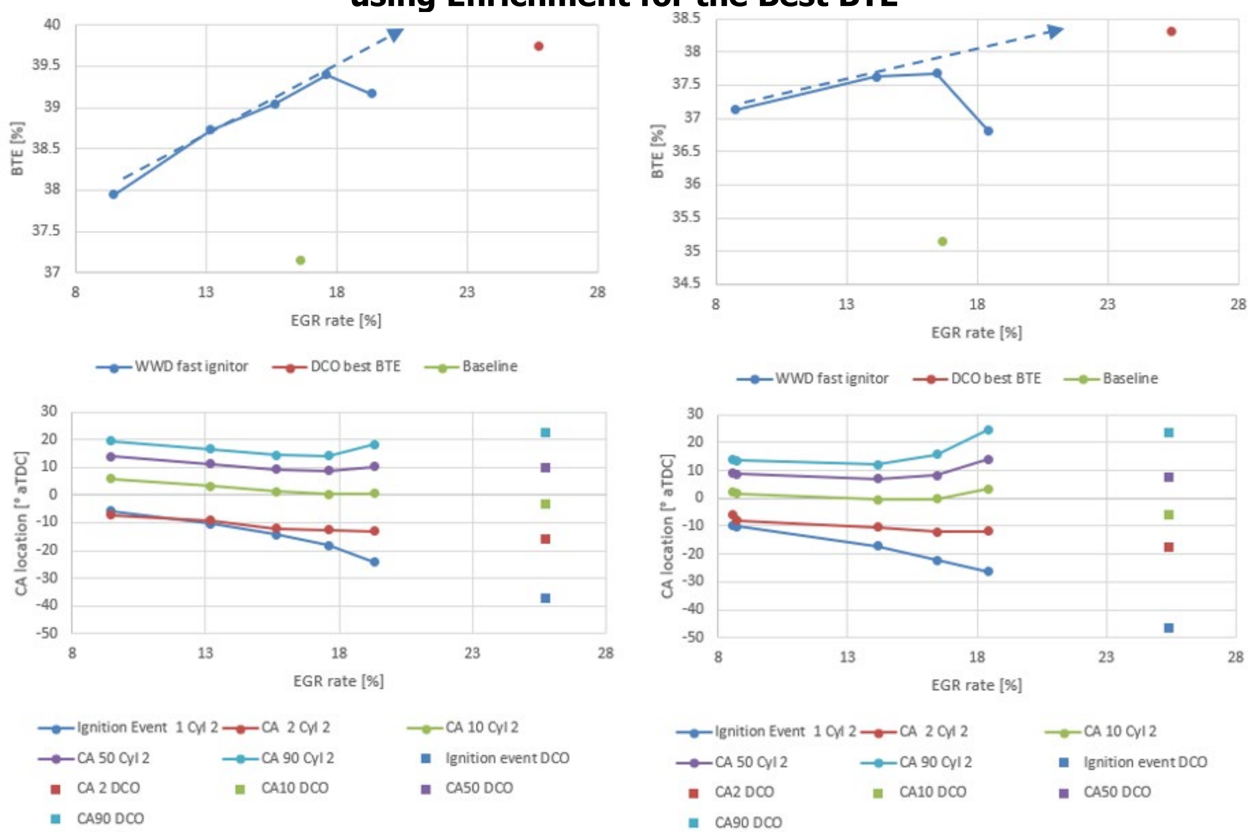

Source: Southwest Research Institute

The EGR limits shown in Figure D-18 can be further understood by reviewing a timing sweep at higher EGR concentrations. An ignition timing sweep at the A50 point with 18 percent EGR is shown in Figure D-19. At later ignition timing, the MFB 50 location responds as expected as timing is retarded. For spark timing earlier than -20° (aTDC), however, the combustion phasing remains fixed as the timing is advanced, and there no mechanism to advance combustion phasing for higher EGR rates resulting in increasing instability.

Figure D-19: Ignition Timing Sweep at A50 with 18 percent EGR to Show the Ignition Timing Window Limits of the Advanced Ignitors due to Scavenging and Late Combustion Phasing

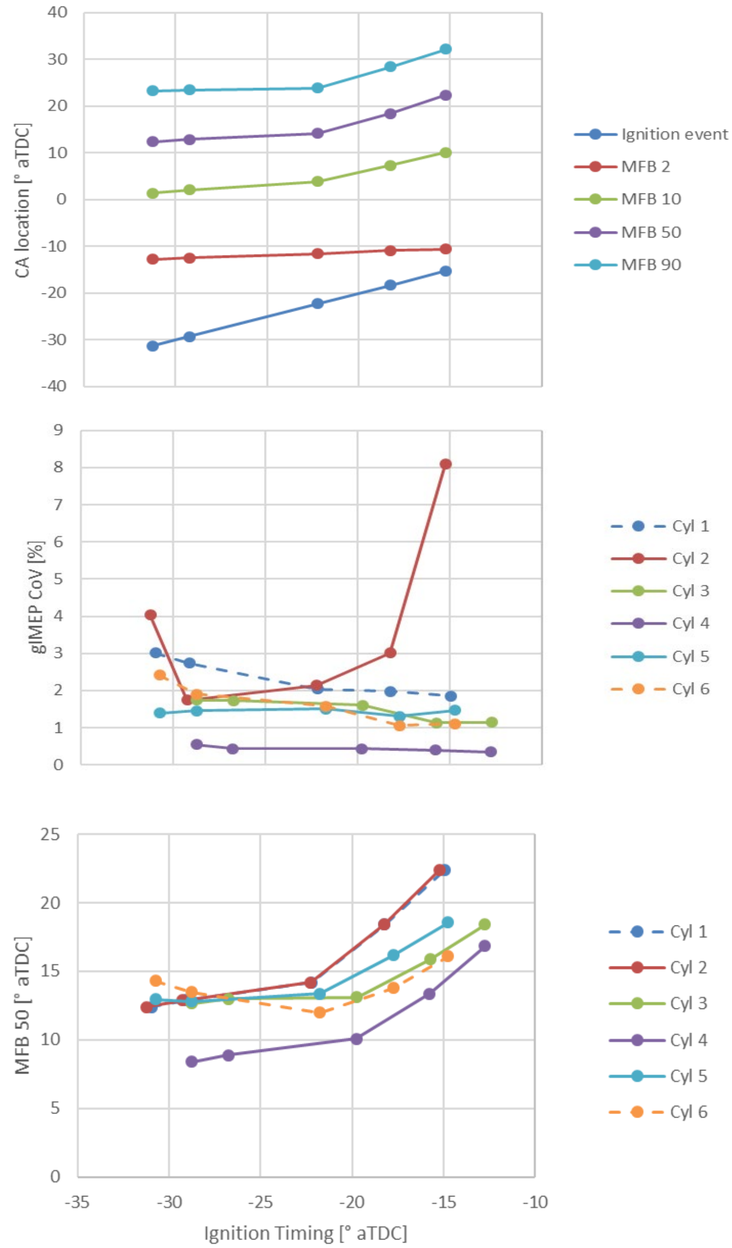

Source: Southwest Research Institute

The previous EGR sweeps were performed at a stoichiometric air-fuel ratio to prevent reformate products from enriched combustion from being bled-off to the exhaust (which has a negative impact on catalyst performance and thermal efficiency). However, in order to understand the impact of the enriched EGR on the non-dedicated cylinders, an EGR sweep was performed at A50 with 10 percent dedicated cylinder enrichment. As expected, the dedicated cylinders became unstable sooner as a result of the additional charge dilution of excess fuel, while the main cylinders benefited from increased stability as a result of the presence of reformate products. In Figure D-20, the stoichiometric EGR sweep is represented with solid lines and the enriched EGR sweep with dashed lines. For the stoichiometric sweep, cylinders 1 and 2 were the first to become unstable. During the enriched EGR sweep both dedicated cylinders, 1 and 6, become unstable. The mass fraction burn development for the

EGR sweep with and without enrichment are presented in Figure D-21. The enrichment did not show much of an effect on burn rates except at the highest EGR level.

Figure D-20: CoV of gIMEP for EGR Sweeps at A50 with Stoichiometric and 10 percent Enrichment for the Dedicated Cylinders

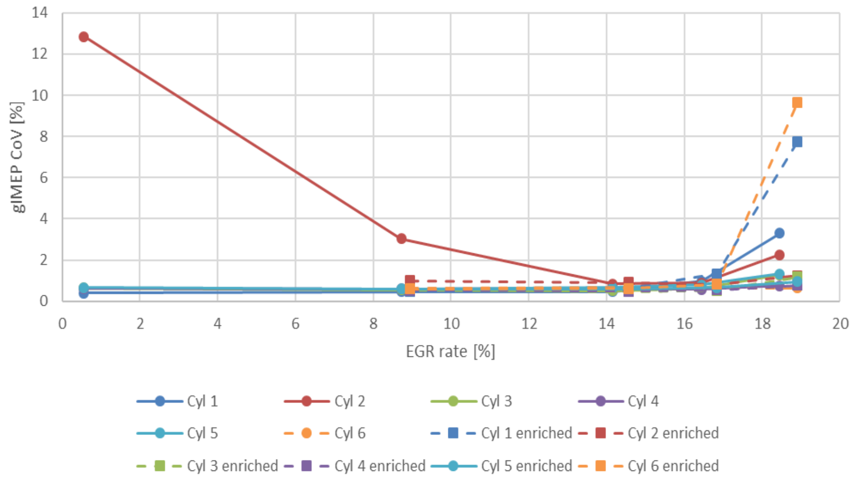

Source: Southwest Research Institute

Figure D-21: Mass Fraction Burn Development for EGR Sweeps at A50 for Stoichiometric and 10 percent Enrichment Dedicated Cylinder Operation

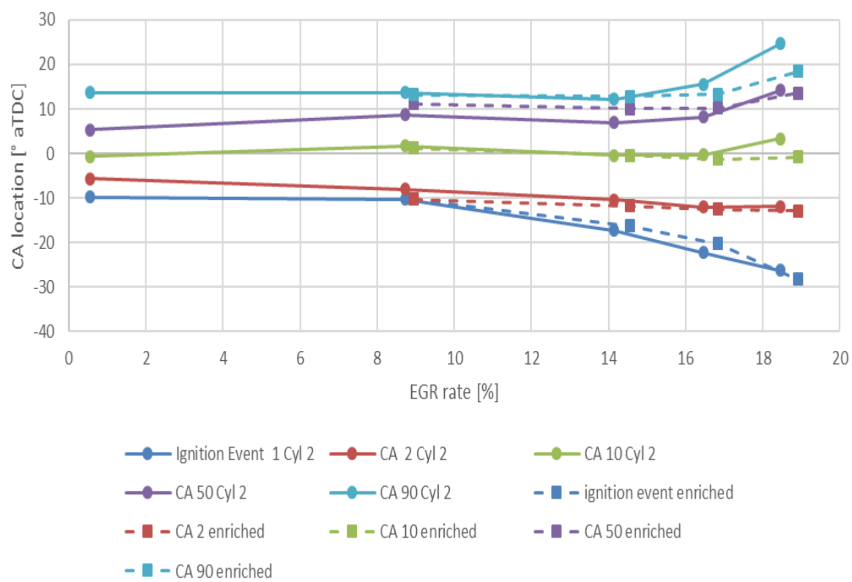

Source: Southwest Research Institute

To study the interactions between the reformed EGR and pre-chambers, an enrichment sweep was performed at each of the modal points. The EGR rate was reduced slightly from the stability limit to provide enrichment margin for the dedicated cylinders. The results in Figure D-22 show the enrichment had no noticeable effect on the burn rates. The pre-chamber already demonstrated a marked improvement in the MFB 0-10 duration where the introduction of enrichment typically shows the greatest benefit. In this case, the presence of reformate did not further improve the MFB 0-10 rates.

Figure D-22: Mass Fraction Burn Development for an Enrichment Sweep at A75 with 14 percent EGR

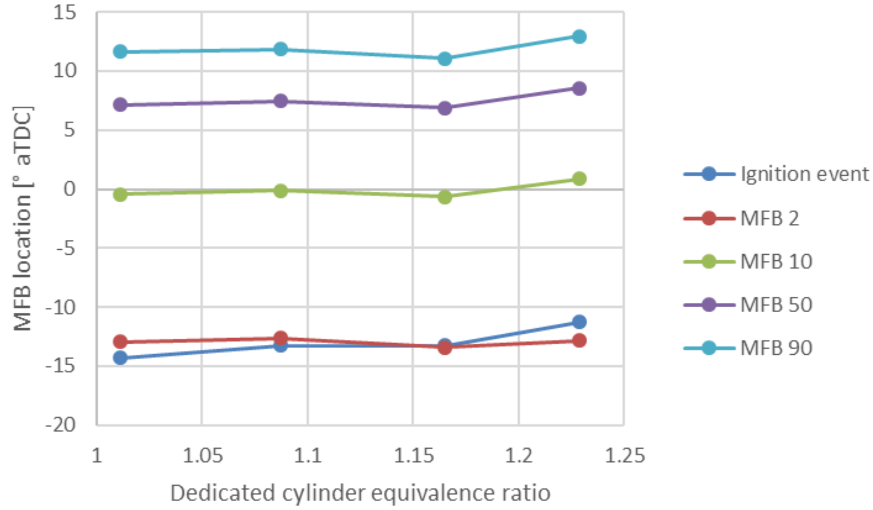

Source: Southwest Research Institute

In summary, up to the stability limit, the Advanced Fast Ignitors showed diesel-like stability with CoV of ~0.6 percent and marked improvement in combustion duration over the baseline at the same EGR level. Ultimately, however, it was not possible to advance ignition timing sufficiently to counteract combustion phasing degradation with increasing EGR. As a result, the maximum EGR rate that could be tolerated with the Advanced Fast Igniter was reduced, and the engine operation was therefore simultaneously limited by knock and CoV around 75 percent load and 18 percent EGR. As mentioned previously, it is expected that further design iterations on the pre-chamber geometry could be performed to adjust the ignition timing window and extend the overall EGR tolerance of the Advanced Fast Ignitor, but the timeline of the project did not allow for testing of a second set of ignitors.

Ignition System Comparison

The overall performance of the Advanced Fast Ignitors was comparable to the DCO ignition system. The BTE shown in are similar for most of the modal points even with the Advanced Fast Ignitors having lower EGR rates.

Figure D-23: Best BTE Points for the DCO and Fast Igniter Compared to the Baseline

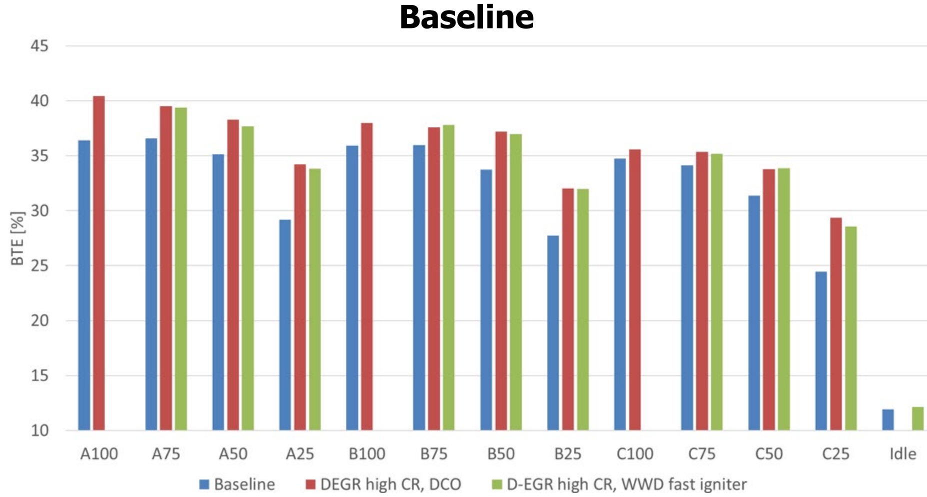

Source: Southwest Research Institute

Each of the three ignition systems have been compared on a relative scale for an overall indication of dilution tolerance, efficiency benefits, reliability and cost. The comparison is presented in Table D-1. The DCO system demonstrated full D-EGR at each of the modal conditions. The increased EGR rate enables a higher compression and a large benefit in efficiency. The cost of the system is greater than the stock engine coils as there are two coils per spark plug with the DCO system. The reliability is the same as the stock engine since the stock spark plugs can be used and the electrical circuits have not shown reliability problems. The pre-chamber plugs are similar in cost to the stock spark plugs and fully compatible with the DCO system. However, the pre-chamber plugs were not able to improve the dilution tolerance and therefore not able to improve the efficiency compared to the baseline. Additionally, pre-ignition concerns with both pre-chamber concepts affected their reliability ratings.

Table D-1: Relative Comparison of the DCO, Pre-Chamber and Advanced Fast Ignitor Ignition Systems

Ignition system	DCO	Pre-chamber	Advanced Fast Ignitor
Efficiency benefit	+	0	+
Increased dilution tolerance	+	-	-
Reliability	+	-	-
Cost	+	+	++

Source: Southwest Research Institute

Ignition System Evaluation Summary

Throughout the project, the Cummins Westport ISX12 G was tested in multiple configurations with different ignition systems. The baseline engine was modified to operate with D-EGR and tested with the DCO ignition system. With the DCO system, the engine was able to run at the full D-EGR rate and achieve between 5 and 40 percent dedicated cylinder enrichment. The two other ignition systems used pre-chamber type spark plugs. The first ignition system was a standard type pre-chamber plug and the second was an Advanced Fast Ignitor with a larger pre-chamber volume. The Advanced Fast Ignitors showed diesel-like stability with CoV of ~0.6 percent and marked improvement in combustion duration over the baseline at the same EGR level. This led to similar brake thermal efficiency as the DCO system even though the EGR rate was lower. However, both systems experienced similar issues: pre-ignition, narrow ignition timing authority for stable combustion, low EGR tolerance, and misfires at EGR rates below the 33 percent EGR target. Neither pre-chamber system was able to successfully operate at full load conditions as the EGR tolerance was not high enough to mitigate the pre-ignition. Even though the Advanced Fast Ignitors showed high efficiency potential, further refinement of the design to the specific combustion chamber is required to fully realize the potential. Therefore, the DCO ignition system with stock J-gap plugs was chosen as the optimal ignition system.